Optimisation-based approaches for multi-floor process plant layout

Jude O. Ejeh

Supervisors: Professor Lazaros Papageorgiou

Dr Songsong Liu

A dissertation submitted in partial fulfillment of the requirements for the degree of

Doctor of Philosophy

of

University College London

Department of Chemical Engineering

University College London

September 2020

To Shera Kyau Ejeh . . .

DECLARATION

I, Jude O. Ejeh, confirm that the work presented in this thesis is my own. Where information has been derived from other sources, I confirm that this has been indicated in the thesis.

_____

Jude O. Ejeh

September 2020

ACKNOWLEDGEMENTS

I thank God! He has been my rock and solid shield, and words cannot accurately capture all He has done for me and my family through the course of this programme. Thank you!

A number of people have contributed towards making this research a success. First, I would like to thank my supervisors Professor Lazaros Papageorgiou and Dr Songsong Liu for the opportunity to work with them on this project. I appreciate your patient guidance, for taking the chance with me and providing the necessary tools and support that I required to learn about mathematical programming.

I am grateful to the Petroleum Technology Development Fund (PTDF), Nigeria for the funding provided through the Overseas Scholarship Scheme (OSS), as well as all the support given through the course of the programme. I also acknowledge the immense support given by the administrative and technical staff of the Department of Chemical Engineering, University College London.

I appreciate the help and support of Andreas, Masha, Adrian, Mayowa, Vassilis, Deema, Ioannis, and a host of other members of the CPSE research group. Your help at different points during the programme made it successful and easier to get through.

A huge gratitude goes to my wife Shera and daughter Ora without whom I would not have been able to cope. Thank you for being there and for all the sacrifices made. I truly cannot repay it. To every member of my family - Professor & Mrs Stephen Ejeh, Engr. & Mrs Joel Agwai, David, Ene Ayi, Sim, Stephen, Sindah - thank you for your love, support, prayers, help and encouragement. They all have been building blocks in what I have and am now.

ABSTRACT

The layout configuration of a chemical process plant has an immense impact on its efficiency of operation, energy consumption, environmental impact and safety levels. This design decision usually lasts throughout the life span of a plant but with the advent of smart manufacturing systems, changes can be made as often as required. At present, there is also a growing need for new chemical plants to meet the increasing demand for chemical products. Hence, automating the layout design process using highly efficient and realistic mathematical models is vital. To aid this, mixed integer linear programming (MILP) models are proposed in this thesis for the efficient determination of multi-floor chemical process plant layout designs.

These MILP models proposed obtain the layout configurations factoring in equipment inter-connectivity by pipes, pumping, construction, land purchase and a more realistic description for tall equipment that span through floors, with/without the availability of pre-defined production sections. Using novel integer cuts, each model obtains globally optimal solutions for larger problem instances in short computational times.

Safety factors are also introduced with risk being quantified using the Dow's fire and explosion index and the Domino Hazard Index. Hazardous events including jet fires, pool fires, fireballs, flash fires, explosions and/or the resulting blast wave effects are quantified as a function of inter-equipment distances. The associated financial risks in the event of an accident are also determined using a more accurate evaluation of the separation distance between equipment. The resulting MILP model estimates the optimal layout configuration and protection device choices for a chemical process plant.

In each of these cases, the unique characteristics and limitations of the proposed models are shown using industry-relevant case studies having a varying number of equipment and requirements, with the models handling all features described with improved computational performance.

IMPACT STATEMENT

By reason of this research, improved mathematical programming models have been developed to obtain solutions to the multi-floor process plant layout problem. These mixed integer programming models successfully obtain multi-floor layout configurations for process plant equipment items within a plant site, whilst ensuring a good balance of economical and safety factors.

These models are useful in providing optimal layout designs for new chemical process plants which site engineers may modify where necessary. When paired with popular CAD software e.g. Autodesk AutoCAD Plant 3D, it also serves as a toolkit to proffer a range of alternative layout configurations, each with its associated layout costs, operational costs and financial risk. As such, site engineers are provided with as much data as may be required to make an informed decision on factors that deal with plant safety, construction efficiency and future operational costs.

Such toolkit is also quite important for smart manufacturing plants, as in such plants, perpetual re-design of its layout is required to meet changing product demands and/or production schedules. These models may be integrated into existing smart systems within the plant to automate layout design and re-design based on pre-specified criteria. This will also lead to savings in time and cost as 20 - 50% of the operating costs of a manufacturing plant have been linked to material handling, which is layout dependent (Moran, 2017; Tompkins et al., 2010).

Although each of the models proposed in this thesis was applied to the layout of chemical process plants, the modelling concepts are transferable to other forms of the layout problem. Faster and/or automated solutions can be obtained for the layout of warehouse

facilities storing goods shipped to customers and/or end users, for the optimal arrangement of electronic device components, or in urban planning of new communities.

TABLE OF CONTENTS

LIST OF FIGURES

LIST OF TABLES

LIST OF ACRONYMS

Acronyms / Abbreviations

BW	Blast wave
BWl	Blast wall
DHI	Domino Hazard Index
DHS	Domino Hazard Score
DI	Damage Index
F&EI	Fire and explosion index
FB	Fire ball
FF	Flash fire
FI	Fire insulation
FW	Firewall
HZ1	Potential hazard scenario 1
HZ2	Potential hazard scenario 2
JF	Jet fire
MILP	Mixed integer linear programming
MINLP	Mixed integer non-linear programming
PF	Pool fire
SF	Safe scenario

CHAPTER *1*

INTRODUCTION

1.1 Background

In 2019, the world's population figure stood at 7.7 billion, with an estimated increase to 8.5 billion in 2030 (United Nations Department of Economic and Social Affairs, Population Division, 2019). For each individual represented, chemical products have been identified to play an indispensable role in their day-to-day lives - healthcare, consumables, housing, food, communication, e.t.c. - with demand projected to rise by up to 4.5% in the next 20 years. Because of this, chemical companies are building more chemical plants especially in emerging economies (Alpizar et al., 2019), and re-optimising existing ones to meet this growing demand in an efficient and sustainable way.

Building these chemical plants typical involves a number of stages (Peters and Timmerhaus, 2003). First, feasibility studies of the economics and market are carried out followed by design data development, detailed engineering designs and economics, procurement and construction, with step by step results testing at each stage. The detailed engineering designs comprise the estimation of process operating conditions, equipment specifications, costs and the overall layout; with the last consideration of particular concern to this thesis.

Chemical process plant layout design seeks to determine how best equipment items and associated structures required in a chemical plant can be spatially arranged within a given physical location, considering their interconnections, the general safety and operability of the

plant, as well as the ease and efficiency of construction and operation (Moran, 2017). This stage of the plant's design has a tremendous impact on its energy consumption, environmental impact, safety levels for plant personnel and the immediate environment, and the overall construction and operational costs. Research has shown that 20 - 50% of the operating costs of manufacturing plants are linked to material handling, which is quite dependent on its layout (Moran, 2017; Tompkins et al., 2010). Such layout designs have traditionally been addressed via intuitive, 'engineering judgement'-based approaches in the past, however there is an emerging need for more systematic and automated approaches, especially with the current transition to smart manufacturing systems and Industry 4.0. A proven way to achieve this is by using mathematical programming techniques.

1.2 Mathematical programming

Mathematical programming or mathematical optimisation can be described as the science of decision making, in which an existing problem is represented as a mathematical model with a specific goal governed by predefined conditions. This goal is represented by an objective function, the conditions by mathematical constraints and its solution, a set of variables that proffer an optimal decision to the problem. A typical mathematical programming problem is represented as follows:

$$\begin{aligned} \textit{min} \quad & f(x) \\ \textit{s.t.} \quad & g(x) \leq 0 \\ & h(x) = 0 \\ & x \in X \end{aligned} \tag{1.1}$$

where $f(x)$ is the objective function to be optimised, $g(x) \in \mathbb{R}^b$ and $h(x) \in \mathbb{R}^c$ are b inequality and c equality constraints respectively, and X is the set of decision variables. If all of the objective function(s) and constraints are defined by linear functions of the variables, a *Linear Programming* (LP) problem results, else a *Non Linear Programming* (NLP) problem. When any of the variables in the problem is restricted to take discrete or integer values, the problem is referred to as a *Mixed-integer Programming* (MIP) problem.

This method has played a key role in tackling a variety of real-life problems in several industries in a systematic and precise manner. Efficient models have been proposed to handle problems in supply chain and energy system management, production planning, scheduling and control, e.t.c. Models have also been developed for the layout design of chemical process plants (Barbosa-Póvoa et al., 2001, 2002; Dan et al., 2015; de Lira-Flores et al., 2014; Díaz-Ovalle et al., 2013, 2010; Georgiadis and Macchietto, 1997; Han et al., 2013; Hwang and Lee, 2014; Jung et al., 2011, 2010b; Ku et al., 2014a,b; Latifi et al., 2017; Lee and Lee, 2017; López-Molina et al., 2013; Medina-Herrera et al., 2014; Papageorgiou and Rotstein, 1998; Park et al., 2011; Patsiatzis and Papageorgiou, 2002; Penteado and Ciric, 1996; Vázquez-Román et al., 2010; Westerlund et al., 2007; Wrigley et al., 2019; Xu and Papageorgiou, 2007, 2009). However, a great deal of these existing models have either been unable to simultaneously handle industrial-sized problems, had a limited amount of realistic problem features, and/or were not able to obtain the best possible solution for a given problem set in a short amount of time (less than 4 hours).

1.3 Project objectives

This work is thus aimed at developing more efficient mathematical programming models to handle the process plant layout problem towards its use in the systematic design of a process plant's layout configuration. Improving model efficiency will be one of the key focuses of this work. This is to ensure that resulting models are more suited to automated design and/or re-design of layout configurations in short computational times. This work will also ensure that additional realistic features are included to the layout problem for a more robust application.

To achieve this, first more efficient mathematical programming models to handle larger problem sizes than previously recorded are needed. As such, mixed integer linear programming (MILP) models with additional constraints to improve computational performance and expand the layout features considered will be presented. Each of these models will be able to simultaneously handle larger-sized problem instances with the same

or a greater number of features than obtainable in the literature. Exact solution techniques will also be adopted to solve these proposed models to ensure the best possible (globally optimal) solutions are obtained for every problem instance.

Each of these models should also handle a range of realistic features for the process plant layout problem. As such, the spatial arrangement of chemical process plant equipment items will be determined considering the interconnection costs by pipes, the horizontal and vertical pumping costs, area dependent purchase cost of the layout site, fixed and area-dependent floor construction costs, purchase and installation of protection devices to mitigate hazardous events, as well as the financial risks associated with those events quantified using industry-accepted safety indices. Hazardous events such as pool fires, jet fires, flash fires, fireballs and blast waves resulting from explosions will be considered in order to obtain safe and economical layout designs. These layout design will be across multiple floors having tall equipment items allowed to span across consecutive floors with pre-specified connection points along their heights based on design specifications.

Models will also be proposed to incorporate the feature of production sections. With production sections, equipment items are segregated in common areas on the plant site to ease construction, operation and/or maintenance activities. The proposed models will simultaneously assign equipment items to floors and pre-defined production sections with an objective to minimize the total layout costs considering all previously mentioned features.

Each of these model features will be tested using industry-relevant case studies. These case studies will demonstrate the performance, applicability, unique characteristics and limitations of each of the proposed models. For the purpose of this thesis, all proposed models will be solved using GAMS (GAMS Development Corporation, 2018) modelling system v25.0.2 and CPLEX v12.8.0.0 solver on an Intel® Xeon® E5-1650 CPU using 12 threads with 32GB RAM.

1.4 Structure of the thesis

The rest of the thesis is structured as follows:

In Chapter 2, past efforts by researchers to tackle the process plant layout problem is reviewed. The definitions and details of the layout problem are presented identifying the features addressed in the past using mathematical programming approaches, the underlying assumptions, formulation techniques and solution methodologies. The merits and limitations encountered from past research are also highlighted.

In Chapter 3 efficient MILP models for the multi-floor process plant layout problem are presented, building on the works from literature. These models handle larger-sized problem instances considering connectivity, pumping and construction costs, and tall equipment items with unique connection points. Case studies having 7 - 25 equipment items are investigated to show the capabilities and limitations of the proposed models.

Chapter 4 further develops the layout problem, introducing pre-defined production sections. Constraints to model this feature in a multiple floor scenario are introduced with previous case studies revisited from Chapter 3 to demonstrate its applicability and performance. The resulting MILP models obtain the optimal decisions for equipment item spatial arrangement within and among production sections, as well as for floor construction in each section.

Safety considerations are introduced in Chapter 5. The probability, magnitude and impact of fire and explosion events on equipment items are quantified using the Dow's Fire & explosion index. Using these data, an MILP model is proposed to minimise the total layout and safety costs. Safety costs are estimated as the sum of the financial risk in the event of an accident as well as the purchase and installation of protection devices for the plant.

Additional hazardous events are incorporated in a more detailed way using the Domino Hazard index in Chapter 6. Pool fire, Jet fire, flash fire, fireball and blast wave events are included in an MILP model to minimise the domino effects such incidents have on neighbouring equipment items, and these features are demonstrated using a case study. A more accurate linear formulation of inter-equipment separation distance is introduced for both cases with safety considerations to properly capture the probability and impact of hazardous events within the plant.

Chapter 7 gives a conclusion of the findings of the thesis with possible areas for future work highlighted.

CHAPTER 2

LITERATURE REVIEW

In this chapter, literature on the process plant layout problem is reviewed. Unique terminologies to the problem are defined and past research efforts are explained towards identifying current gaps to be tackled.

2.1 Introduction

Over the past three decades, the layout of equipment items in process plants has gained increasing relevance (Anjos and Vieira, 2017; Mecklenburgh, 1985). Research has shown that to operate an efficient production and/or service system, attention needs to be given not only to its operational and planning procedures but also to its layout design (Hosseini-Nasab et al., 2018). Such design generally entails finding the optimal spatial location of facilities primarily accounting for how they are connected to each other, as well as a number of other factors (Anjos and Vieira, 2017; Drira et al., 2007). The process of accomplishing this task gave rise to what is often referred to as the "facility layout problem". Fig 2.1 gives a pictorial structure of the problem showing its subclasses, applications, general considerations, objectives, constraints explored and solution approaches. Facilities here refer to an entity used directly or indirectly to perform a job e.g. work centres, manufacturing cells, departments in an organisation, machine tools, process plant equipment, etc. (Drira et al., 2007). When such set of facilities solely comprise of items directly associated with the manufacturing

processes in a chemical process plant, the problem may be referred to as the "process plant layout problem".

In this chapter, a review of past efforts to tackle the process plant layout problem is presented, highlighting the criteria considered, underlying assumptions, solution techniques and limitations realized.

2.2 Process plant layout problem

As earlier explained, the process plant layout problem is regarded as a subset of the facility layout problem (Fig 2.1). Here, the facilities considered are typically process vessels and equipment (also referred to as units), and sometimes associated structures such as control rooms, plant personnel areas, offices, etc. (Jayakumar and Reklaitis, 1994; Mecklenburgh, 1985). Connection considerations between process units are mostly by pipes and/or ducts, but can be by conveyors in processes involving solids or by automated guided vessels or vehicular transportation in pipeless plants (Patsiatzis et al., 2005). Pre-specified criteria such as the general safety and operability of the plant, ease and efficiency of construction and operation, effective, economical and ergonomic use of space, are also considered in the final layout of the process plant (Moran, 2016). Fianl layout decisions are then determined through a combination of intuition, economic optimisation, critical examination, equipment ratings, mathematical modelling, and/or 3D CAD software.

In practice, layout considerations can be classified into three forms as outline by Moran (2016) in a "brownfield":

- *site layout* - which relates to how plots are placed relative to each other in a site. A plot is a section of a plant site mostly defined as being bounded by a road system (Moran, 2017);
- *plot layout* - referring to the spatial arrangement of process units within a plot; *and*
- *equipment layout* - referring to the arrangement of process unit auxiliaries about the individual unit.

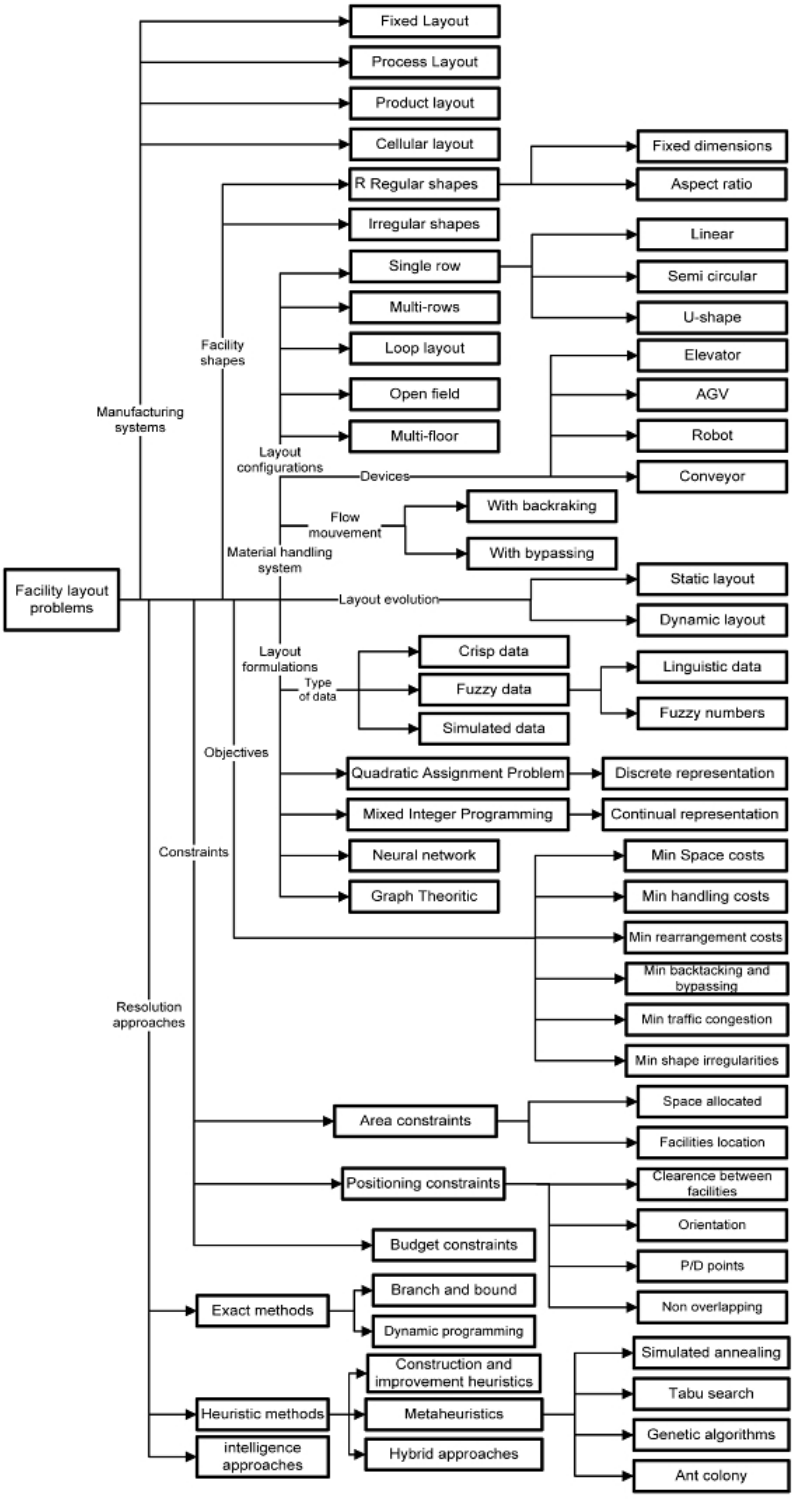

Fig. 2.1 Overview of the facility layout problem (Drira et al., 2007)

In most cases, equipment layout are carried out by equipment manufacturers prior to its installation on the plant site, and a bulk of the decision making process relates to the plot and site layout. Details of past considerations for the process plant layout problem - its characteristics, problem formulations, objectives and solution methodologies - are reviewed below.

2.2.1 Problem characteristics

Process plant layout design has gradually transitioned from methods based solely on past experience and engineering judgement towards more deterministic methods. As such, a number of mathematically representative ways to model the process plant layout problem has arisen. From basic considerations of just the cost of material flow between units by Jayakumar and Reklaitis (1994) to more realistic considerations having connection costs, pumping costs, financial risk, safety device installations, etc. (Ejeh et al., 2019a). Fig. 2.2 shows a summary of the major features, formulations, and solution approaches of the process plant layout problem considered in literature from a deterministic point of view.

Layout cost components

The basic consideration of the process plant layout problem from the start has been on the cost of material flow between process units (Jayakumar and Reklaitis, 1994). As process plant units are mainly connected by pipes, the objective was to minimise the cost per unit distance of flow between connected units. At first, this cost was a lump consideration of the properties of the process fluids, the amount being transferred, and nature of the piping material to be used (Jayakumar and Reklaitis, 1994). Later on, representative costs were included to separately describe the cost associated with laying a unit distance of an appropriate pipe for a process fluid stream (Penteado and Ciric, 1996), and pumping such process streams horizontally and/or vertically across multiple floors (Coulson J. M.; Richardson, 1994; Georgiadis and Macchietto, 1997). Decision variables relating to area dependent costs of land were introduced by Georgiadis et al. (1999). In such situations, the total layout area was also determined. Fixed and area dependent floor construction costs (Patsiatzis and

Papageorgiou, 2002) were further introduced to better account for the individual factors that make up the total costs for a proper layout estimation.

Space and geometry representations

In each of these works, the process plant layout area was either represented using a discrete or continuous domain. In a discrete representation, the layout area is divided into a set of candidate locations with each process unit allocated to one or more of such locations. This representation was adopted by Georgiadis and Macchietto (1997) and Georgiadis et al. (1999). The size of each candidate location is a choice of the decision maker, and although this representation is a more convenient approach from a modelling point of view, the final solutions obtained are suboptimal as each candidate location is always greater than or equal to the process unit's actual size. Hence, the exact size of each unit can hardly be captured no matter how 'fine' the set of locations are defined. Papageorgiou and Rotstein (1998) first adopted the use of a continuous representation for a detailed layout determination in which exact sizes of process units were used to obtained the final layout design. This was a more accurate representation and has since been adopted by subsequent researchers in the field.

Earlier considerations of the layout problem were restricted to single floor considerations (Barbosa-Póvoa et al., 2001; Georgiadis and Macchietto, 1997; Jayakumar and Reklaitis, 1994; Papageorgiou and Rotstein, 1998; Penteado and Ciric, 1996), where the spatial arrangement of process units was considered over a 2 dimensional space. However, owing to increasing land costs, limited space availability, as well as the fact that certain plant sites exist by default as multiple floor structures e.g. offshore facilities (Hosseini-Nasab et al., 2018), considerations have been extended to multi-floor and/or 3 dimensional representations of the process plant layout problem (Barbosa-Póvoa et al., 2002; Georgiadis et al., 1999; Patsiatzis and Papageorgiou, 2002). For such cases, the floor location and spatial arrangement of each process unit in each floor is simultaneous determined. A bulk of previous considerations assumed that all process units considered for multi-floor layout occupied only a single floor. This assumption is valid for the parent facility layout problem, however the presence of tall process units in chemical process plants such as distillation columns, flare stacks,

e.t.c., invalidates such assumption. Ku et al. (2014b) proposed a mixed integer non-linear programming (MINLP) model for multi-floor layout with tall process units. Such units were described by a set of consecutive single-floor units, and the location of each of these units in subsequent floors was fixed relative to the previous. The resulting MINLP was solved using local solvers and global optimality could not be guaranteed.

Aside from the single vs multiple floor viewpoint, additional consideration has also been given to the representative geometry of process units in a continuous domain. As process plant equipment items have differing shapes, past researchers have made assumptions on a representative geometry in their proposed models. Penteado and Ciric (1996) approximated process unit geometries/foot print as circles, and euclidean distances from the mid-points of units were used to calculate the piping distances. This is a valid assumption as most units have a cylindrical geometry e.g. separation columns, reactors, e.t.c., however, with units like heat exchangers and tubular reactors, a circular footprint gives a large error. A more valid assumption of equipment geometry is that of a rectangle as adopted by Papageorgiou and Rotstein (1998) and following authors. Papageorgiou and Rotstein (1998) also used a rectilinear metric to model the piping distance between process units which mimics how actual pipes are laid in process plants. The euclidean distances evaluated between equipment item midpoints, although a more accurate representation in terms of equipment separation distances, also presents a non-linear term in the formulation which is difficult to solve.

Safety considerations

As noted by Moran (2017), a good process plant layout design should provide a healthy balance of not only efficient, economic and ergonomic factors, but of safety factors as well. The layout of chemical process plant has been identified as playing a significant role in the overall safety level of a plant (Kidam and Hurme, 2012) and has been considered by past researchers of the process plant layout problem. Penteado and Ciric (1996) addressed safety from the view point of the financial risk associated with accidents. Such risk was quantified as the net present financial loss associated with an accident based on its probability and severity as a function of the distance of the accident source to neighbouring units. Passive

protection devices (with their associated costs) were made available to reduce the risk level. Patsiatzis et al. (2004) quantified financial risk using the Dow's Fire and Explosion Index (F&EI) system (American Institute of Chemical Engineers, 1994), with protection devices also being made available to reduce the impact an accident had on neighbouring equipment items. The proposed model was formulated as an MILP problem and considered single-floor layout scenarios. Park et al. (2018) extended the work of Patsiatzis et al. (2004) to multi-floor scenarios, while Wang et al. (2017) also employed the F&EI system but over a discrete domain for single floor layouts.

More recently, researchers have employed the Domino Hazard index (DHI) system (Tugnoli et al., 2008a) which assesses the domino effects hazards originating from a particular process unit have on other components of the chemical plant. Unlike the F&EI which accounts majorly for fire and explosion incidents, the DHI allows for other hazards such as toxic release, human risk, blast wave, e.t.c. Tugnoli et al. (2008b) first applied the DHI to assess safety levels of different layout configurations, but de Lira-Flores et al. (2014) developed an MINLP model to handle single floor cases. The model accounted for pool fires, jet fires, fireballs, flash fires and explosions, and the domino effect such incidents have on secondary units as a function of separation distances and the presence of protection devices.

Other risk estimating methods have also been developed apart from the F&EI and DHI system of estimation. Using dispersion models, Díaz-Ovalle et al. (2010) accounted for toxic release incidents based on a worst-case scenario, with mitigation systems later on introduced in Díaz-Ovalle et al. (2013). Using the individual risk, Han et al. (2013) also formulated an MILP model to determine layout configurations with minimal risk to human beings.

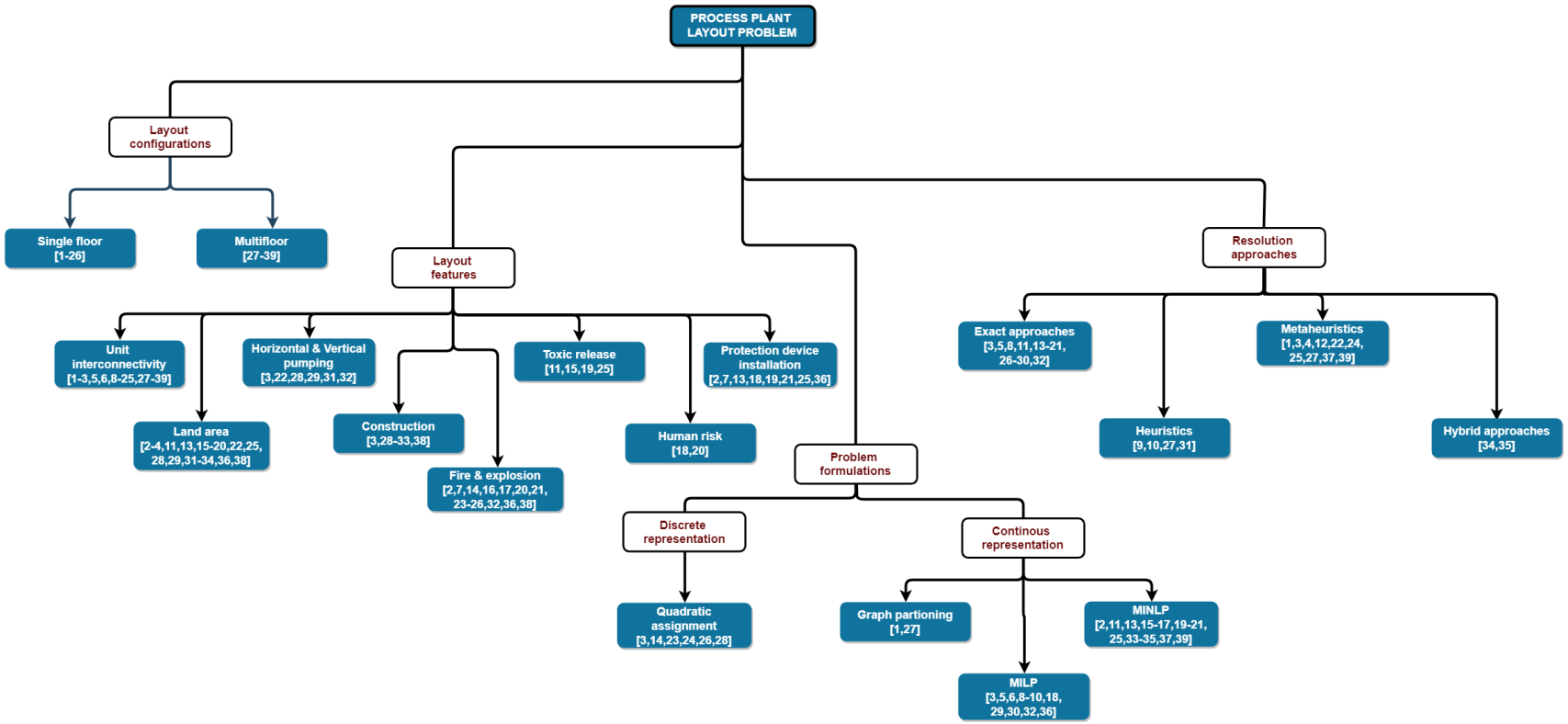

1 Jayakumar and Reklaitis (1994)	2 Penteado and Ciric (1996)	3 Georgiadis and Macchietto (1997)	4 Castell et al. (1998)	5 Papageorgiou and Rotstein (1998)
6 Barbosa-Póvoa et al. (2001)	7 Patsiatzis et al. (2004)	8 Westerlund et al. (2007)	9 Xu and Papageorgiou (2007)	10 Xu and Papageorgiou (2009)
11 Vázquez-Román et al. (2010)	12 Furuholmen et al. (2010)	13 Jung et al. (2010b)	14 Jung et al. (2010a)	15 Díaz-Ovalle et al. (2010)
16 Jung et al. (2011)	17 López-Molina et al. (2013)	18 Han et al. (2013)	19 Díaz-Ovalle et al. (2013)	20 Medina-Herrera et al. (2014)
21 de Lira-Flores et al. (2014)	22 Caputo et al. (2015)	23 Jung (2016)	24 Wang et al. (2017)	25 Latifi et al. (2017)
26 de Lira-Flores et al. (2018)	27 Jayakumar and Reklaitis (1996)	28 Georgiadis et al. (1999)	29 Patsiatzis and Papageorgiou (2002)	30 Barbosa-Póvoa et al. (2002)
31 Patsiatzis and Papageorgiou (2003)	32 Park et al. (2011)	33 Hwang and Lee (2014)	34 Ku et al. (2014b)	35 Ku et al. (2014a)
36 Dan et al. (2015)	37 Lee and Lee (2017)	38 Park et al. (2018)	39 Wrigley et al. (2019)	

Fig. 2.2 Review of past literature on the process plant layout problem

Other features

Some other important features have also been considered in the process plant layout problem. One of such is the determination of piping routes. Guirardello and Swaney (2005) incorporated this feature in the layout problem. They proposed to simultaneously and/or sequentially obtain the layout and piping routes for a process plant. Particular attention has also been given to pipeless plants in the literature (Patsiatzis et al., 2005; Realff et al., 1996). In pipeless plants, transfer of materials between process units/stages is achieved using mobile vessels instead of pipes (Realff et al., 1996). A major part of the research in the layout of pipeless plants, though, has been in combination with the plant's design and scheduling. Realff et al. (1996) adopted a discrete representation in an MILP model and obtained solutions by a rigorous decomposition procedure while Patsiatzis et al. (2005), adopting a continuous representation of the layout area, proposed an MILP model which was solved by exact approaches. More recently, Shaik and Mathur (2018) considered simultaneous scheduling, vessel routing and layout for pipeless plants. The final layout was selected from three pre-defined layout configuration types and the solution was obtained by a simultaneous approach using an MILP model. Irregularly-shaped process units have also been studied. This feature is important in modelling process units having geometries that do not fit the assumption of a rectangular footprint with negligible error. Barbosa-Póvoa et al. (2001) modelled such items as a combination of regular-shaped items (ie. fitting a rectangular geometry) in 2D and 3D (Barbosa-Póvoa et al., 2002) with items having different input and output points.

A final feature worthy of mention is that of production sections. With production sections, processing units are segregated/grouped in a common area. This has been common practice in most plant layout design endeavours (Mecklenburgh, 1985). Units may be grouped based on the functions they perform, similarity in type or on special considerations of the process at hand. Jayakumar and Reklaitis (1994) achieved such grouping by minimizing the inter-section flow costs using graph partitioning. However, these groupings are most times decided prior to layout design. Researchers have incorporated predefined production section considerations for the determination of optimal single (Barbosa-Póvoa et al., 2001; Papageorgiou and Rotstein, 1998) and multi-floor (Barbosa-Póvoa et al., 2002) layout designs

in a continuous space. The site and plot layout were determined with an objective to minimise unit interconnectivity costs (Barbosa-Póvoa et al., 2001; Papageorgiou and Rotstein, 1998) and pumping costs (Barbosa-Póvoa et al., 2002) alone.

2.2.2 Problem formulation

One of the earlier ways of mathematically representing the process plant layout problem was based on graph theory (Jayakumar and Reklaitis, 1994, 1996). Here, the problem is represented as a graph $G = (V, E)$ having a set of vertices V and edges E. Edges are defined as a set of unordered pairs of distinct vertices. Each vertex was used to represent a process unit and an edge for interconnection. Weights are assigned to each edge corresponding to the magnitude/cost of flow. Jayakumar and Reklaitis (1994) adopted this approach to segregate process units by minimizing the total inter-section connection cost alone. This was further extend to a multi-floor case (Jayakumar and Reklaitis, 1996). Both problems were solved using heuristic approaches as obtaining an optimal solution proved difficult using exact approaches for plants of industrial sizes. The nature of the formulation also made it difficult to incorporate additional features to the layout problem apart from interconnectivity costs.

As earlier stated, the process plant layout problem can be regarded as a subclass of the facility layout problem. This dependency also extends to the problem formulation methods and solution. A popular way of formulating the facility layout problem is the quadratic assignment problem (QAP) formulation (Koopmans and Beckmann, 1957). The QAP applied to facility layout seeks to assign a set of facilities to pre-defined locations with a goal of minimizing the weighted sum of their relative distances (Hanan and Kurtzberg, 1972). As such, the layout area is represented by a discrete domain. The original problem formulation can be further modified to include additional features aside from unit interconnectivity such as land area, pumping and construction costs (Georgiadis and Macchietto, 1997; Georgiadis et al., 1999), safety (de Lira-Flores et al., 2018; Jung, 2016; Jung et al., 2010a; Wang et al., 2017), e.t.c. However, solutions obtained are almost always suboptimal. This is because the set of pre-defined locations are, by default, of equal area. The exact dimensions of process unit can, therefore, not be accurately captured. The difference in areas creates

unwanted/unoccupied space which increases layout costs. The formulation, though, proffers an easier-to-solve method when compared with other methods having a continuous domain representation. Exact and heuristic approaches have been adopted by authors to solve this problem as exact approaches cannot handle problems with more than 15 units considering only unit interconnectivity in modest computational times (Hosseini-Nasab et al., 2018).

A more common formulation approach is by mixed integer programming (MIP) models (Fig. 2.2). MIP models consist of an objective function having a mixture of integer and non-integer decision variables subject to a number of equality and inequality constraints (Hosseini-Nasab et al., 2018). This formulation type allows for a continuous domain representation of the layout area with a more accurate calculation of the process unit/equipment dimensions, as well as the inclusion of additional features to the layout problem. A range of features have been formulated as mixed integer linear (Barbosa-Póvoa et al., 2001, 2002; Dan et al., 2015; Georgiadis and Macchietto, 1997; Han et al., 2013; Papageorgiou and Rotstein, 1998; Park et al., 2011; Patsiatzis and Papageorgiou, 2002; Westerlund et al., 2007; Xu and Papageorgiou, 2007, 2009) or non-linear (de Lira-Flores et al., 2014; Díaz-Ovalle et al., 2013, 2010; Hwang and Lee, 2014; Jung et al., 2011, 2010b; Ku et al., 2014a,b; Latifi et al., 2017; Lee and Lee, 2017; López-Molina et al., 2013; Medina-Herrera et al., 2014; Penteado and Ciric, 1996; Vázquez-Román et al., 2010; Wrigley et al., 2019) programming models, with the latter having non-linear terms in the objective function or constraints, or both. Both cases, as with the previous formulation types can be solved using exact approaches, heuristics, metaheuristics or a hybrid approach.

2.2.3 Solution methodologies

The main solution approaches to the process plant layout problem have been by exact methods, heuristics, metaheuristics or an intuitive combination of some or all of them. Exact approaches refer to resolution methods used to find the optimal/best solution to the layout problem. They generally comprise methods such as dynamic programming, semi-definite programming, the branch and bound method, cutting plane algorithms, e.t.c. (Hosseini-Nasab et al., 2018); with the branch and bound method being the most popularly adopted for the

layout problem. The branch and bound algorithm employs a binary tree to represent the integer variable combinations. The feasible region is methodologically partitioned into subdomains and valid upper and lower bounds computed at every level of the tree (Floudas, 1995). Cutting planes or valid inequalities can be incorporated into the branch and bound algorithm, in what is referred to as the branch and cut method, to improve its performance. Current literature, however, have shown that this solution method is unable to obtain final solutions for MIP layout problems having more than 15 units in modest computational times, either using a discrete or continuous representation (Hosseini-Nasab et al., 2018). This has led to the use of approximated approaches or heuristics in recent times.

Heuristic methods generally employ problem-specific rules to find, in a quick way, good-enough solutions to an optimisation problem. For example, Patsiatzis and Papageorgiou (2003) proposed a rigorous decomposition approach and an iterative scheme to solve the multi-floor process plant layout problem. Xu and Papageorgiou (2007) also proposed a construction-based approach for the single-floor process plant layout problem, later including an improvement-phase (Xu and Papageorgiou, 2009). Each of these methods were able to obtain optimal or near-optimal solutions to the problem at hand in shorter times than exact methods, however their performance in terms of solution quality were unpredictable and computational times were also problem specific and could not be extrapolated to other cases.

Meta-heuristics on the other hand are problem-independent and have also been used extensively in the literature for the process plant layout problem. Methods such as particle swarm optimisation (Park and Lee, 2015), genetic algorithm (Xin et al., 2016), hyper heuristics (Furuholmen et al., 2010), e.t.c., have been adopted to obtain approximate solutions to the layout problem in reasonable computational time for large problem sizes. Hybrid techniques have also been used. Ku et al. (2014b) used a hybrid optimisation technique consisting of genetic algorithm and sequential quadratic programming (initial proposed by Lee et al. (2005)) on an MINLP formulation with an objective to minimise the total area allotted for the layout. All these methods have been adopted in recent times by a number of authors (Caputo et al., 2015; Castell et al., 1998; Furuholmen et al., 2010; Latifi et al., 2017; Lee and Lee, 2017; Wang et al., 2017; Wrigley et al., 2019) owing to their problem-

independence and computational performance, but they still have the same issue as heuristic methods relating to solution quality.

2.3 Current consideration

It is evident that a considerable amount of research has gone into the process plant layout problem, but a gap still exists. First is with the scalability of mixed integer programming models using exact solution approaches. Although a number of heuristic and metaheuristic methods exist in solving the layout problem, globally optimal solutions or at least the obtained solution quality, cannot be guaranteed and/or inherently determined. The performance of heuristic methods is also directly related to the efficiency of the model used. Hence, more efficient models need to be proposed to address industrial-sized processes in reasonable computational times. These models should be able to handle basic considerations of equipment interconnectivity and pumping considerations, to more complex determination of safety factors such as the choice of safety device installations to mitigate the propagation of accidents within the chemical process plant.

Second is the incorporation of more realistic considerations, particularly the modelling of tall process units/equipment items. These are process units whose heights exceed the standard floor height in industrial plants e.g. distillation columns, flare stacks, contacting columns, etc. and will span through multiple floors. Although this feature has been considered in the past (Ku et al., 2014b), globally optimal solutions were not obtained using the proposed MINLP model. In addition to tall equipment item modelling, unique connections points need to be considered as opposed to the mid-point connection assumption in previous literature. With this feature, connection points between items will be taken from their respective design-specified heights.

More efficient MILP models with safety considerations are also needed. At present, MINLP models covering a range of possible incidents such as flash fires, pool fires, jet fires, blast waves, e.t.c., with allowance being made for the installation of protection devices to mitigate the level of damage from accidents, have been proposed. However, the actual layout

features considered were limited to connection costs in a single floor design with sub-optimal results obtained. There is therefore a need for models which simultaneously determine the multi-floor layout design of chemical process plants considering unit interconnectivity, pumping, area-dependent construction costs, as well as safety factors. These models should also be able to obtain globally optimal solutions in modest computational times for a larger number of equipment items than previously recorded in literature.

The following chapters seek to address these gaps. The proposed models will simultaneously handle equipment interconnectivity with unique interconnection points, availability of production sections, a more precise modelling of tall equipment with associated constraints, vertical and horizontal pumping, and fixed and area-dependent construction costs of the process plant in a continuous domain. Allowances being made for multi-floor placement of units, with safety levels estimated using industry-accepted safety metrics directly affected by layout designs, and each MILP model handling more units than previous recorded in literature for the multi-floor layout design of chemical process plants using an exact solution approach.

In the next chapter (Chapter 3), five models are proposed considering equipment interconnectivity, tall equipment items, vertical and horizontal pumping, and fixed and area-dependent construction costs for multi-floor process plants.

CHAPTER 3

MULTI-FLOOR PROCESS PLANT LAYOUT

In this chapter, mixed integer linear programming (MILP) models are proposed for a more efficient handling of the multi-floor process plant layout problem. The proposed models consider tall equipment items that span through multiple floors with unique connection points along their heights, connection costs, vertical and horizontal pumping costs, and fixed and area-dependent construction costs. Case studies with 7 - 25 equipment items are presented to shown model performance and unique capabilities.

3.1 Introduction

The proposed models build on the work of Patsiatzis and Papageorgiou (2002) with additional features to account for tall equipment items, unique connection points along the height of each item, with novel valid inequalities for more efficient solution evaluation. Tall equipment items here refer to process plant equipment having heights greater than the height of each floor, as such, they extend through consecutive floors. For all items considered, the connection points at design specified heights are taken as opposed to mid-point connections on the equipment item.

This rest of this chapter is structured as follows: Section 3.2 gives a detailed description and assumptions of the layout problem being considered. Section 3.3 describes the proposed mathematical models. The applicability and performance of each model is illustrated with

relevant case studies in Section 3.4. Additional constraints are introduced to the proposed models in Section 3.5 to improve computational performance with added benefits of one of the proposed models highlighted in Section 3.6. Finally, concluding remarks are given in Section 3.7.

3.2 Problem description

The multi-floor process plant layout problem considered is described as follows:

Given:

- a set of equipment items and their dimensions (length, breadth and height);
- a set of potential floors for layout;
- the connectivity network amongst equipment items;
- cost data (connection, pumping, land, and construction);
- floor height of each potential floor;
- space and equipment allocation limitations;
- minimum safety distances between equipment items;

determine:

- the total number of floors required for the final layout;
- the base land area occupied;
- the area of each selected floor;
- spatial equipment item allocation to floors;

so as to: minimise the total plant layout cost.

The total plant layout cost comprises the cost of connecting equipment items by pipes, pumping process fluids through such pipes with differing considerations for horizontal vs vertical pumping, purchasing the land for the layout based on its area, and the fixed cost of constructing each floor as well as that dependent on its area. It is assumed that:

- each equipment item is approximated with a rectangular geometry;
- every item is connected to the other from its geometrical centre in the x-y plane, and from a predefined height along the z-plane, based on design considerations;

- an item is allowed to rotate through 90° angles about the x-y plane as deemed optimal but it must start at the base point of the floor it has been assigned to;
- floors are numbered from bottom to top with a fixed floor height;
- rectilinear distances are taken between items; and
- equipment items tall enough to exceed the fixed floor height are allowed to extend through successive floors.

3.3 Mathematical formulation

The mathematical formulations proposed constitutes an extension to the model proposed by Patsiatzis and Papageorgiou (2003) as enumerated in Appendix A. Five models are proposed, each primarily differing in how tall/multi-floor equipment items are modelled. Models A.x handle tall equipment items as one continuous unit/entity starting on one floor k, spanning through consecutive floors and terminating on a higher floor k'. In model B, multi-floor items are divided into pseudo single-floor units. These pseudo units are basically single-floor-sized units which when combined vertically make up the multi-floor equipment item. Each pseudo unit has the same length and breadth as the multi-floor item, but its height is always equal to the floor height of the plant, with the exception of the top-most pseudo unit, which takes the remainder of the height of the multi-floor item.

Nomenclature

Indices

θ	floor count index
i, j, n	equipment item in models A.1 - A.4
i', j', n'	equipment item in model B
k, k'	floor number
p	pseudo units
s	rectangular area sizes

Sets

I	set of equipment item for models A.1- A.3
I'	set of equipment item for model B; $I' = (I \setminus MF) \cup \bigcup_{i \in MF} P_i$
K	set of available floors for layout
MF	set of multi-floor equipments
P_i	sets of pseudo units for equipment i

Parameters

$\alpha_i, \beta_i, \gamma_i$	dimensions of equipment item i
$\delta_{i\theta}$	1 for equipment item i if $\theta \leq M_i$; 0 otherwise
BM	a large number
C^c_{ij}	connection costs between items i and j
C^h_{ij}	horizontal pumping costs between items i and j
C^v_{ij}	vertical pumping costs between items i and j
De^{min}_{ij}	minimum safety distance between items i and j
f_{ij}	1 if flow direction between equipment items i and j is positive; 0, otherwise
$FC1$	fixed floor construction cost
$FC2$	area-dependent floor construction cost
FH	floor height
IP_{ij}	distance between the base and input point on item j for the connection between items i and j
LC	area-dependent land purchase cost
M_i	number of floors required by equipment item i
OP_{ij}	distance between the base and output point on equipment i for the connection between items i and j
$\overline{X}_s, \overline{Y}_s$	x-y dimensions of pre-defined rectangular area sizes s

Integer variables

NF	number of floors

Binary variables

$E1_{ij}, E2_{ij}$	non-overlapping binary, a set of values which prevents equipment overlap in one direction in the x-y plane
N_{ij}	1 if items i and j are assigned to the same floor; 0, otherwise
O_i	1 if length of item i is equal to α_i; 0, otherwise
Q_s	1 if rectangular area s is selected for the layout; 0, otherwise
S^s_{ik}	1 if item i begins on floor k; 0, otherwise
S^f_{ik}	1 if item i terminates on floor k; 0, otherwise
V_{ik}	1 if item i is assigned to floor k
W_k	1 if floor k is occupied; 0, otherwise

Continuous variables

ω_i	number of floors by which a multi-floor item $i \in MF$ extends over the topmost floor
A_{ij}	distance in the y plane between items i and j, if i is above j
AR_s	predefined rectangular floor area s
B_{ij}	distance in the y plane between items i and j, if i is below j
d_i	breadth of item i
D_{ij}	distance in the z plane between items i and j, if i is lower than j
FA	base land area
l_i	length of item i
L_{ij}	distance in the x plane between items i and j, if i is to the left of j
NQ_s	linearisation variable expressing the product of NF and Q_s
R_{ij}	distance in the x plane between items i and j, if i is to the right of j
TD_{ij}	total rectilinear distance between items i and j

U_{ij}	distance in the z plane between items i and j, if i is higher than j
x_i, y_i	x,y coordinates of the geometrical centre of item i
X^{max}, Y^{max}	dimensions of base land area

3.3.1 Model A.1

Floor constraints

Every equipment item is assigned to an equivalent number of floors, M_i, based on its height:

$$\sum_k V_{ik} = M_i \qquad \forall\, i \tag{3.1}$$

V_{ik} is a binary variable which determines if an equipment i is assigned to floor k. A variable, N_{ij}, is introduced to determine if items i and j are assigned to the same floor k, given by:

$$N_{ij} \geq V_{ik} + V_{jk} - 1 \qquad \forall\, i, j > i, k \tag{3.2}$$

The variable N_{ij} takes the value of 1 if items i and j are on any same floor, and 0 otherwise.

As not all available floors may be required for layout, it is necessary to define which floors are chosen and so exist. For a floor to exist, an equipment item must start on it. Additional variables - S^s_{ik} and $S^f_{ik'}$ - are introduced taking values of 1 if an equipment i starts at floor k and terminates at floor k' respectively. Thus:

$$S^s_{ik} \leq W_k \qquad \forall\, i, k \tag{3.3}$$

where W_k takes a value of 1 if a floor k is chosen for the layout, and thus exists. Such floors will exist only if an equipment is starting on it, and not just passing through it (for multi-floor equipment items), and that the preceding floor is also occupied. Ensuring that the preceding floor is occupied eliminates empty intermediate floors and reduces solution degeneracy. The

later consideration is described by equation (3.4).

$$W_k \leq W_{k-1} \qquad \forall\, k > 1 \tag{3.4}$$

A lower bound on the number of floors required is then determined by equation (3.5).

$$NF \geq \sum_k W_k \tag{3.5}$$

Equipment orientation constraints

A 90° rotation of equipment orientation is permitted in the x-y plane only. Rotation in the z-axis is deemed unrealistic as such equipment orientation is fixed for construction in virtually all cases. This is represented by equations (3.6) and (3.7).

$$l_i = \alpha_i O_i + \beta_i (1 - O_i) \qquad \forall\, i \tag{3.6}$$

$$d_i = \alpha_i + \beta_i - l_i \qquad \forall\, i \tag{3.7}$$

Multi-floor equipment constraints

In order for equipment items requiring more than one floor to span across successive floors, the constraints below are introduced.

$$-V_{ik} + V_{i,k-1} + S^s_{ik} \geq 0 \qquad \forall\, i,k \tag{3.8}$$

$$-V_{ik} + V_{i,k+1} + S^f_{ik} \geq 0 \qquad \forall\, i,k \tag{3.9}$$

Equations (3.8) and (3.9) ensures that the binary variables S^s_{ik} and $S^f_{ik'}$ take a value of 1 if an equipment starts and ends on a particular floor (k and k') respectively, with each equipment being restricted to start and end on only one floor by:

$$\sum_k S^s_{ik} = 1 \qquad \forall\, i \tag{3.10}$$

$$\sum_k S^f_{ik} = 1 \qquad \forall\, i \tag{3.11}$$

The constraint to restrict equipment to occupy successive floors is then given as:

$$\sum_{k'=k}^{k+M_i-1} V_{ik'} \geq M_i \cdot S^s_{ik} \qquad \forall\, i,k \tag{3.12}$$

Non-overlapping constraints

It is also necessary for two or more equipment items assigned to the same floor not to occupy the same spatial area/overlap. Constraints (3.13) - (3.16), adapted from Patsiatzis and Papageorgiou (2003) are introduced to prevent such occurrence. The pairwise values of the binary variables $E1_{ij}$ and $E2_{ij}$ determine if an equipment item i is forced to the right, left, above or below another item j if they exist on the same floor ($N_{ij} = 1$):

$$x_i - x_j + BM(1 - N_{ij} + E1_{ij} + E2_{ij}) \geq \frac{l_i + l_j}{2} + De^{min}_{ij} \qquad \forall\, i,j > i \tag{3.13}$$

$$x_j - x_i + BM(2 - N_{ij} - E1_{ij} + E2_{ij}) \geq \frac{l_i + l_j}{2} + De^{min}_{ij} \qquad \forall\, i,j > i \tag{3.14}$$

$$y_i - y_j + BM(2 - N_{ij} + E1_{ij} - E2_{ij}) \geq \frac{d_i + d_j}{2} + De^{min}_{ij} \qquad \forall\, i,j > i \tag{3.15}$$

$$y_j - y_i + BM(3 - N_{ij} - E1_{ij} - E2_{ij}) \geq \frac{d_i + d_j}{2} + De^{min}_{ij} \qquad \forall\, i,j > i \tag{3.16}$$

The parameter De^{min}_{ij} is added to the right hand side of each constraint to enforce a minimum spacing between each pair of items on a floor.

Distance constraints

Distance constraints are described by equations (3.17) - (3.19), to determine the horizontal and vertical distances between two connected items i and j. The horizontal rectilinear distances are adapted from Patsiatzis and Papageorgiou (2002) in equations (3.17) and (3.18). For the vertical distance, provision is made for connections at varying points along the height of either equipment as determined from design calculations. This is described by equation (3.19;

$$R_{ij} - L_{ij} = x_i - x_j \qquad \forall\, i,j : f_{ij} = 1 \tag{3.17}$$

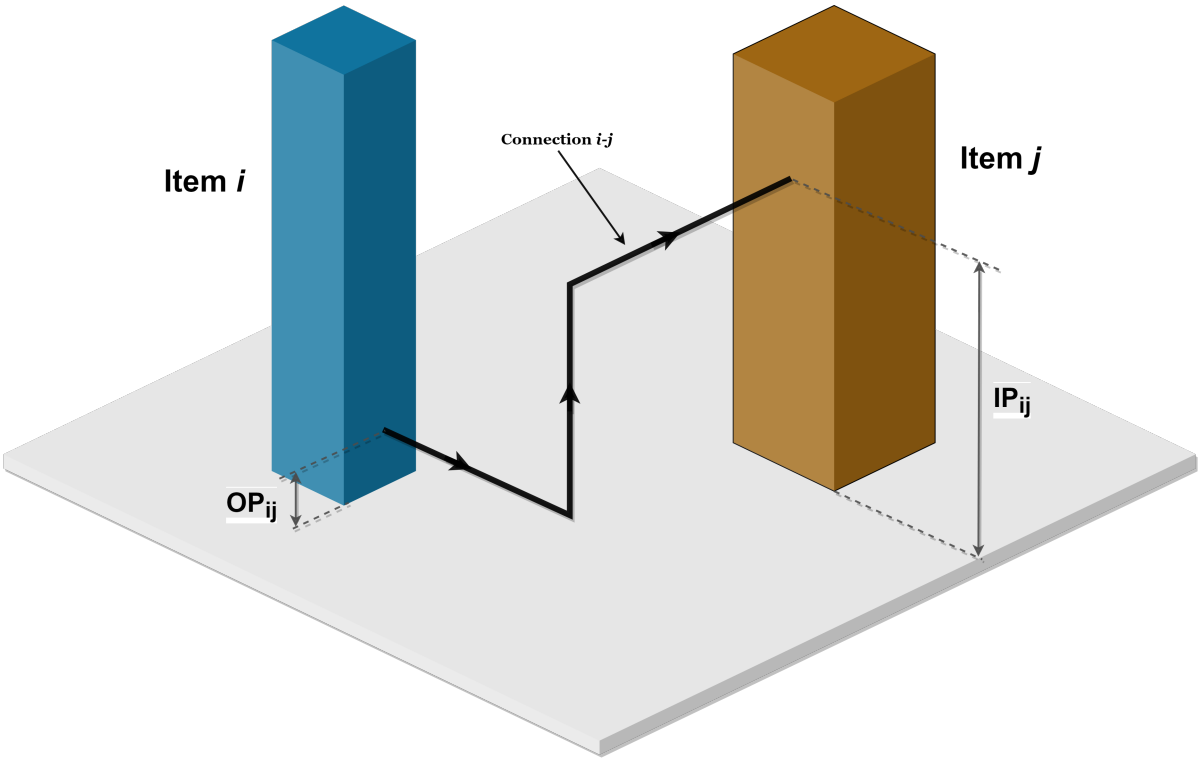

Fig. 3.1 Design-specified connection point illustration

$$A_{ij} - B_{ij} = y_i - y_j \qquad \forall i,j : f_{ij} = 1 \tag{3.18}$$

$$U_{ij} - D_{ij} = FH\sum_k (k-1)(S^s_{ik} - S^s_{jk}) + OP_{ij} - IP_{ij} \qquad \forall (i,j) : \ f_{ij} = 1 \tag{3.19}$$

OP_{ij} represents the vertical distance from the base of equipment i to its output point, and IP_{ij} represents the vertical distance from the base of equipment j to its input point for connection i-j (Fig. 3.1). The total rectilinear distance is then calculated as:

$$TD_{ij} = R_{ij} + L_{ij} + A_{ij} + B_{ij} + U_{ij} + D_{ij} \qquad \forall i,j : f_{ij} = 1 \tag{3.20}$$

Layout design constraints

Layout design constraints, (3.21) - (3.24), ensure that equipment items are placed within the boundaries of a floor. Lower bounds on the x and y coordinates of every item i are defined as:

$$x_i \geq \frac{l_i}{2} \qquad \forall\, i \tag{3.21}$$

$$y_i \geq \frac{d_i}{2} \qquad \forall\, i \tag{3.22}$$

and the upper bound:

$$x_i + \frac{l_i}{2} \leq X^{max} \qquad \forall\, i \tag{3.23}$$

$$y_i + \frac{d_i}{2} \leq Y^{max} \qquad \forall\, i \tag{3.24}$$

X^{max} and Y^{max} are the maximum floor length and width.

Area Constraints

The area of each floor is then determined as the product of X^{max} and Y^{max}. However, to avoid such bilinear term, the value of the floor area, FA, is selected from a set S of predefined rectangular area sizes, AR_s, with dimensions $(\overline{X}_s, \overline{Y}_s)$.

$$FA = \sum_s AR_s Q_s \tag{3.25}$$

$$\sum_s Q_s = 1 \tag{3.26}$$

The floor length and breadth is selected from the chosen rectangular area size dimensions:

$$X^{max} = \sum_s \overline{X}_s Q_s \tag{3.27}$$

$$Y^{max} = \sum_s \overline{Y}_s Q_s \tag{3.28}$$

Also, a continuous variable NQ_s is introduced to linearise the cost term associated with the area dependent floor construction costs in the total cost having the product of the floor area and the number of floors.

$$NQ_s \leq \mid K \mid Q_s \qquad \forall s \tag{3.29}$$

$$NF = \sum_s NQ_s \tag{3.30}$$

Objective function

The objective function then minimizes the total cost associated with the connection cost, pumping cost, land area cost, fixed floor construction cost and floor area dependent cost. This is given as:

$$\begin{aligned} min \sum_{i,j:f_{ij}=1} \left(C^c_{ij} T D_{ij} + C^v_{ij} D_{ij} + C^h_{ij}(R_{ij} + L_{ij} + A_{ij} + B_{ij})\right) \\ + FC1 \cdot NF + FC2 \cdot \sum_s AR_s \cdot NQ_s + LC \cdot FA \end{aligned} \tag{3.31}$$

subject to equations (3.1) - (3.31). This constitutes model A.1.

3.3.2 Model A.2

Model A.2 is similar to model A.1 except that some of the constraints for the multi-floor equipment descriptions - (3.9), (3.11) and (3.12) - are replaced with equation (3.32) below:

$$\sum_{\theta=1}^{M_i-1} V_{i,k+\theta} \geq (M_i - 1) \cdot (V_{ik} - V_{i,k-1}) \qquad \forall\, i,k \tag{3.32}$$

Equation (3.32) ensures that multi-floor equipment occupy consecutive floors, the total number equalling the required number of floors M_i. Model A.2 then comprises of equations (3.1) - (3.8), (3.10), (3.13) - (3.32).

3.3.3 Model A.3

Model A.3 makes use of the binary variables S^s_{ik} and S^f_{ik} and is described using equations (3.10), (3.11) and (3.33) below.

$$V_{ik} - V_{i,k-1} = S^s_{ik} - S^f_{i,k-1} \qquad \forall\, i,k \tag{3.33}$$

Model A.3 is then composed of equations (3.1) - (3.7), (3.10) - (3.11), (3.13) - (3.31) and (3.33).

3.3.4 Model A.4

In model A.4, in addition to the floor constraints (equations (3.1) - (3.5)), the following constraint is included:

$$\mid K \mid +1 \geq \sum_k k \cdot S^s_{ik} + M_i \qquad \forall\, i \in MF \tag{3.34}$$

This ensures that each equipment item occupies the required number of floors amongst the available floors for the layout design. Each of these units must, however, start on only one floor:

$$\sum_k S^s_{ik} = 1 \qquad \forall\, i \tag{3.35}$$

Multi-floor equipment item constraints from model A.1 (equations (3.8) - (3.12)) are also reformulated as follows: Equation (3.36) ensures that such items occupy consecutive floors:

$$V_{ik} = \sum_{\theta=1}^{M_i} \delta_{i\theta} \cdot S^s_{i,k-\theta+1} \qquad \forall\, i,k \tag{3.36}$$

where V_{ik} is still a binary variable which determines if an equipment i is assigned to floor k and $\delta_{i\theta} = 1$ for all $\theta \leq M_i$.

Thus, model A.4 consists of objective function (equation 3.31) subject to constraints (3.1) - (3.7), (3.13) - (3.30) and (3.34) - (3.36).

3.3.5 Model B

Model B is a linearised formulation of Ku et al. (2014b) with adaptations from Patsiatzis and Papageorgiou (2003). Multi-floor equipment items are split into pseudo single-floor units. This modelling approach has the advantage of correctly describing equipment items which have varying sizes along their height. Example of such units are the fluidized catalytic cracking (FCC) unit, vacuum distillation unit, e.t.c., where an assumption of a constant cross-sectional area may not always be valid. The following additional constraints are included to account for the multi-floor equipment items and multi-point connections.

Floor constraints

Equation (3.1) is re-written as (3.37) as all units now occupy only one floor. In addition to equation (3.2) for all $i', j' > i', k'$, equations (3.39) and (3.40) are included, and (3.3) is modified to (3.41).

$$\sum_k V_{i'k} = 1 \qquad \forall\, i' \tag{3.37}$$

$$N_{i'j'} \geq V_{i'k} + V_{j'k} - 1 \qquad \forall\, i',\, j' > i',\, k \tag{3.38}$$

$$N_{i'j'} \leq 1 - V_{i'k} + V_{j'k} \qquad \forall\, i',\, j' > i',\, k \tag{3.39}$$

$$N_{i'j'} \leq 1 + V_{i'k} - V_{j'k} \qquad \forall\, i',\, j' > i',\, k \tag{3.40}$$

$$V_{i'k} \leq W_k \qquad \forall\, i', k \tag{3.41}$$

Multi-floor equipment constraint

Multi-floor equipment are split into pseudo units equivalent to the number of floors they occupy (Fig. 3.2). For all multi-floor equipment, $i \in MF$, requiring M_i number of floors, each unit is split into M_i pseudo units. The first $M_i - 1$ units having heights equal to the floor height, and the last pseudo unit with the remainder.

So, for each $i \in MF$, there exists pseudo units, $p \in P_i$; and the modified set of all equipments, I', becomes:

$$I' = (I \wedge (\neg MF)) \vee P_i$$

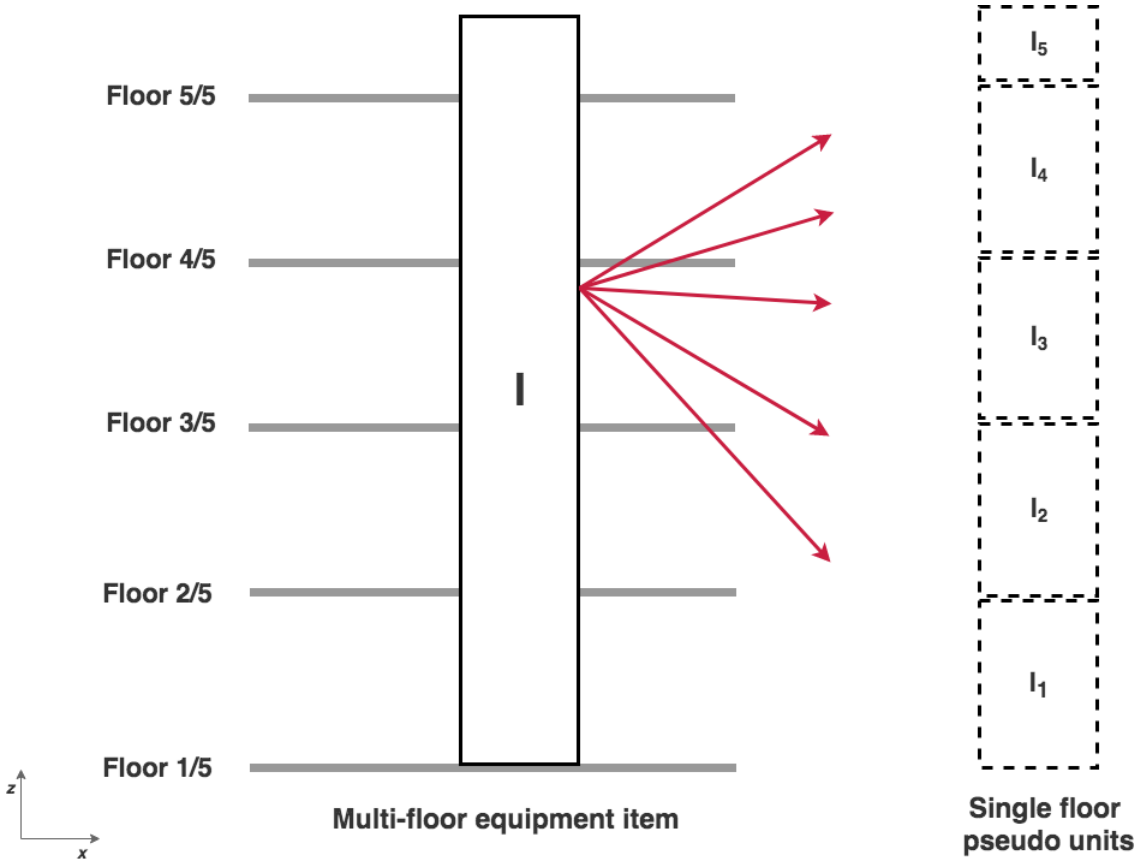

Fig. 3.2 Pseudo-unit illustration

Subsequent pseudo units, $p+1$, for each pseudo unit set, P_i, are then made to occupy successive floors by the constraint:

$$V_{p,k} = V_{p-1,k-1} \qquad \forall\, p \in P_i, k \tag{3.42}$$

These pseudo units are also placed directly above their preceding counterpart:

$$x_p = x_{p+1} \qquad \forall\, p \in P_i \tag{3.43}$$

$$y_p = y_{p+1} \qquad \forall\, p \in P_i \tag{3.44}$$

and finally, consistency in 90° rotation is ensured for all pseudo units of a multi-floor equipment:

$$O_p = O_{p+1} \qquad \forall\, p \in P_i \tag{3.45}$$

Distance constraints

For connection between equipment i' and j' at varying points along the height of either equipment, equation (3.19) in models A.x is modified to:

$$U_{i'j'} - D_{i'j'} = FH\sum_{k}(k-1)(V_{i'k} - V_{j'k}) + OP_{i'j'} - IP_{i'j'} \qquad \forall (i',j') \in I' : \; f_{i'j'} = 1 \tag{3.46}$$

Model B thus consists of constraints (3.4) - (3.7) and (3.13) - (3.30) written for any equipment item i', j' in I' instead; (3.37) - (3.46) and objective function:

$$\begin{aligned} min \sum_{i',j':f_{i'j'}=1} \left(C^c_{i'j'} TD_{i'j'} + C^v_{i'j'} D_{i'j'} + C^h_{i'j'}(R_{i'j'} + L_{i'j'} + A_{i'j'} + B_{i'j'})\right) \\ + FC1 \cdot NF + FC2 \sum_{s} AR_s \cdot NQ_s + LC \cdot FA \end{aligned} \tag{3.47}$$

3.4 Case studies

In this section, a description of the case studies applied to each model is given. Models A.1 - A.4 and B are each applied to the case studies. All runs were solved to global optimality or a maximum time of 10,000s. The choice of pre-defined floor area sizes were based on estimates from the equipment dimensions for a particular case study. Five alternative sizes were used for the predefined floor dimensions in the ethylene oxide (10 - 50 m, with a step size of 10m) and urea production (5 - 45 m, with a step size of 10m) plants and twelve sizes were used for all the other examples (5 - 60m, with a step size of 5m). The layout plots of model A.1 alone is presented in this section, while the models A.2 - B plots are presented in Appendix C.

To ensure a globally optimal solution, the value of BM used in equations (3.13) - (3.16) were such that:

$$BM \geq \max_{s}(\overline{X}_s, \overline{Y}_s) + \max_{i,j}(De^{min}_{ij}) \tag{3.48}$$

The term on the right hand side is the sum of the maximum allowable length or breadth from the pre-defined area dimensions, and the minimum separation distance. This removes any restriction on the position coordinates of an item i by the inactive non-overlapping constraints of equations (3.13) - (3.16).

3.4.1 Ethylene oxide (EO) plant

The first example is an ethylene oxide plant used in Patsiatzis and Papageorgiou (2002), originally presented by Penteado and Ciric (1996) but extended for multi-floor considerations. The process flow diagram of the plant is shown in Fig. 3.3 having a total of 7 units. Data on the connectivity and construction costs, as well as the connection points along the heights of the equipment, are shown in Section B.1. The summary of the model statistics is shown in Table 3.1 and the optimal layout in Fig. 3.4.

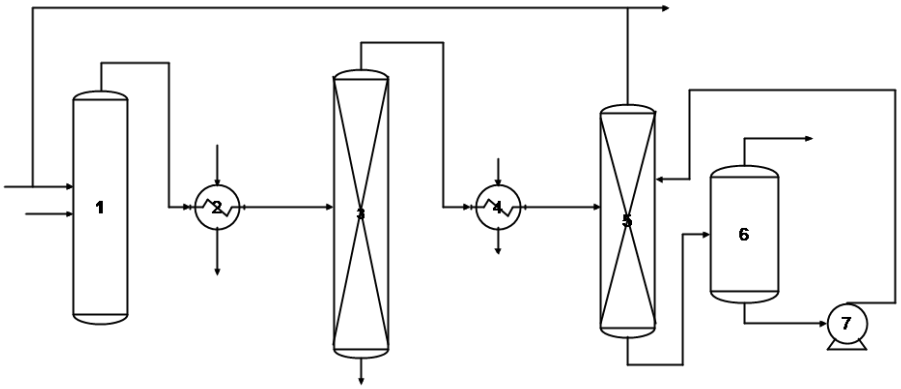

Fig. 3.3 Flow diagram of ethylene oxide plant (Ejeh et al. (2018a)) (See Table B.1 in Appendix B for a description of the equipment item labels)

Table 3.1 Model statistics & computational performance for EO Plant

	EO plant (7 units)				
	A.1	A.2	A.3	A.4	B
Total cost (rmu[1])	66,262.0				
CPU (s)	1.3	1.2	1.6	1.4	2.0
Number of discrete variables	92	92	92	92	132
Number of continuous variables	176	155	176	157	157
Number of equations	360	317	318	313	630

[1] relative monetary units

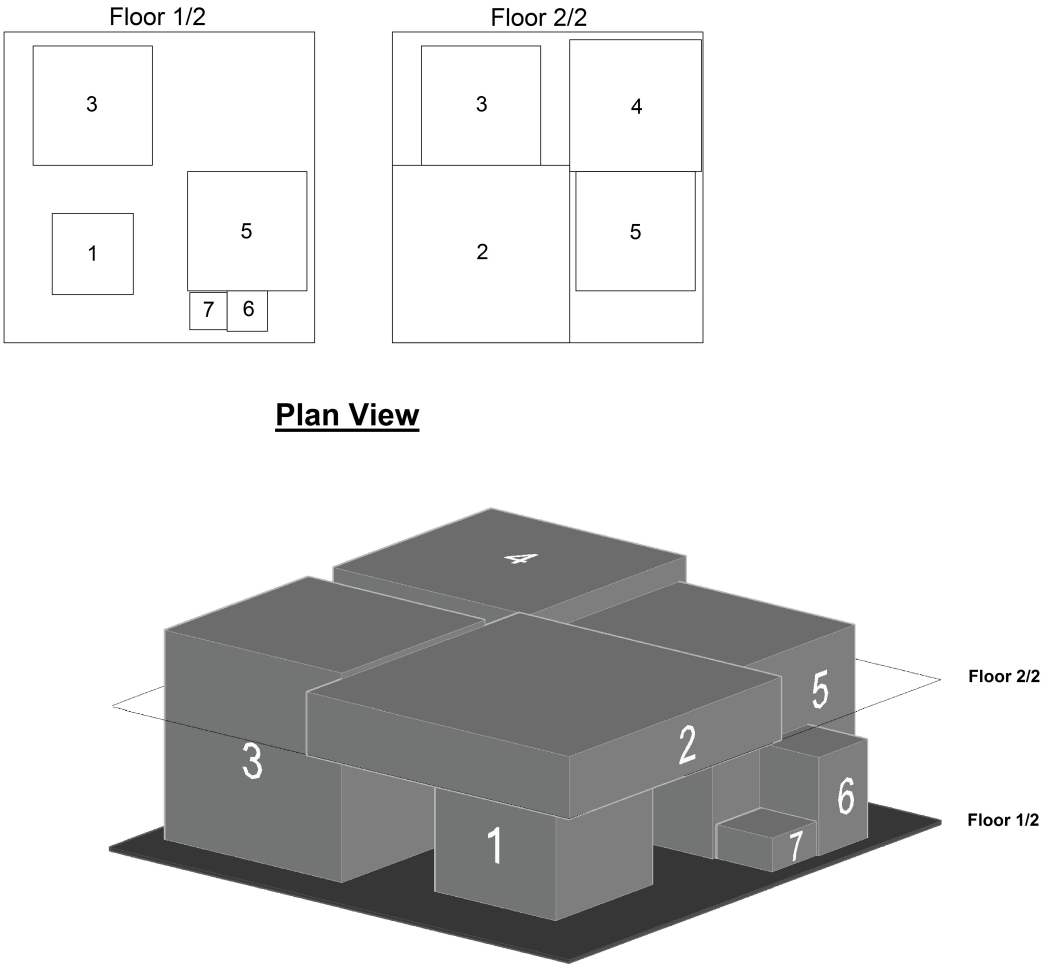

Fig. 3.4 Optimal layout of EO plant

The results obtained gave a total cost of 66,262 rmu across all models - 22% connection costs, 44% pumping costs and 34% construction costs. Each floor had an area measuring 20m$\times$ 20m, with a total of two (2) floors selected from an available four(4); models A being more computationally efficient. Model B was inherently larger in size owing to a greater number of units handled compared to models A. All models, however, solved the problem in at most 2s showing a great computational improvement when compared to similar exact approaches in literature of the same example with a smaller number of layout features (Patsiatzis and Papageorgiou, 2003). Tall/multi-floor items 3 (ethylene oxide absorber) and 5 (CO_2 absorber) were also successfully modelled to span through floors 1 and 2 (Fig. 3.4) as both required two floors based on their heights relative to the floor height.

The total cost value obtained (66,262 rmu) is also 30% higher than that obtained by Patsiatzis and Papageorgiou (2002) (50,817 rmu). This cost difference is mainly attributed to the connection point consideration where design-specified heights are used as opposed to mid-point connections along the height of each equipment item. This shows that previous assumptions were not entirely realistic.

3.4.2 Urea production (UR) plant

An urea production plant is also considered. It consists of 8 units, with 2 (unit 2 - Reactor 1, and 4 - Distillation column 1) exceeding the floor height of 8m. A minimum inter-unit distance of 4m is required across all floors. The process flow diagram of the plant is shown in Fig. 3.5 and data on the connectivity and construction costs, and equipment dimensions are available in Section B.2. The summary of the model statistics and computational performance is shown in Table 3.2 and the optimal layout in Fig. 3.6.

All 4 floors made available for the layout were assigned units, with each floor having an area measuring 15m$\times$ 5m, and a total layout cost of 117,430 rmu. The two multi-floor units (units 2 and 4) occupied successive floors proportional to their height (floors 1-4 and 2-3 respectively). Computational results showed global optimality was achieved by all models in a short time (under 3s), with models A being computationally superior to B. Fig. 3.6 also shows that the minimum inter-equipment spacing of 4m was enforced across floors. This

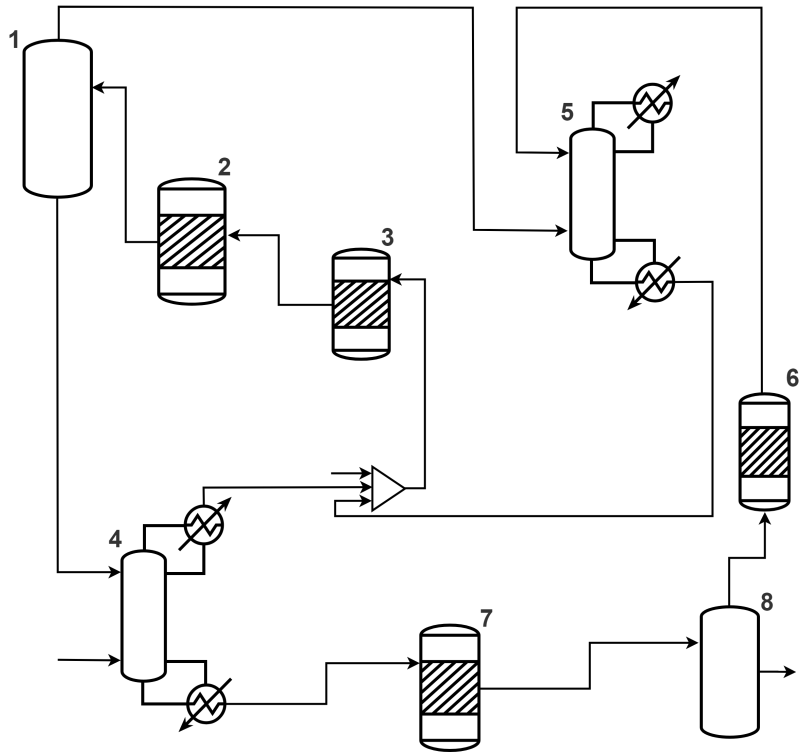

Fig. 3.5 Flow diagram of urea production plant (Ejeh et al. (2019b)) (See Table B.6 in Appendix B for a description of the equipment item labels)

feature allows for easy inclusion of minimum safety distances for all units, even for specific unit pairs.

Table 3.2 Model statistics & computational performance for UR Plant

	UR plant (8 units)				
	A.1	A.2	A.3	A.4	B
Total cost (rmu)	117,431.0				
CPU (s)	1.5	1.3	1.5	1.5	2.8
Number of discrete variables	118	118	118	118	216
Number of continuous variables	223	191	223	193	213
Number of equations	499	435	435	429	1275

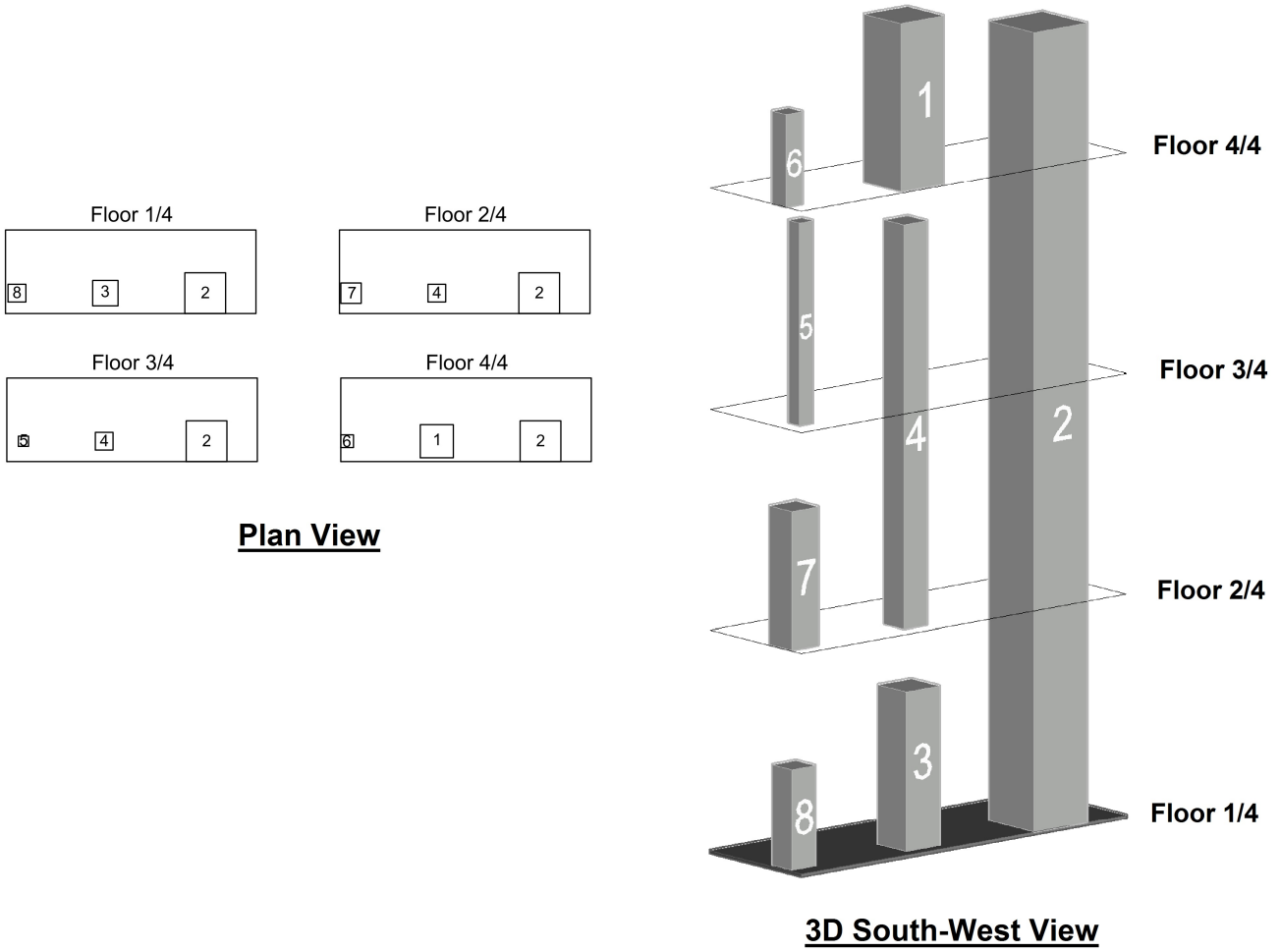

Fig. 3.6 Optimal layout of UR plant

3.4.3 Crude distillation (CDU) plant

The third example is a crude distillation (CDU) plant with preheating train. It consists of 17 units, with five (unit 5 - Pre-flash drum, 7- Crude distillation tower, 6, 12 - the two Fired heaters, and 15 - Debutaniser) exceeding the floor height of 5m. The process flow diagram of the plant is shown in Fig. 3.7 and data on the equipment dimensions, connectivity and construction costs are available in Section B.3.

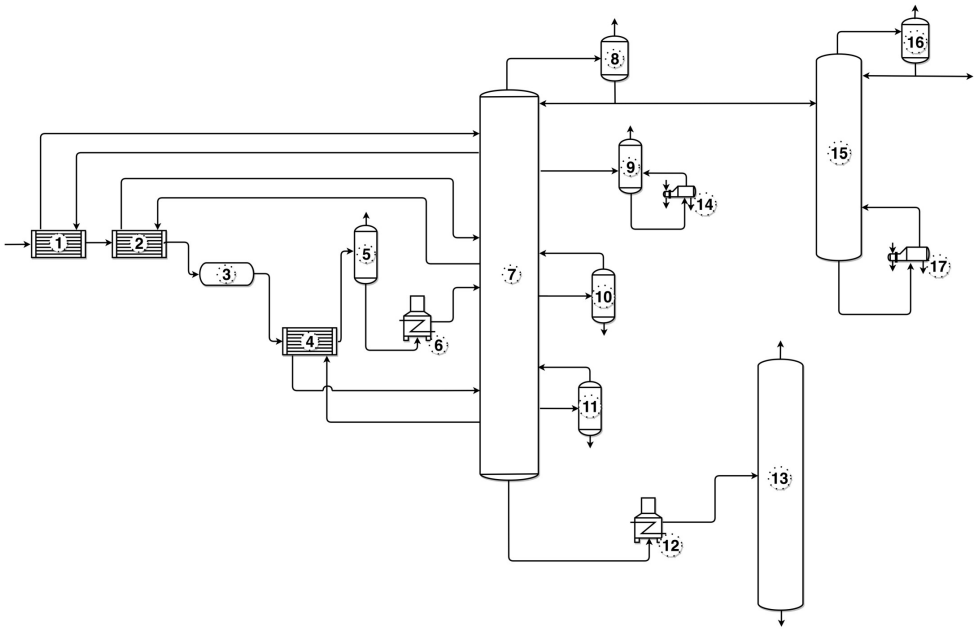

Fig. 3.7 Flow diagram of crude distillation plant (Ejeh et al. (2019b)) (See Table B.8 in Appendix B for a description of the equipment item labels)

The results obtained for the CDU plant gave a total of five possible floors, out of seven. A total cost of 603,886.5 rmu was obtained across all models with each floor measuring 15m$\times$ 20m. The layout of equipment items is shown in Fig. 3.8. The optimal starting floors of all equipment items (especially the multi-floor items) and floor locations were simultaneously determined by each model (Figs. C.9 - C.12), with each model allowing multi-floor unit 15 extend above the topmost floor without the need to construct floors 6 and 7. These floor constructions were deemed unnecessary as no other item was to be place on such floors. Hence, although a multi-floor item can span a specified number of floors based on its height, not every one of those floors need to be constructed. This feature has practical

applications for items such as fired heaters with long stacks, distillation columns and flare stacks, where not all floors need to be constructed through the length of the equipment item, saving cost.

Table 3.3 Model statistics & computational performance for CDU plant

	CDU plant (17 units)				
	A.1	A.2	A.3	A.4	B
Total cost (rmu)	603,886.5				
CPU (s)	0.4%[1]	2142.4	2078.4	956.6	5.5%[1]
Number of discrete variables	551	551	551	551	1258
Number of continuous variables	793	674	793	679	906
Number of equations	2398	2178	2160	2148	11607

[1] Relative gap quoted at CPU limit of 10,000s

Table 3.3 shows the computational performance of each model. Although all models obtained the globally optimal cost value of 603,886.5 rmu, models A.1 and B did not prove this value within the CPU limit of 10,000s. Model A.4, on the other hand, obtained this value in less than 1000s. This shows a higher degree of computational efficiency as compared to previous literature model with similar considerations (Patsiatzis and Papageorgiou, 2003) where the globally optimal solution for a smaller total number of units (12) could not be obtained within the same time limit.

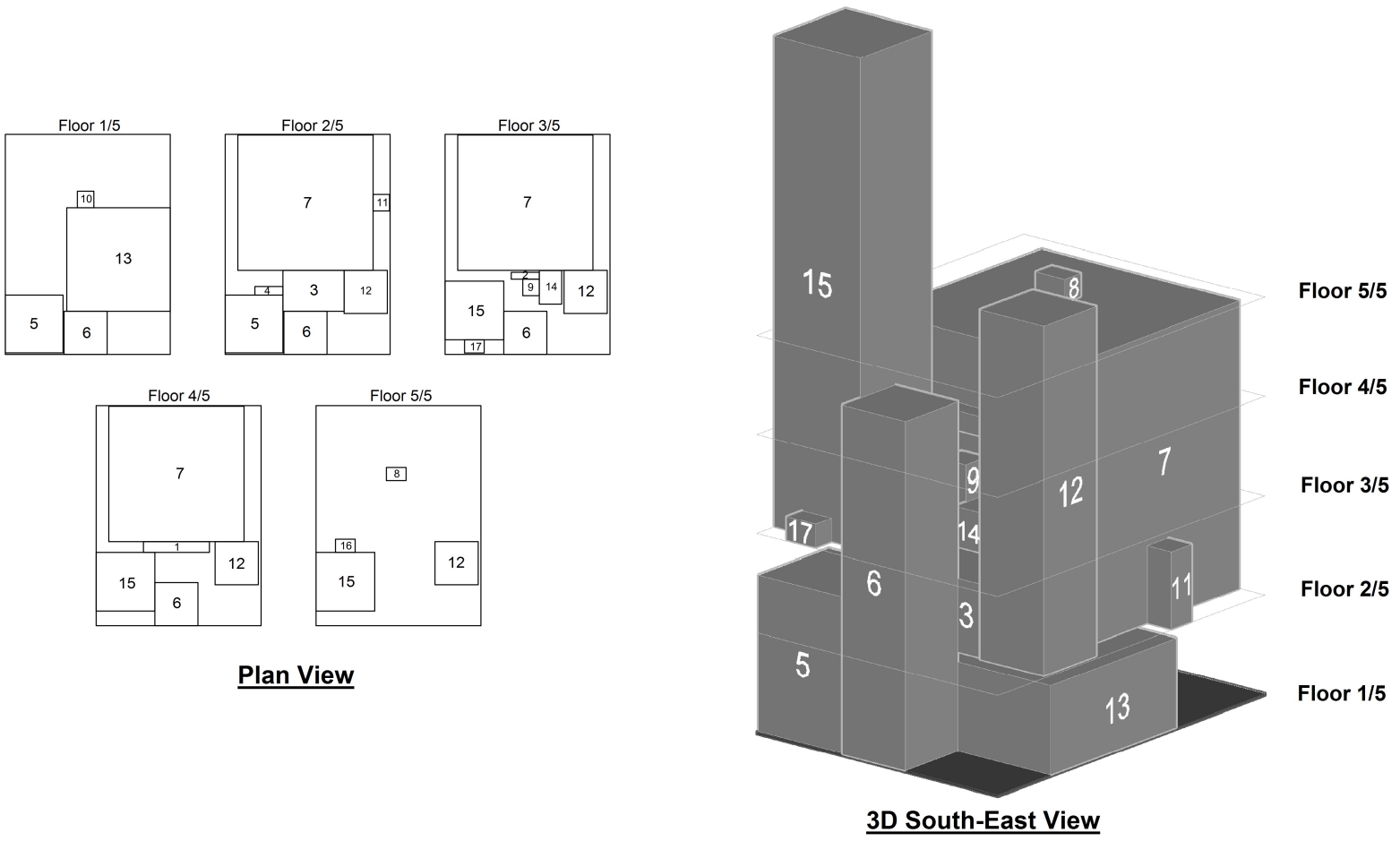

Fig. 3.8 Optimal layout of CDU plant

3.4.4 Liquefied natural gas liquefaction (LNG) plant

To further test the limits of the proposed model, a fourth example is presented - a liquefied Natural Gas liquefaction plant (LNG Plant) originally presented in Hwang and Lee (2014). It consists of 22 units as shown in Fig. 3.9 to be arranged within five decks of a ship. Required equipment information and cost data are provided in Section B.4.

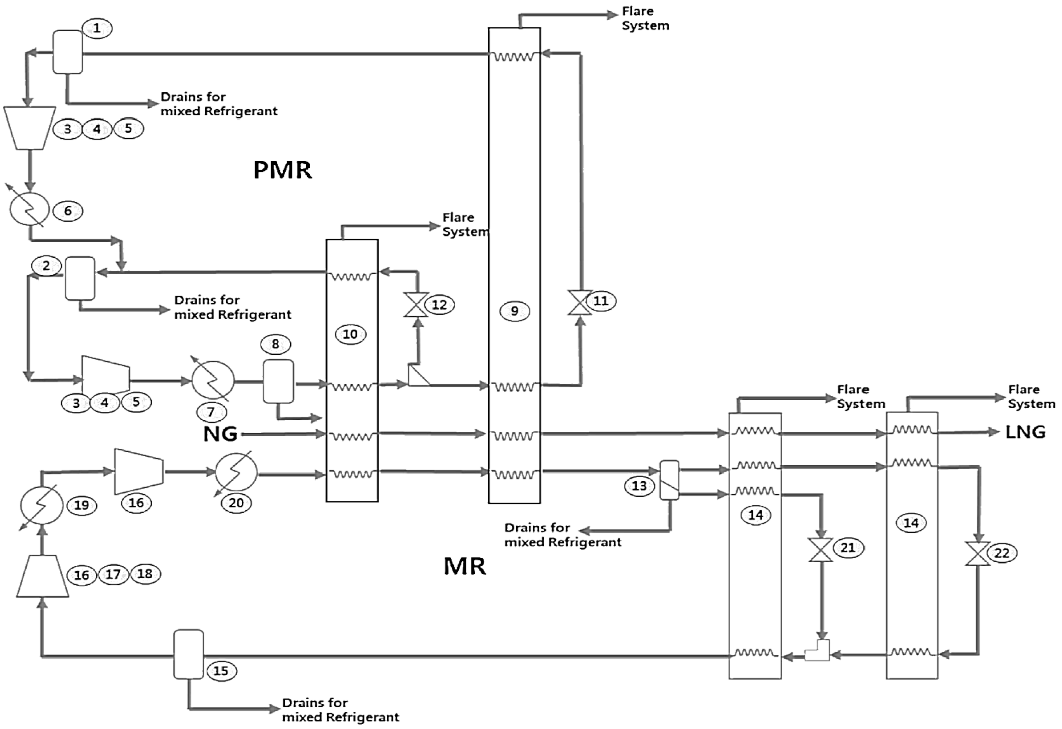

Fig. 3.9 Flow diagram of LNG liquefaction plant (Hwang and Lee (2014)) (See Table B.10 in Appendix B for a description of the equipment item labels)

Additional features to this case study were that the MR compressor (unit 16) had to be located directly above the MR compressor cooler (17), and below the overhead crane (18); the PMR compressor (3) above its cooler (4) and below its overhead crane (5); the minimum distance between each unit, be 4m; and, a workspace area of not more than 50%, and an emergency area of not more than 60% of the floor area on the ground and topmost floor respectively must be available. These additional features are modelled as follows:

$$V_{ik} = V_{j,k+1} \qquad \forall\,(i,j) \in I^{LNG} \tag{3.49}$$

$$x_i = x_j \qquad \forall\,(i,j) \in I^{LNG} \tag{3.50}$$

$$y_i = y_j \qquad \forall\,(i,j) \in I^{LNG} \tag{3.51}$$

$$FA - \left(\sum_i V_{i,1}\alpha_i\beta_i - 9X^{max}\right) \geq 0.5FA \tag{3.52}$$

$$FA - \left(\sum_i V_{i,5}\alpha_i\beta_i - 9X^{max}\right) \geq 0.6FA \tag{3.53}$$

where $I^{LNG} = \{(3,5),(4,3),(16,18),(17,16)\}$. The relative equipment item allocations are modelled by equations (3.49) - (3.51), and (3.52) and (3.53) ensure that a portion of the area on the first and last floor is left free by at least 50% and 60% of the total floor area for the workspace and emergency area respectively. The total floor area is the total equipment layout area plus an additional free area of $X^{max}\times$9m.

Table 3.4 Model statistics & computational performance for LNG plant

	LNG plant (22 units)				
	A.1	A.2	A.3	A.4	B
Total cost (rmu)	1,467,009.7	1,466,654.2			1,467,009.7
CPU (s)	2.3%[1]	3.1%[1]	2.4%[1]	3.0%[1]	3.7%[1]
Number of discrete variables	732	732	732	732	1398
Number of continuous variables	890	780	890	786	1011
Number of equations	3018	2806	2798	2782	10762

[1] Relative gap quoted at CPU limit of 10,000s

Table 3.4 show the computational statistics of the proposed models. None of the proposed models proved the globally optimal solution (1,466,654.2 rmu) within the specified time limit of 10,000s, but models A.1 and A.3 were more efficient than A.2, A.4 and B, with model A.1 having the smallest relative gap at termination.

A floor area of 35m$\times$ 30m was obtained across all five floors selected in the final layout result (Fig. 3.10). All models were able to successfully incorporate the requirements of relative item positioning, additional free space on the first and last floor and the minimum equipment spacing. As required, item 16 was located on floor 2 directly above 17 (on floor 1) and below 18 on floor (3); item 3 (floor 3) is directly above item 4 (floor 2) and below 5 (floor 4). Floors 1 and 5 also have the required free space as a workspace and emergency area

respectively. Additionally, all six multi-floor equipment items (8, 9, 10, 13, 14, 15) spanned through the required number of floors based on their height.

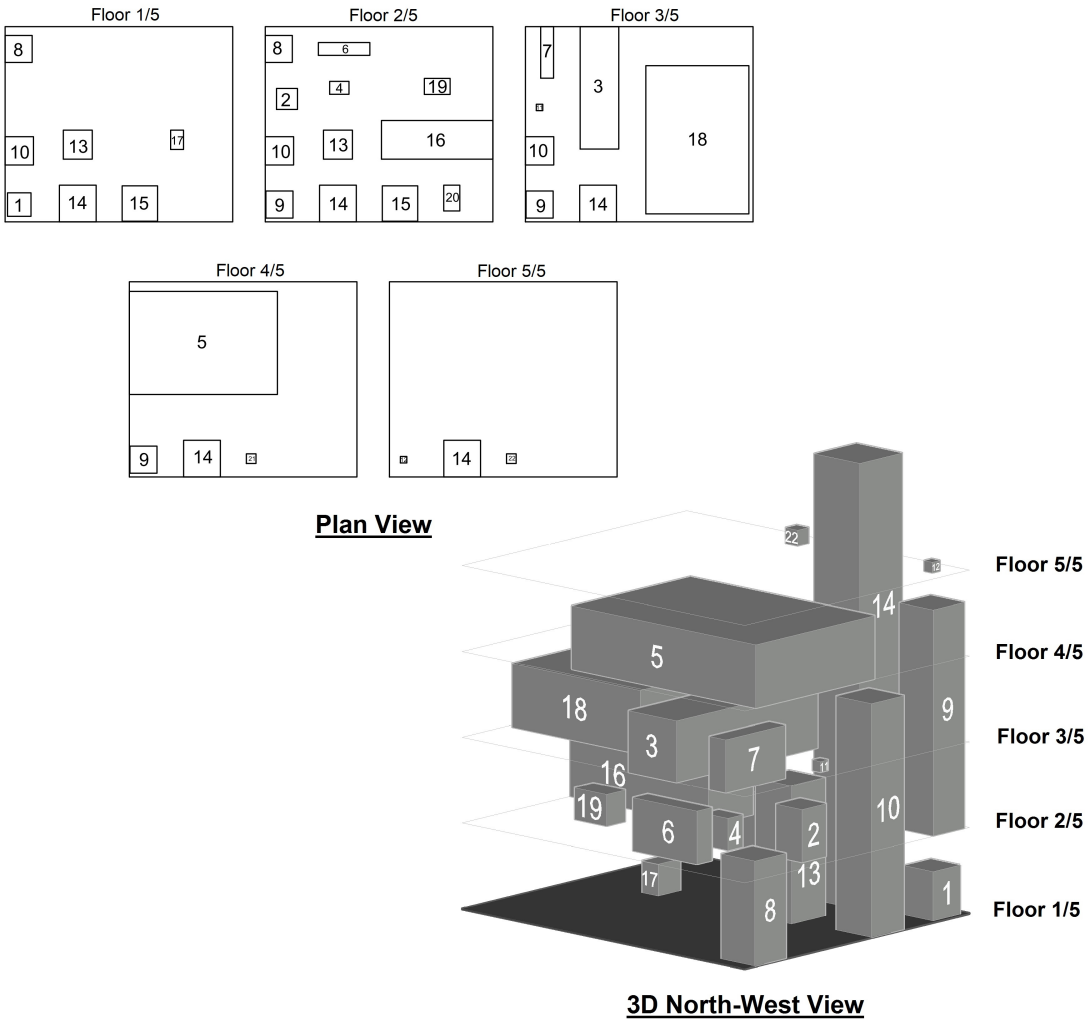

Fig. 3.10 Layout results of LNG plant

3.4.5 Crude oil & gas processing (COGP) plant

The final example is a crude oil & gas processing (COGP) plant (Fig. 3.11) consisting of 25 units adapted from Xu and Papageorgiou (2009) and extended for multi-floor considerations. A total of 9 units - all 8 Contactors (units 3, 4, 11, 12, 13, 20, 21 and 22) and the Separator

(1) - have heights greater than the floor height of 5m, and 7 floors are made available for layout.

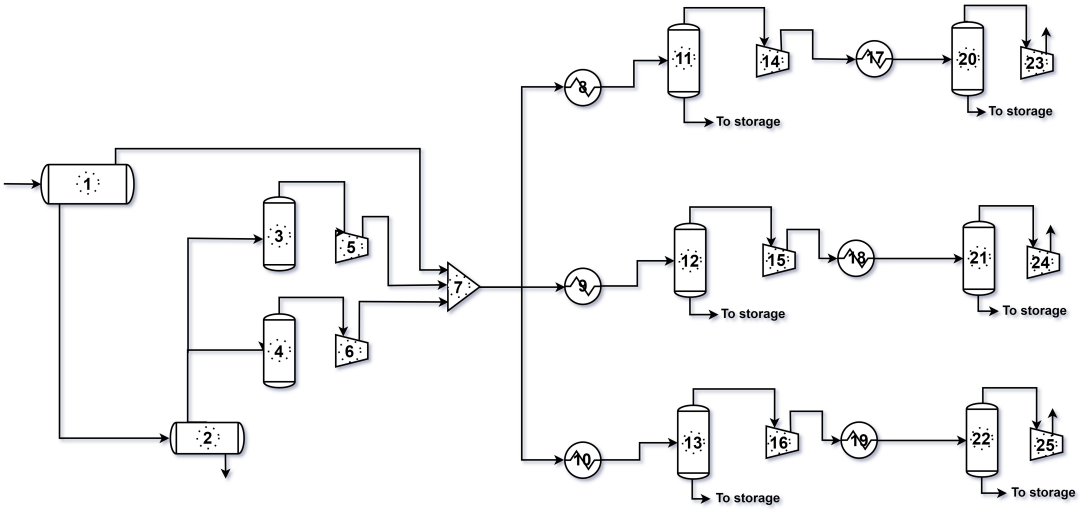

Fig. 3.11 Flow diagram of crude oil & gas processing plant (Ejeh et al. (2019b)) (See Table B.12 in Appendix B for a description of the equipment item labels)

Fig. 3.12 (and Figs. C.17 - C.20) show the layout results obtained. Across all models a floor area of 10m$\times$ 25m was obtained with all seven floors being assigned units. None of the proposed models solved to global optimality but each of them was able to obtain a solution with a relative gap less than 30%.

Table 3.5 Model statistics & computational performance for COGP Plant

	COGP plant (25 units)				
	A.1	A.2	A.3	A.4	B
Total cost (rmu)	290,975.4	290,965.1	297,173.9	295,672.4	291,306.9
CPU (s)	25.4%[1]	25.1%[1]	28.9%[1]	24.6%[1]	25.7%[1]
Number of discrete variables	943	943	943	943	1861
Number of continuous variables	1080	905	1080	914	1185
Number of equations	4486	4174	4136	4120	18407

[1] Relative gap quoted at CPU limit of 10,000s

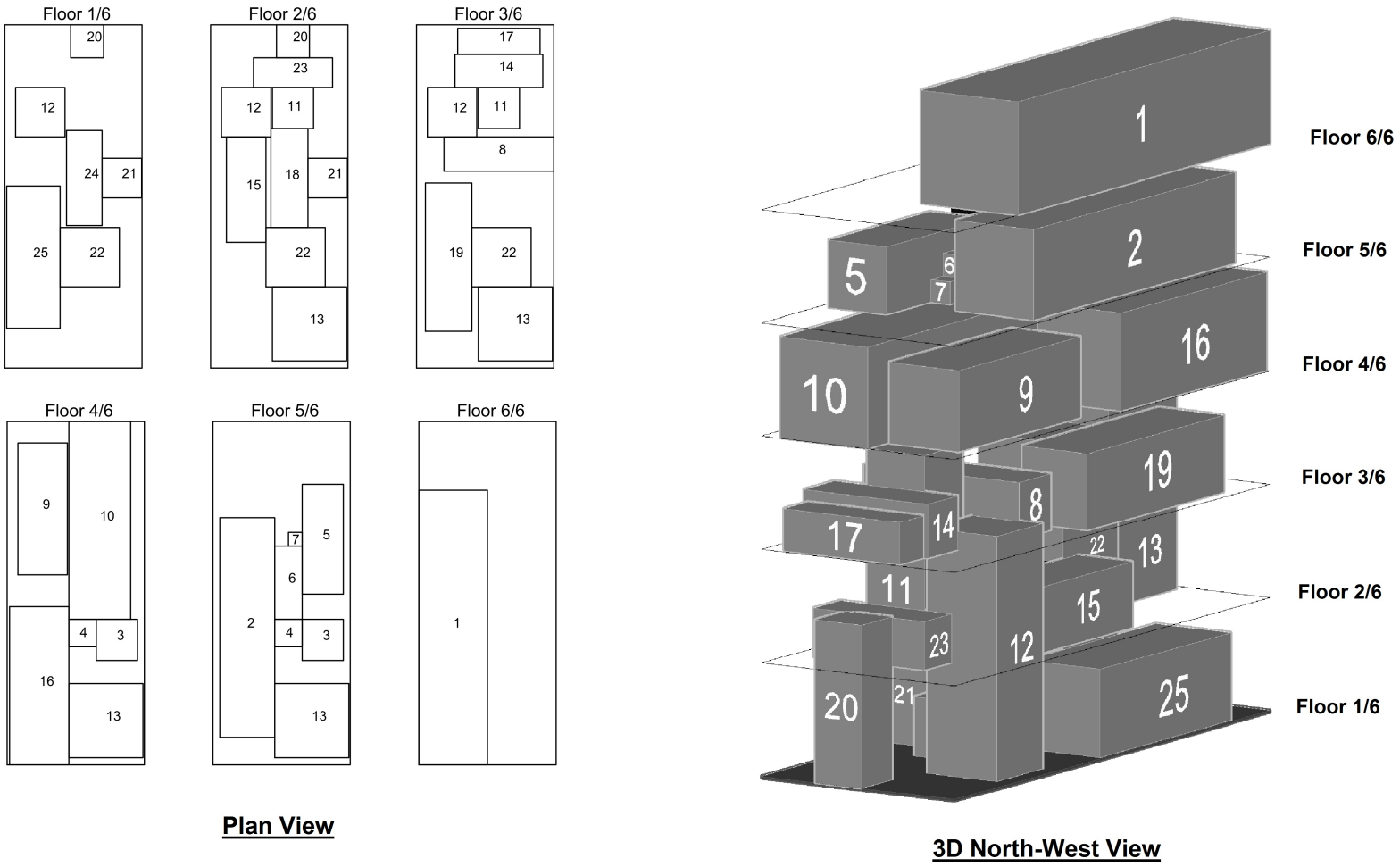

Fig. 3.12 Layout results of COGP plant

3.5 Model improvements

As observed from the case studies discussed, although the proposed models (specifically, models A.x) are capable of handling larger number of equipment items that previous recorded in literature, additional improvements are necessary to obtained good enough solutions for larger case studies (20+ items). It is also evident from the layout results shown (and in Appendix C) that there exists variations of the globally optimal solution for each problem. These solutions are basically layout reflections and/or rotations of equipment items, or having orientational changes to the plot geometry. These have a negative impact on the computational performance of the proposed models (Westerlund and Papageorgiou, 2004). In this section, symmetry breaking constraints are proposed to reduce such symmetric solution occurrence. Valid inequalities/integer cuts are also proposed for model improvement for the proposed models and their impact evaluated with the previously presented case studies.

3.5.1 Symmetry breaking constraints

Symmetry breaking constraints seek to prevent the occurrence of multiple equivalent/symmetry solutions in the search for the final layout solution. For the models proposed, the following constraints are introduced as extended from Westerlund and Papageorgiou (2004):

$$x_i + y_i - x_j - y_j \geq \delta \cdot N_{ij} \qquad \forall\,(i,j) = \underset{i \in MF, j \in MF}{\arg\max}\; C^c_{ij} \tag{3.54}$$

$$E1_{ij} = 0 \qquad \forall\,(i,j) = \underset{i \in MF, j \in MF}{\arg\max}\; C^c_{ij} \tag{3.55}$$

where $\delta = min\left(\frac{l_i}{2}, \frac{d_i}{2}\right) + min\left(\frac{l_j}{2}, \frac{d_j}{2}\right)$. Equations (3.54) and (3.55) fix the relative position of i to j. Item i will be located such that it is always to the right of j, above j, or both on the x-y plane; in effect, item i is locked to the North-east quadrant of j. The RHS of equation (3.54) ensures that should the global optimal solution require item i to be directly above j, this is not excluded. Units i and j are chosen as the two multi-floor units having the highest

connection costs as they logically seem to have the most effect on the total layout cost and configuration.

3.5.2 Integer cuts

The following valid inequalities are applied to the model to reduce the solution space:

$$\frac{E1_{in}+E2_{in}}{2} \geq E1_{ij}+E2_{ij}+E1_{jn}+E2_{jn}-3 \qquad \forall\, i<j<n \tag{3.56}$$

$$N_{ij} \geq E1_{ij} \quad \forall\, i,j>i \tag{3.57}$$

$$N_{ij} \geq E2_{ij} \quad \forall\, i,j>i \tag{3.58}$$

Given an equipment item trio i,j,n, when item i is strictly below j, and j is strictly below n, equation (3.56) prevents the non-overlapping constraints in equations (3.13) - (3.16) from considering the impractical configuration where n is below i. This is achieved as when the RHS of equation (3.56) is equal to 1 (corresponding to i being strictly below j and j strictly below n), the LHS is forced to 1 (corresponding to i being strictly below n). Equations (3.57) and (3.58), force the non-overlapping binary variables $E1_{ij}$ and $E2_{ij}$ to zero if two items i and j are on different floors.

The inclusion of equations (3.54) - (3.58) to models A.x and B constitutes models A.x_IC and B_IC respectively, and do not introduce any additional variables.

3.5.3 Case studies revisited

Each of the previous case studies were re-solved using models A.x_IC and B_IC. Table 3.6 gives a summary of the computational performance of each model with and without the symmetry breaking constraints and integer cuts.

Table 3.6 Comparison of the computational performance of models with and without improvement constraints

		Layout model				
		A.1	**A.2**	**A.3**	**A.4**	**B**
		EO plant - 7 units				
Without IC	TC	66,262.0				
	CPU (s)	1.3	1.2	1.6	1.4	2.0
With IC	TC	66,262.0				
	CPU (s)	0.6	0.6	0.8	0.9	1.5
		Urea plant - 8 units				
Without IC	TC	117,431.0				
	CPU (s)	1.5	1.3	1.5	1.5	2.8
With IC	TC	117,431.0				
	CPU (s)	0.4	0.6	0.6	0.5	0.6
		CDU plant - 17 units				
Without IC	TC	603,886.5				
	CPU (s)	0.4%[1]	2142.4	2078.4	956.6	5.5%[1]
With IC	TC	603,886.5				
	CPU (s)	1771.2	187.7	502.5	166.5	3604.1
		LNG plant - 22 units				
Without IC	TC	1,467,009.7	1,466,654.2			1,467,009.7
	CPU (s)	2.3%[1]	3.1%[1]	2.4%[1]	3.0%[1]	3.7%[1]
With IC	TC	1,466,654.2				1,467,009.7
	CPU (s)	1.6%[1]	1.0%[1]	1.4%[1]	1.5%[1]	2.1%[1]
		COGP plant - 25 units				
Without IC	TC	290,975.4	290,965.1	297,173.9	295,672.4	291,306.9
	CPU (s)	25.4%[1]	25.1%[1]	28.9%[1]	24.6%[1]	25.7%[1]
With IC	TC	296,773.0	295,909.6	303,545.0	259,754.5	296,884.3
	CPU (s)	26.1%[1]	26.6%[1]	28.8%[1]	15.7%[1]	26.1%[1]

[1] Relative gap quoted at CPU limit of 10,000s

TC - Total Cost in rmu

In most of the examples, computational improvements were observed for all the proposed models. The EO and UR plant problems were solved well below 2s to global optimality. The 17 unit CDU plant was also solved by all models in at most an hour, with model A.4_IC obtaining the globally optimal solution in less than 3 mins. The globally optimal solution was obtained by models A.x_IC at solution termination with a smaller relative gap, and model A.4_IC an optimal solution with a much smaller relative gap (16%).

The inclusion of the symmetry breaking constraints and integer cuts allowed for the solution of examples with up to 17 units by all the proposed models. In most of the examples, however, no particular model proved to be consistently more computationally efficient than the rest. models A.x_IC though showed superiority to B_IC with A.4_IC showing better efficiency amongst the larger examples.

3.6 Model A.4$^+$

Model A.4$^+$ builds on the same assumptions of the previous models with the added characteristic that equipment items are allowed to span well above the available floors. In the previous models A.1 - A.4, the available number of floors must never be less than the number of floors required by the tallest equipment item for a feasible solution. In model A.4$^+$, this restriction is removed as it is sometimes necessary to allow equipment items extend beyond the topmost available floor especially where maximum height restrictions on sites do not exist. In such situations, the decision maker may set the maximum number of floor he/she desires to construct (available floors, K), but equipment items can extend well above this floor level. This feature is achieved by reformulating the floor constraints in model A.4.

Floor constraints

The initial floor constraints in model A.4 are reformulated as follows. Every non-multi-floor equipment i available should be assigned to one floor:

$$\sum_k V_{ik} = 1 \qquad \forall\, i \notin MF \tag{3.59}$$

For tall/multi-floor equipment items ($i \in MF$), to ensure that they can extend well above the top-most available floor if required, equations (3.60) and (3.61) are introduced:

$$\sum_k V_{ik} = M_i - \omega_i \qquad \forall\, i \in MF \tag{3.60}$$

$$\omega_i \geq \sum_k k \cdot S^s_{ik} + M_i - \mid K \mid -1 \qquad \forall\, i \in MF \tag{3.61}$$

ω_i represents the number of floors by which a multi-floor equipment item i extends over the top-most available floor. This allows the potential/available number of floors for the layout design to be less than the maximum number of floors required by any equipment item if necessary.

All units must also start on only one floor:

$$\sum_k S^s_{ik} = 1 \qquad \forall\, i \tag{3.62}$$

Model A.4$^+$ thus consists of objective function (3.31) subject to constraints (3.2) - (3.7), (3.13) - (3.30), (3.36) and (3.59) - (3.62).

Model A.4$^+$ layout results

The benefits of this reformulation is shown by revisiting some of the case studies considered. With the previous models, the total number of floors selected in the final layout may be less than or equal to the number of available floors. Floors were only selected for construction if an item started on it and not just passed through it. However, the number of floors a multi-floor item spans through must always be amongst those available. This is demonstrated with a sensitivity analysis on the number of available floors for the UR plant example.

Table 3.7 shows the results of the sensitivity analysis on the globally optimal solution obtained by models A.1 - A.4, to the number of floors made available for layout for the UR plant. The tallest unit (2) requires a minimum number of 4 floors based on its height, as such, feasible solutions could not be obtained for models A.1 - A.4. Model A.4$^+$ on the other hand was able to provide single floor layout solutions were required. This feature allows for a

more informed decision making process were compromises can be ascertained between the total number of floors and the total layout cost. Layout solutions can also be obtained were there are restrictions on the maximum heights of all constructed floors due to government policies, plant site load balancing constraints, or were the number of floors are fixed in a site e.g. in offshore platforms.

Table 3.7 Sensitivity analysis on the number of available floors for UR plant

Available	**Model A.4$^+$**		**Models A.1 - A.4**	
floors, $\lvert K \rvert$	NF	Total Cost (rmu)	NF	Total Cost (rmu)
1	1	260,942.2	-	-[1]
2	2	167,298.8	-	-[1]
3	3	149,498.0	-	-[1]
4	4	117,431.0	4	117,431.0

[1]Infeasible model

Additional benefits of the features in model A.4$^+$ are also demonstrated with the CDU plant example. Table 3.8 shows the results of the sensitivity analysis. A similar situation is observed for models A.1 - A.4 when the number of floors available are less than that required by the tallest item (item 15; 5 floors). Additionally, reduced total layout costs are also observed for model A.4$^+$ when 5,6 and 7 floors were made available. This is because, allowing equipment items to extend well above the topmost available floor gives greater flexibility to the position of multi-floor items which can lead to lower layout costs. This is observed in Fig. 3.13 which shows the layout plot of model A.4$^+$ when the number of available floors is set at 7 (same as in the previous consideration of models A.1 - B). Item 6 particular extends above floor 7 reaching the elevation of floor 8. This, and the associated re-arrangement of all other items, is the prime reason for the reduction in layout costs.

Table 3.8 Sensitivity analysis on the number of available floors for CDU plant

Available	**Model A.4^{+}**		**Models A.1 - A.4**	
floors, $\mid K \mid$	*NF*	Total Cost (rmu)	*NF*	Total Cost (rmu)
1	1	1,112,094.7	-	-[1]
2	2	855,465.8	-	-[1]
3	3	697,672.4	-	-[1]
4	4	624,452.8	-	-[1]
5	5	603,886.5	5	614,820.0
6	5	603,886.5	5	614,820.0
7	7	592,322.2	5	603,886.5

[1]Infeasible model

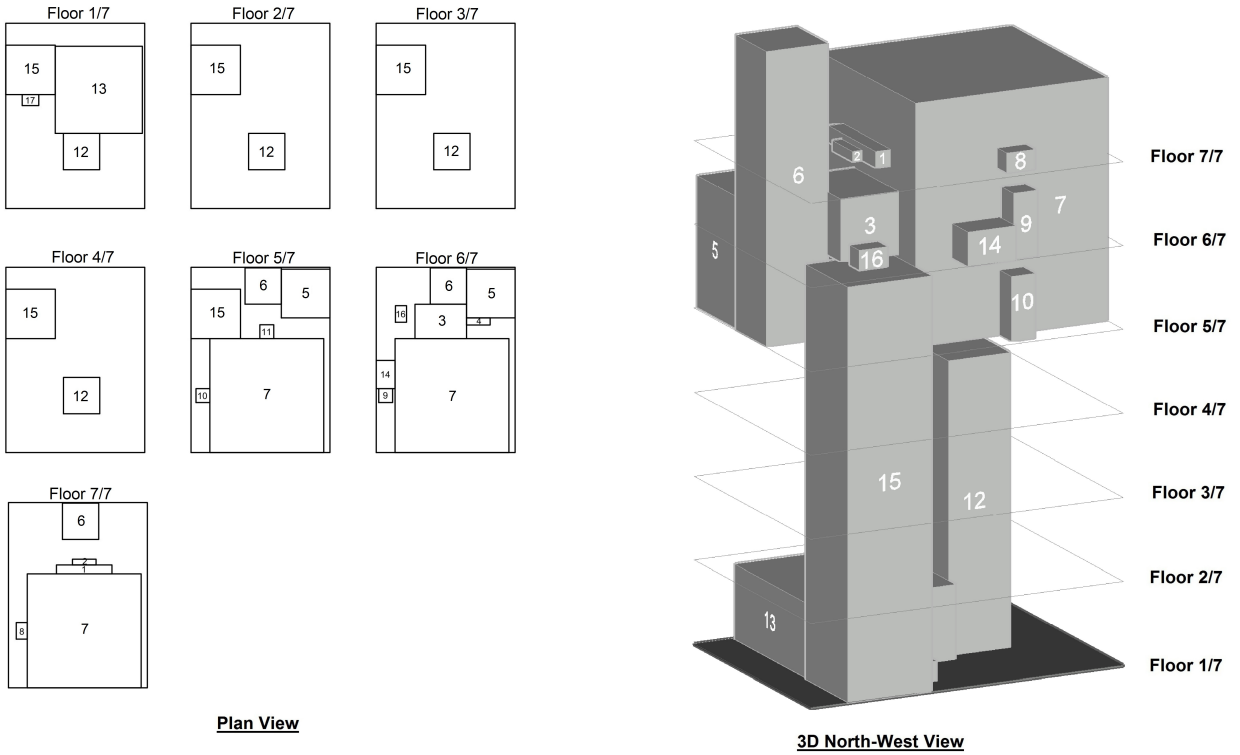

Fig. 3.13 Layout results of CDU plant; model A.4^{+}

3.7 Concluding remarks

In this chapter, novel mixed integer linear programming (MILP) models were proposed to address the multi-floor process plant layout problem. Each of the five models proposed successfully considered important features for the layout of chemical process plants in a continuous domain. These features included unit interconnectivity by pipes, vertical and horizontal pumping, fixed and area-dependent construction whilst accounting for tall/multi-floor equipment items with unique connection points obtained from equipment design calculations. Symmetry breaking constraints and integer cuts were also proposed to improve model performance.

Each of the proposed models were broadly grouped into two: models A and B, primarily differing in how tall/multi-floor equipment items were described. Models A described tall items as single continuous units spanning through consecutive floors, from which four models were presented - A.1, A.2, A.3 and A.4. Model B on the other hand described tall items as a set of single-floor pseudo units assigned to the same positions on consecutive floors. The proposed models' capabilities and performance were demonstrated using industry relevant case studies of 7 - 25 equipment items each having problem-specific considerations.

The layout results showed that each of the proposed models successfully handled all the required layout considerations and unique case study features. Tall items occupied consecutive floors proportional to their height with the optimal starting floors of each item simultaneously decided. The optimal number of floors was also determined from those made available for layout by the proposed models, with floors selected for construction only if an item was assigned to it. This allowed for construction costs savings as well as a provision for tall items to extended well above the topmost selected floor. The impact of considering unique connection points about the height of an equipment item was also highlighted in terms of the final layout costs. Unique characteristics of some of the proposed models were also highlighted with model A.4^{+}, an extension of model A.4, able to allow for tall items to extended well above the top most available floor, and model B being able to model items with uneven cross-sectional area.

Although no consistent trend was observed in a specific model's relative performance across case studies, all proposed models were able to obtain a globally optimal solution for a larger problem size (17 units) than previous recorded in literature using the same solution approach. Inclusion of the proposed symmetry breaking constraints and integer cuts showed considerable performance improvement in all models in most case studies considered. Models A showed superior performance to B obviously due to the smaller amount of decision variables required for each case study, with model A.4_IC showing a better performance for case studies with a greater number of items.

In the next chapter, the current models are extended to incorporate the feature of having pre-defined production sections in the process plant layout design.

CHAPTER 4

MULTI-FLOOR PROCESS PLANT LAYOUT WITH PRODUCTION SECTIONS

In the previous chapter, more efficient MILP models were proposed to address the multi-floor process plant layout problem considering a range of features. In this chapter, new constraints are introduced in the previously proposed models to address the feature of pre-defined production sections. Two case studies from the previous chapter are revisited to show model performance and changes in layout results owing to the new feature.

4.1 Introduction

As noted by Mecklenburgh (1985) and as is common practice in the layout of chemical process plant, equipment items having the same or similar functions should be placed within a common area - referred to as a production section/module. With process plant sections/segregations, different items in the chemical process plant are grouped in a common area and placed adjacent to each other (Fig. 4.1). Such groupings aid in safety and loss prevention, housekeeping, workforce management and efficient construction and maintenance of equipment items (Mecklenburgh, 1985). As such, the proposed models in this chapter will simultaneously obtain the site and plot layout of a multi-floor chemical process plant. Aside from unit connectivities and pumping considerations previously considered in literature,

construction costs and the modelling of tall equipment items with unique connection points are included. Each of models A.x_IC and B_IC are extended with considerations to prevent overlapping among sections/modules and allow for placement of equipment items in the module to which they are pre-assigned..

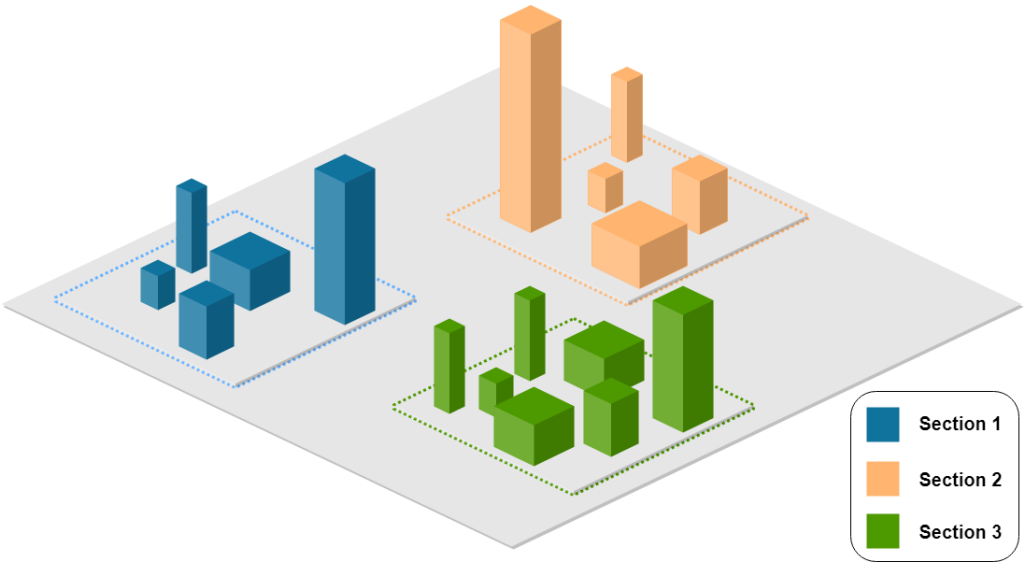

Fig. 4.1 Production section illustration

In the next section (4.2), a modified problem description is given. Section 4.3 highlights the mathematical formulation, and some case studies from Chapter 3 are revisited in Section 4.4 comparing model performance and layout results. A summary of the chapter is given in Section 4.5.

4.2 Problem description

In addition to the assumptions made for the multi-floor process plant layout problem in Chapter 3, it also assumed that:

- the geometries of all production sections are rectangles;
- distances between sections are rectilinear from their geometrical centres in the x-y plane;
- each equipment must belong to only one section, and such section is predefined.

- each of the available sections starts from the ground floor upwards, having an optimal number of floors less than or equal to the total number of available floors.
- the position coordinates of production sections are calculated with respect to the origin of the base land area, and the equipment items position coordinates with respect to the origin of the production section to which they belong.
- both equipment and production sections can be rotated 90° in the x-y plane as deemed optimal, but must start from the base of the floor it has been assigned.

The problem description is given as follows.

Given:

- a set of equipment items and their dimensions (length, breadth and height);
- a set of sections with equipment allocation;
- a set of potential floors;
- connectivity network amongst process units;
- cost data (connection, pumping, land, and construction);
- floor height;
- space and unit allocation limitations;
- minimum safety distances between equipment and production sections;

to determine:

- total number of required floors for each section for the layout;
- base land area occupied by all sections;
- area of floors for each section as well as the base land area;
- equipment item floor location;
- site and plot layout;

so as to: minimise the total plant layout cost associated with connection, pumping, land purchase and floor construction within and across production sections.

4.3 Mathematical formulation

Nomenclature

The symbols used are redefined as follows:

Indices

i, j	equipment item in models A.x
i', j'	equipment item in model B
t, u, u'	sections/production modules
k, k'	floor number
p	pseudo units
s	rectangular area sizes

Sets

I	set of equipment item for models A.1 - A.3
I^{δ}	pair of multi-floor equipment items i, j with highest connection costs; $(i, j) = \underset{i,j \in MF}{\arg\max}\, C^{c}_{ij}$
I'	set of equipment item for model B; $I' = (I \setminus MF) \cup \bigcup_{i \in MF} P_i$
I_t	set of equipment item i in section t
I'_t	set of equipment item i' in section t
MF	set of multi-floor equipment
P_i	sets of pseudo units for multi-floor equipment i
P^1	set of pseudo units of each multi-floor equipment item i assigned to the lowest floor

Parameters

BM, BM'	large numbers

C^c_{ij}	connection costs between items i and j
C^h_{ij}	horizontal pumping costs between items i and j
C^v_{ij}	vertical pumping costs between items i and j
De^{min}_{ij}	minimum safety distance between items i and j
Ds^{min}_{tu}	minimum safety distance between sections t and u
f_{ij}	1 if flow direction between equipment items i and j is positive; 0, otherwise
$FC1$	fixed floor construction cost
$FC2$	area-dependent floor construction cost
LC	land cost
M_i	number of floors required by equipment item i
$\overline{X}_s, \overline{Y}_s$	x-y dimensions of pre-defined rectangular area sizes s

Integer variables

NF^{max}	maximum number of floors required across all sections
NF'_t	number of floors required by section t

Binary variables

$E1_{ij}$, $E2_{ij}$	non-overlapping binary, a set of values of which prevents equipment overlap in one direction in the x-y plane
N_{ij}	1 if items i and j are assigned to the same floor; 0, otherwise
$S1_{tu}$, $S2_{tu}$	non-overlapping binary, a set of values which prevents production section overlap in one direction in the x-y plane
V_{ik}	1 if item i is assigned to floor k
Q_s	1 if rectangular area s is selected for the layout; 0, otherwise
Q'_{st}	1 if rectangular area s is selected for section t in the layout; 0 otherwise
W'_{kt}	1 if floor k in section t is occupied; 0, otherwise

Continuous variables

ω_i	number of floors by which a multi-floor item $i \in MF$ extends over the topmost floor
A_{ij}	distance in the y plane between items i and j, if i is above j
AR_s	predefined rectangular floor area s
AR'_{st}	predefined rectangular floor area s for section t
B_{ij}	distance in the y plane between items i and j, if i is below j
d_i	breadth of item i
D_{ij}	distance in the z plane between items i and j, if i is lower than j
dt_t	breadth of production section t
FA	base land area
FA'_t	area of section t
$FA2'_{kt}$	area of floor k in section t
l_i	length of item i
L_{ij}	distance in the x plane between items i and j, if i is to the left of j
lt_t	length of production section t
NQ_s	linearisation variable expressing the product of NF and Q_s
NQ'_{st}	linearisation variable expressing the product of NF'_t and Q'_{st}
R_{ij}	distance in the x plane between items i and j, if i is to the right of j
TD_{ij}	total rectilinear distance between items i and j
U_{ij}	distance in the z plane between items i and j, if i is higher than j
x_i, y_i	x,y coordinates of the geometrical centre of item i relative to the origin of production section it belongs
xt_t, yt_t	absolute coordinates of the geometrical centre of production section t on base land area
X^{max}, Y^{max}	dimensions of base land area

4.3.1 Models A.x

The following changes to models A.x are made to incorporate the production section features. Additional constraints are included and in some cases previously proposed ones in Chapter 3 are modified.

Non-overlapping constraints

In order to prevent an overlap of production section within each floor k, the following additional constraints are introduced:

$$xt_t - xt_u + BM(S1_{tu} + S2_{tu}) \geq \frac{lt_t + lt_u}{2} + Ds_{tu}^{min} \qquad \forall t,\ u > t \qquad (4.1)$$

$$xt_u - xt_t + BM(1 - S1_{tu} + S2_{tu}) \geq \frac{lt_t + lt_u}{2} + Ds_{tu}^{min} \qquad \forall t,\ u > t \qquad (4.2)$$

$$yt_t - yt_u + BM(1 + S1_{tu} - S2_{tu}) \geq \frac{dt_t + dt_u}{2} + Ds_{tu}^{min} \qquad \forall t,\ u > t \qquad (4.3)$$

$$yt_u - yt_t + BM(2 - S1_{tu} - S2_{tu}) \geq \frac{dt_t + dt_u}{2} + Ds_{tu}^{min} \qquad \forall t,\ u > t \qquad (4.4)$$

where $S1_{tu}$ and $S2_{tu}$ are binary variables with pairs of values determining which of equations (4.1) - (4.4) is active. For $(S1_{tu}, S2_{tu}) = (0,0)$, equation (4.1) becomes $xt_t - xt_u \geq \frac{lt_t+lt_u}{2} + Ds_{tu}^{min}$ forcing section t to the right hand side of u with at least Ds_{tu}^{min} spacing. Ds_{tu}^{min} represents the minimum distance between sections t and u, and must be greater than or equal to the minimum safety distance (De_{ij}^{min}) between equipment $i \in I_t$ and $j \in I_u$. Other pairs of values for the two binary variables activate one of equations (4.2) - (4.4) to prevent overlap in one direction.

The non-overlapping constraints for equipment item pairs only needs to written for items in the same section. Hence equations (3.13) - (3.16) are re-written as:

$$x_i - x_j + BM(1 - N_{ij} + E1_{ij} + E2_{ij}) \geq \frac{l_i + l_j}{2} + De_{ij}^{min} \qquad \forall\, i \in I_t, j \in I_t, j > i, t \qquad (4.5)$$

$$x_j - x_i + BM(2 - N_{ij} - E1_{ij} + E2_{ij}) \geq \frac{l_i + l_j}{2} + De_{ij}^{min} \qquad \forall\, i \in I_t, j \in I_t, j > i, t \qquad (4.6)$$

$$y_i - y_j + BM(2 - N_{ij} + E1_{ij} - E2_{ij}) \geq \frac{d_i + d_j}{2} + De_{ij}^{min} \qquad \forall\, i \in I_t, j \in I_t, j > i, t \qquad (4.7)$$

$$y_j - y_i + BM(3 - N_{ij} - E1_{ij} - E2_{ij}) \geq \frac{d_i + d_j}{2} + De_{ij}^{min} \qquad \forall\, i \in I_t, j \in I_t, j > i, t \tag{4.8}$$

Additional integer cuts

In addition to the integer cuts proposed for equipment items in Section 3.5.2, a similar constraint is included for production sections. As with the items, equation 4.9 prevents the non-overlapping constraints in equations (4.1) - (4.4) from considering the impossible configuration where section u' is below section t, when t is strictly below u, and u is strictly below u'.

$$\frac{S1_{tu'} + S2_{tu'}}{2} \geq S1_{tu} + S2_{tu} + S1_{uu'} + S2_{uu'} - 3 \quad \forall\, t < u < u' \tag{4.9}$$

Layout design constraints

Layout design constraints are included to ensure that sections are placed within the boundaries of the base land area. Equations (4.10) and (4.11) force any equipment i to be placed within the boundaries of section t to which it belongs:

$$lt_t \geq x_i + \frac{l_i}{2} \qquad \forall t,\ i \in I_t \tag{4.10}$$

$$dt_t \geq y_i + \frac{d_i}{2} \qquad \forall t,\ i \in I_t \tag{4.11}$$

The mid-point coordinates of each section is defined by equations (4.12) and (4.13):

$$xt_t \geq \frac{lt_t}{2} \qquad \forall t \tag{4.12}$$

$$yt_t \geq \frac{dt_t}{2} \qquad \forall t \tag{4.13}$$

and each section is located within the boundaries of the base land area:

$$xt_t + \frac{lt_t}{2} \leq X^{max} \qquad \forall t \tag{4.14}$$

$$yt_t + \frac{dt_t}{2} \leq Y^{max} \qquad \forall t \tag{4.15}$$

Distance constraints

The horizontal distances in the x- and y- directions between units i and j connected to each other (equations (4.16) and (4.17)) are rewritten for situations where the units belong to different production sections. As such, the additional distance between sections has to be included. This is described by equations (4.16) and (4.17):

$$R_{ij} - L_{ij} = (xt_t - \frac{lt_t}{2} + x_i) - (xt_u - \frac{lt_u}{2} + x_j) \quad \forall\, i,j : f_{ij} = 1; i \in I_t; j \in I_u \tag{4.16}$$

$$A_{ij} - B_{ij} = (yt_t - \frac{dt_t}{2} + y_i) - (yt_u - \frac{dt_u}{2} + y_j) \quad \forall\, i,j : f_{ij} = 1; i \in I_t; j \in I_u \tag{4.17}$$

For cases where units i and j belong to the same section ($u = t$), equations (4.16) and (4.17) reduce to equations (3.17) and (3.18).

Floor constraints

Equipment floor constraints from Section 3.3 (equations (3.2) - (3.5)) are modified to equations (4.18) - (4.23) as follows.

Equipment items on the same floor ($N_{ij} = 1$) are only identified if they belong to the same production sections, or if they are the two multi-floor items with the highest connection costs required for the symmetry breaking constraints (equations (3.54 and (3.55)):

$$N_{ij} \geq V_{ik} + V_{jk} - 1 \qquad \forall \left(i \in I_t, j \in I_t, j > i\right) \text{ or } (i,j) \in I^{\delta}; k,t \tag{4.18}$$

There is a possibility of having empty floors if a uniform number of floors is determined for all sections. In order to prevent this, it is necessary to determine the total number of floors required by each section:

$$S^s_{ik} \leq W'_{kt} \qquad \forall\, i \in I_t, k, t \tag{4.19}$$

$$W'_{kt} \leq W'_{k-1,t} \qquad \forall k > 1; t \tag{4.20}$$

Equation (4.19) ensures that for each section t, floor k will only exist if an equipment i belonging to that section starts on it. Empty intermediate floors are eliminated by equation (4.20), and the total number of floors per section is obtained by equations (4.21) and (4.22) - less than or equal to the available number of floors, but just the required number for any equipment that belongs to the section:

$$NF'_t \geq \sum_k W'_{kt} \qquad \forall\, t \tag{4.21}$$

$$NF'_t = \sum_s NQ'_{st} \qquad \forall\, t \tag{4.22}$$

The maximum number of floors, NF^{max}, across sections is calculated in order to determine the total fixed floor construction cost:

$$NF^{max} \geq NF'_t \qquad \forall\, t \tag{4.23}$$

The objective function is then written to account for production sections and area-dependent floor construction cost for floors that exist in each section:

$$\begin{aligned} min \sum_{i,j:f_{ij}=1} & \left(C^c_{ij} TD_{ij} + C^v_{ij} D_{ij} + C^h_{ij}(R_{ij} + L_{ij} + A_{ij} + B_{ij})\right) \\ & + FC1 \cdot NF^{max} + FC2 \sum_{s,t} lt_t \cdot dt_t \cdot NQ_{st} + LC \cdot FA \end{aligned} \tag{4.24}$$

This results in a non-linear objective function which is neither convex nor concave, because of the term $\sum_{s,t} lt_t \cdot dt_t \cdot NQ_{st}$. The objective function is linearised by introducing the following area constraint modifications.

Area constraints

A new term FA'_t representing the area of a section t is first introduced. The sum of the areas of all sections should be less than or equal to the total base land area.

$$FA \geq \sum_t FA'_t \tag{4.25}$$

The area of each section t is also selected from a predefined set of rectangular sizes:

$$FA'_t = \sum_s AR'_{st} \cdot Q'_{st} \qquad \forall\, t \tag{4.26}$$

where Q'_{st} is a binary variable allowing for a unique selection of predefined rectangular areas s for each section t. Such area is calculated from the minimum length and breadth required by each section:

$$lt_t \leq \sum_s \overline{X}_s \cdot Q'_{st} \qquad \forall\, t \tag{4.27}$$

$$dt_t \leq \sum_s \overline{Y}_s \cdot Q'_{st} \qquad \forall\, t \tag{4.28}$$

where $\overline{X}_s$ and $\overline{Y}_s$ are the dimensions of the pre-defined rectangular area sizes. The area of a floor k in section t should only have a non-zero value if it exists (i.e. a non-multi-floor equipment is assigned on or above it):

$$W'_{kt} \leq FA2'_{kt} \qquad \forall\, k,t \tag{4.29}$$

and the value of such area should be the maximum obtained amongst all floors k in section t:

$$FA'_t - BM'(1 - W'_{kt}) \leq FA2'_{kt} \qquad \forall\, k,t \tag{4.30}$$

To ensure only one area size is selected from the predefined set, the following equation is used:

$$\sum_s Q'_{st} = 1 \qquad \forall\, t \tag{4.31}$$

and the objective function becomes:

$$\begin{aligned} min \sum_{i,j:f_{ij}=1} & \left(C^c_{ij} TD_{ij} + C^v_{ij} D_{ij} + C^h_{ij}(R_{ij} + L_{ij} + A_{ij} + B_{ij})\right) \\ & + FC1 \cdot NF^{max} + FC2 \sum_{k,t} FA2'_{kt} + LC \cdot FA, \end{aligned} \tag{4.32}$$

subject to plant-wide constraints (4.1) - (4.4) and (4.10) - (4.17); section-wide constraints (3.1) - (3.2), (3.6) - (3.12), (3.19) - (3.20), (3.54) - (3.58), (4.5) - (4.8), (4.18) - (4.23) and (4.25) - (4.31). This constitutes model A.1_PS, an extension of model A.1_IC.

In model A.2_PS, equations (3.9), (3.11) and (3.12) are replaced with equation (3.32);

In model A.3_PS, equations (3.8), (3.9) and (3.12) in model A.1_PS are replaced with (3.33);

In model A.4_PS, equations (3.8) - (3.12) in model A.1_PS are replaced with (3.34) - (3.36).

4.3.2 Model B

In model B, the following changes are made. Equations (3.38) - (3.40) are modified as follows to account for only unit pairs in the same production section:

$$N_{i'j'} \geq V_{i'k} + V_{j'k} - 1 \qquad \forall \left(i' \in I_t, j' \in I_t, j' > i'\right) \text{ or } (i', j') \in I^{\delta}; k, t \tag{4.33}$$

$$N_{i'j'} \leq 1 - V_{i'k} + V_{j'k} \qquad \forall \left(i' \in I_t, j' \in I_t, j' > i'\right) \text{ or } (i', j') \in I^{\delta}; k, t \tag{4.34}$$

$$N_{i'j'} \leq 1 + V_{i'k} - V_{j'k} \qquad \forall \left(i' \in I_t, j' \in I_t, j' > i'\right) \text{ or } (i', j') \in I^{\delta}; k, t \tag{4.35}$$

Equation 4.36 replaces (3.41) and ensures floors only exist in a section if an item is assigned to it, with the exception of the bottom-most pseudo-unit items of each multi-floor unit.

$$V_{i'k} \leq W'_{kt} \qquad \forall\, i' \in I'_t \setminus P^1, k, t \tag{4.36}$$

The objective function becomes:

$$\begin{aligned} min \sum_{i',j':f_{i'j'}=1} \left(C^c_{i'j'} TD_{i'j'} + C^v_{i'j'} D_{i'j'} + C^h_{i'j'} (R_{i'j'} + L_{i'j'} + A_{i'j'} + B_{i'j'})\right) \\ + FC1 \cdot NF^{max} + FC2 \cdot \sum_{k,t} FA2'_{kt} + LC \cdot FA \end{aligned} \tag{4.37}$$

subject to plant-wide constraints (4.1) - (4.4) and (4.10) - (4.17); section-wide constraints (3.6), (3.7), (3.20), (4.4) - (4.7), (4.19), (4.21) - (4.23), (4.25) - (4.31) $\forall\, i', j' \in I'$; (3.37) - (3.40), (3.42) - (3.46), (4.33) - (4.36).

4.4 Case studies

Two case studies are investigated - the CDU plant and LNG liquefaction plant - introducing production section considerations. The equipment dimensions, connectivity and costs data are given in Appendix B. Each run was solved as previously done - to global optimality or a maximum time of 10,000s - retaining the predefined set of rectangular areas. Layout result plots of model A.1_PS are presented below, and the plots of the other models are available in Section C.2 (Appendix C).

4.4.1 CDU plant with production sections

For the CDU plant, two production section scenarios were considered. The first allocated equipment items to sections based on collective functions (*subsequently referred to as "Function based"*). These functions/categories are: crude oil preheating, crude oil heating, atmospheric distillation, atmospheric-bottoms heating, vacuum distillation, and debutanisation.

The second scenario grouped items based on common properties (*referred to as "Unit based"*): crude oil preprocessing, separation equipment and fired heaters - giving a total of three sections. Table 4.1 shows the production section allocation for each equipment. Data on the equipment dimensions, connectivity and costs are available in Section B.3.

Table 4.1 Production section allocation for items in CDU plant

Unit	Description	Production Sections	
		Unit based	Function based
1	Crude Preheater 1	1	1
2	Crude Preheater 2	1	1
3	Desalter	2	1
4	Preflash Heater	1	1
5	Preflash Drum	2	1
6	Fired Heater CDU	3	2
7	Crude Distillation Tower	2	3
8	Naptha Condenser	2	3
9	Kerosine SS	2	3
10	Diesel SS	2	3
11	AGO SS	2	3
12	Fired Heater VDU	3	4
13	Vacuum Distillation Tower	2	5
14	Kerosine Reboiler	2	3
15	Debutaniser	2	6
16	Stabilised Naptha Condenser	2	6
17	Debutaniser reboiler	2	6

Function based sectioning

The model statistics for the function-based sections are shown in Table 4.2. An expected 26.8% increase in the total cost from 603,886.5 (Section 3.4.3) to 765,740 rmu was realised owing to the additional space requirements of production sections, but with a lower CPU across all models. The models simultaneously handled the optimal layout within each section (plot layout) and amongst sections (site layout).

Fig. 4.2 shows a plan of the layout for all sections. All equipment items were placed in their appropriate production section. All sections are located in Floor 1, but certain floors in some sections (e.g. Section 5 in floors 2-5, Section 3 in floor 5, e.t.c.) were not constructed, as process units in such floors are non-existent. This saves cost in construction, as although the total land area boundary is depicted in the layout of each floor in the figures, floors on sections only need to be constructed if they are required. The choice could also be made for a full construction in all floors to provide additional space that can be allocated to other non-processing units within the process plant, or a workspace area.

A total of 5 floors was selected from an available 7, compared to 4 floors in the case where sections were not considered. A compensation provided was that the total connection distance between all process units was reduced from about 234m (in the case with no sections) to 217m. This translates to a cheaper operating cost in the long run, particularly for pumping, and an increased material transport efficiency amongst units. The availability of sections also presents added advantages in plant operation, maintenance, control and safety. The optimal floor areas obtained for each of sections 1 through 5 measured 9.7m$\times$ 8.9m, 3.9m$\times$ 3.9m, 12.3m$\times$ 14.3m, 3.9m$\times$ 3.9m, 9.4m$\times$ 9.4m and 6.5m$\times$ 5.3m respectively, with a base land area of 15m$\times$ 20m.

All models obtained the globally optimal solution in a much shorter time (less than 70s) when compared to the case without production sections (less than 1hr; Table 3.6) as a reduced number of integer decision variables are required, in addition to the integer cut for the non-overlapping production section binary variables (equation 4.9). Model A.4_PS proved to be the most computational efficient of all the models.

Table 4.2 Model statistics & computational performance for CDU Plant - Function based sectioning

	CDU Plant - Function based sectioning (17 units, 6 sections)				
	A.1_PS	A.2_PS	A.3_PS	A.4_PS	B_PS
Total cost (rmu)			765,742.7		
CPU (s)	42.5	33.0	67.9	17.8	44.8
Number of discrete variables	1485	1485	1485	1485	2192
Number of continuous variables	1586	1467	1586	1472	1699
Number of equations	1672	1452	1434	1422	3864

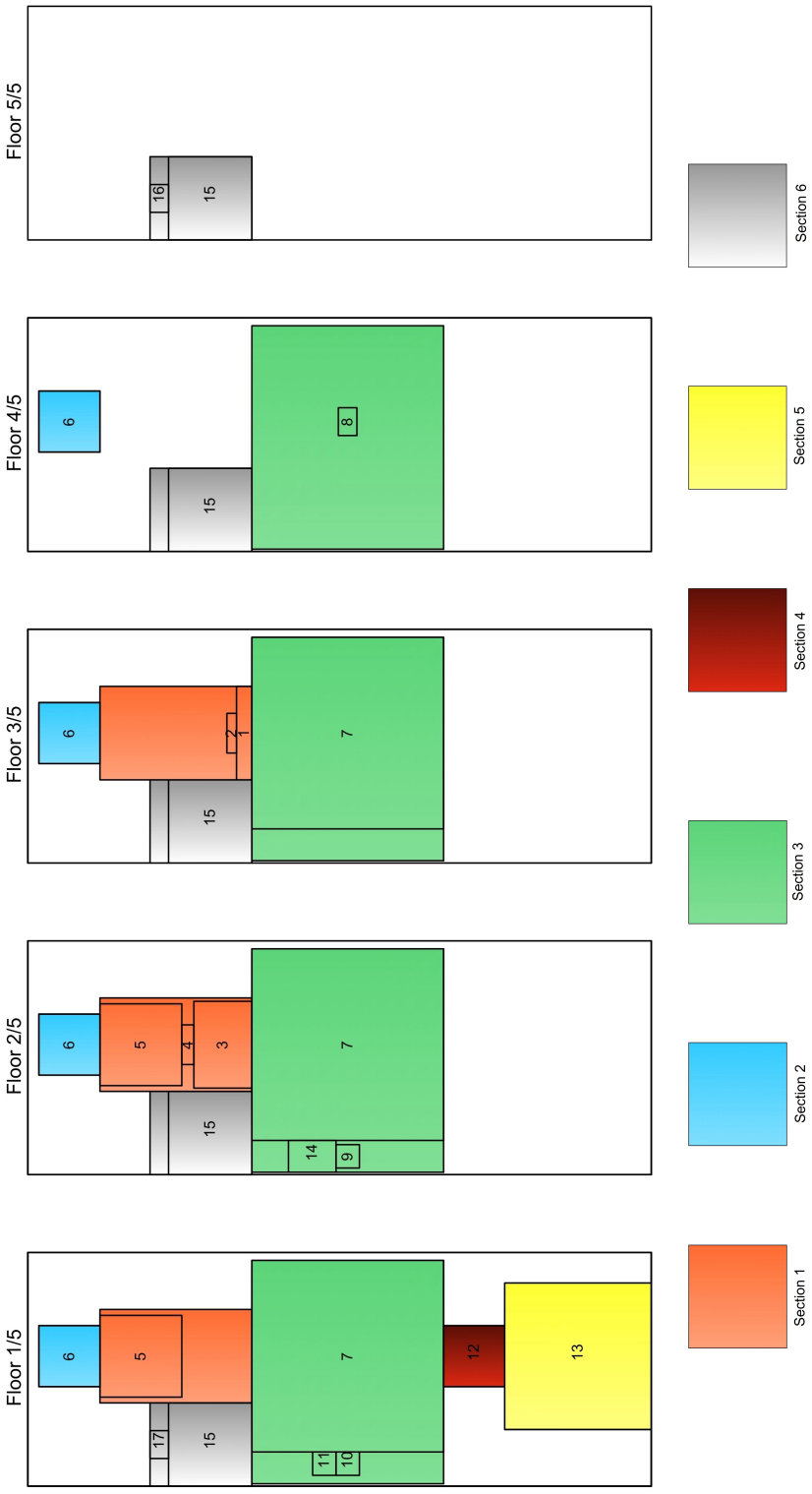

Fig. 4.2 CDU plant - Function based sectioning

Unit based sectioning

The optimal layout for the unit based sections for the CDU plant is shown in Fig. 4.3, and the model performance in Table 4.3. All models obtained the globally optimal solution in relatively shorter times as compared to the function based sectioning case, with model A.4_PS being the most computationally efficient. A smaller CPU usage was realized for models A as a smaller amount of decision variables were required.

A total cost of 740,430 rmu was obtained - 13.4% more than the case without sections, but less than the function based sections earlier calculated. As only 3 sections are required, space initially available in additional sections of the function-based type are allocated to other process units which reduces cost. The total connection length amongst all process units is higher (247m) translating to a higher pumping cost and reduced material transport efficiency in the long run. Having no other consideration but for a layout with a lower initial capital cost, the unit based sectioning is recommended; but for long term operational cost benefits, the function based sectioning should be adopted.

Table 4.3 Model statistics & computational performance for CDU Plant - Unit based sectioning

	CDU Plant - Unit based sectioning (17 units, 3 sections)				
	A.1_PS	A.2_PS	A.3_PS	A.4_PS	B_PS
Total cost (rmu)	684,828.7				
CPU (s)	34.2	29.2	48.8	11.0	85.8
Number of discrete variables	1005	1005	1005	1005	1712
Number of continuous variables	1118	999	1118	1004	1231
Number of equations	2143	1923	1905	1893	7698

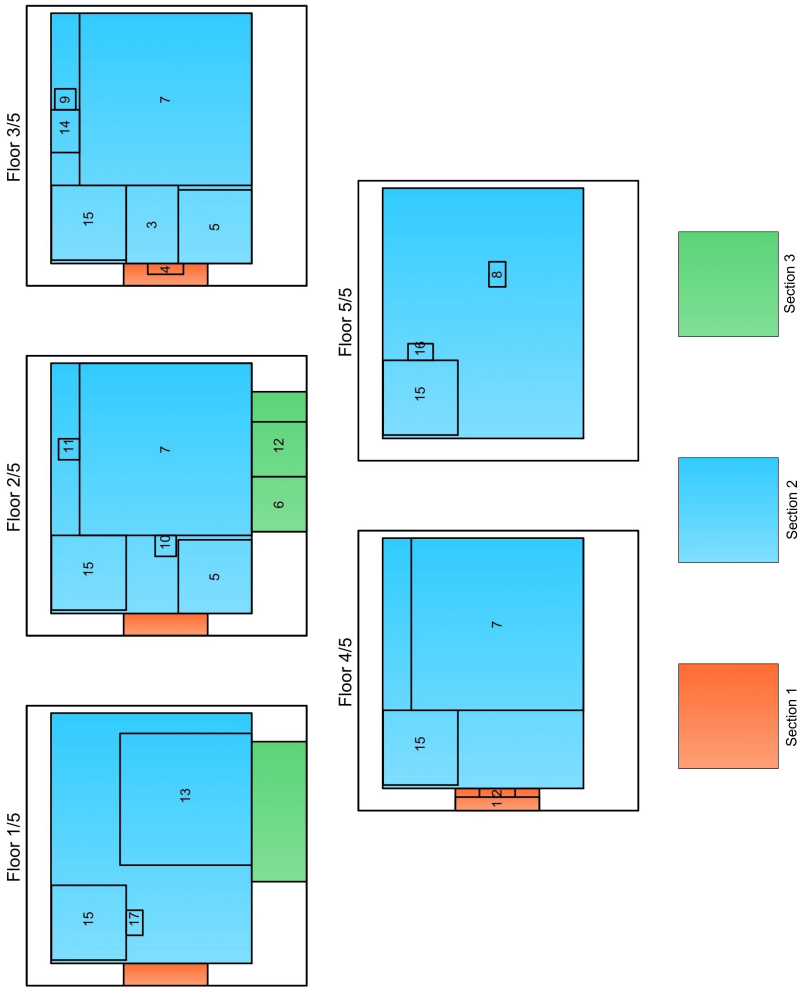

Fig. 4.3 CDU plant - Unit based sectioning

The optimal floor areas obtained for each of sections 1 through 5 measured 1.6m× 10.0m, 17.9m× 14.3m and 10.0m× 3.9m respectively, with a base land area of 20m× 20m. As with the case of function based sectioning, not all floors in some sections were constructed except where equipment items were allocated. Fig. 4.4 compares the total cost distribution for the cases with and without production sections, with construction cost higher with production sections owing to the additional space requirements.

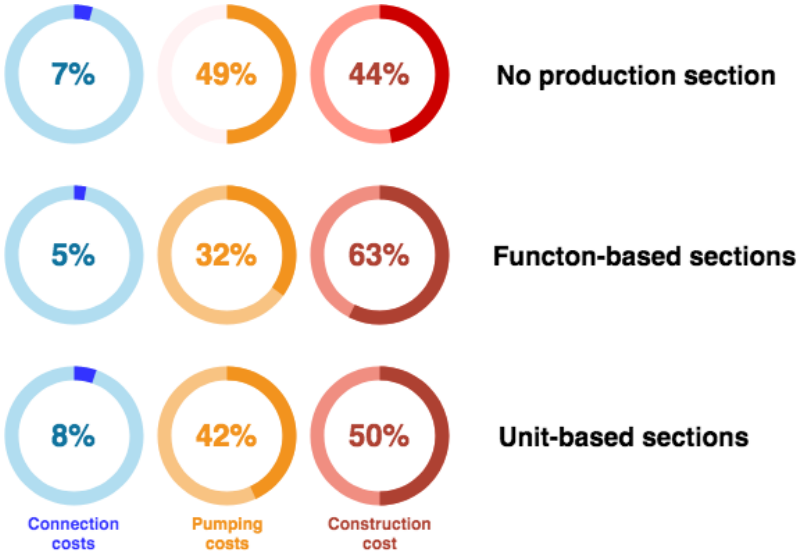

Fig. 4.4 Total Cost Distribution, CDU Plant

4.4.2 LNG plant with production modules

For the LNG liquefaction plant, 3 pre-defined sections were considered as shown in Table 4.4 - Pre-cooled Mixed Refrigerant (PMR) module 1, Pre-cooled Mixed Refrigerant (PMR) module 2, and the Mixed Refrigerant (MR) module. The additional conditions of 4m minimum equipment item spacing, 50% workspace area on the first floor, 60% emergency area on the last floor, and relative equipment item positioning as required in Section 3.4.4 are still enforced.

Table 4.4 Production module allocation for LNG liquefaction plant

Unit	Description	Production Module
1	PMR compressor LP suction drum	PMR Module 1
2	PMR compressor HP suction drum	
3	PMR compressor	
4	PMR compressor cooler	
5	Overhead crane for PMR compressor	
6	SW cooler 1	
7	SW cooler 2	
8	PMR receiver	PMR Module 2
9	LP precool exchanger	
10	HP precool exchanger	
11	Joule–Thomson valve 1	
12	Joule–Thomson valve 2	
13	MR separator 1	MR Module
14	MCHE	
15	MR compressor suction drum	
16	MR compressor	
17	MR compressor cooler	
18	Overhead crane for MR Compressor	
19	SW cooler 3	
20	SW cooler 4	
21	Joule–Thomson valve 3	
22	Joule–Thomson valve 4	

A summary of the solver statistics for each model is shown in Table 4.5. Although being a larger example - based on the number of equipment items and so decision variables - all models obtained the globally optimal solution in less than 3 mins, with model A.4_PS still being the most computational efficient (31.3s). All models simultaneously accounted for the allocation of equipment items to production sections, as well as the additional considerations of minimum equipment spacing, workspace and emergency areas and relative equipment positioning for specific items pairs.

Table 4.5 Model statistics & computational performance for LNG Plant with production sections

	LNG Plant (22 units, 3 sections)				
	A.1_PS	A.2_PS	A.3_PS	A.4_PS	B_PS
Total cost (rmu)	1,690,372.9				
CPU (s)	51.0	78.8	66.5	31.3	182.3
Number of discrete variables	1182	1182	1182	1182	1848
Number of continuous variables	1209	1099	1209	1105	1330
Number of equations	2201	1989	1981	1965	6006

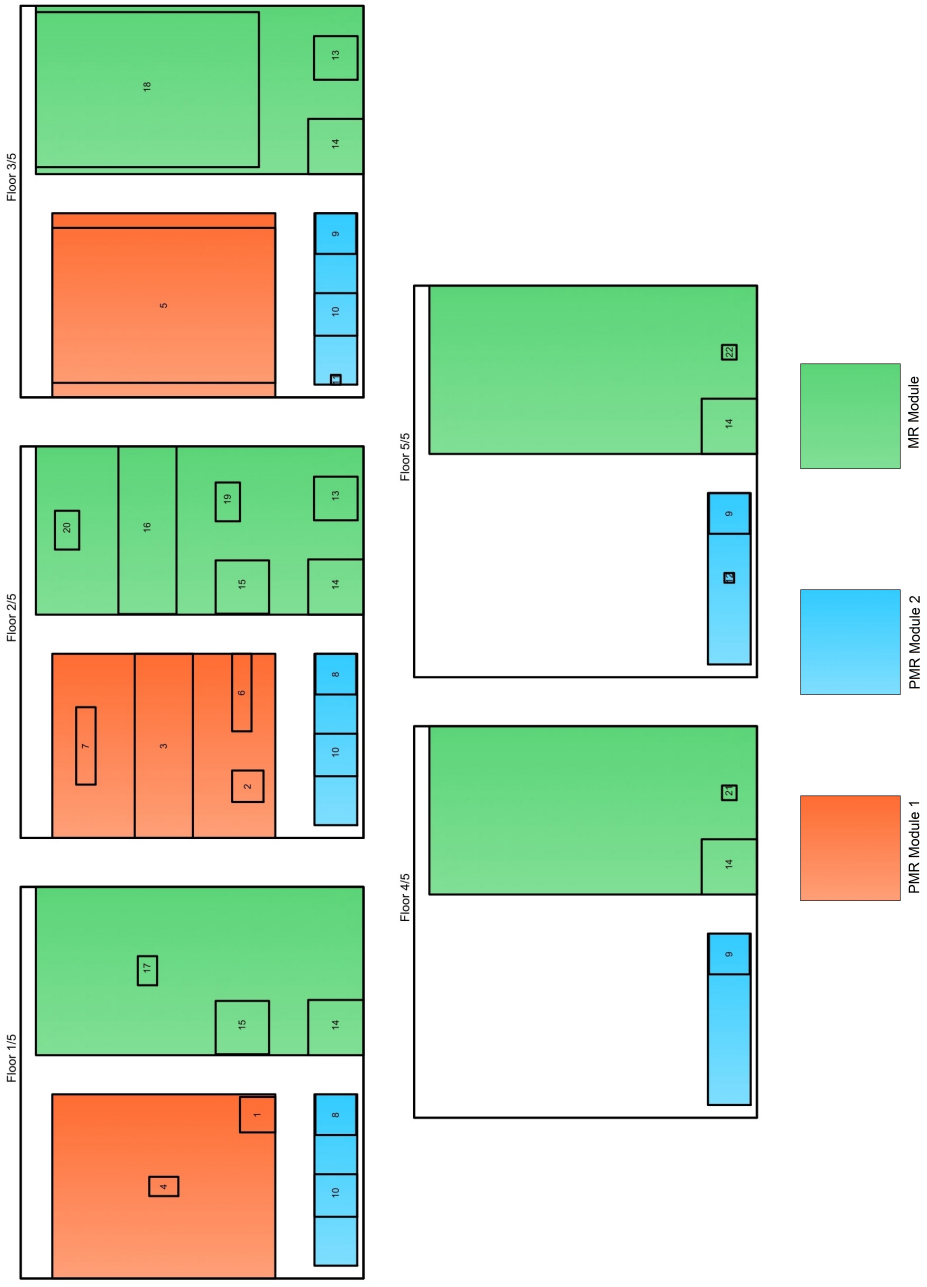

Fig. 4.5 LNG Plant with production sections layout results

The optimal layout with production sections is shown in Fig. 4.5. The total cost of 1,690,372.9 rmu showed a 15.3% increase from the case without sections, although layout results show that floors 4 and 5 do not need to be constructed in the PMR Module 1, and floor 5 in the PMR Module 2. Such increased cost also presents benefits of an increased efficiency in construction, operation and maintenance activities realisable with production sections. The total cost statistic is shown in Fig. 4.6 with a land area of 40m× 35m. PMR module 1 has a floor area of 19.5m× 25.0m, PMR Module 2 - 4.4m× 21.6m and MR Module - 29.6m× 23.9m.

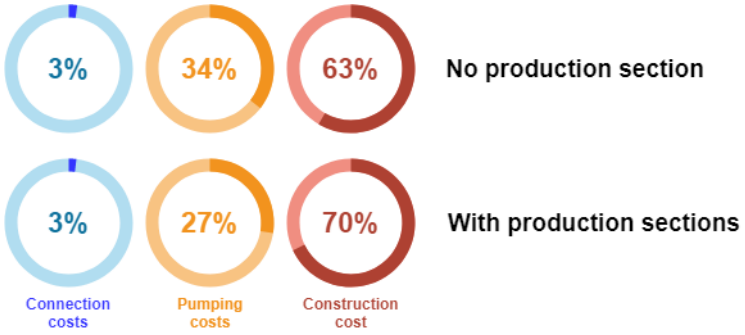

Fig. 4.6 Total Cost Distribution (LNG Liquefaction plant)

4.5 Concluding remarks

In this chapter, the feature of production sections was included in the multi-floor process plant layout models proposed in Chapter 3. Production sections enable grouping of sets of equipment items in a common area to aid construction, maintenance activities and efficient operations within a chemical plant. To incorporate this feature, additional constraints were introduced to ensure that equipment items were placed in the appropriate pre-defined section; simultaneous site and plot layout were determined, as well as the optimal number and area of floors per section. The final models were an extension of models A.x_IC and B._IC proposed in Chapter 3.

Each of the proposed model's capability was tested using the CDU and LNG plant examples each having 17 and 22 total units respectively. For the CDU plants, two cases were

explored: one where production sections were created for items having a common function (called Function-based sectioning), and the other with items grouped majorly according to their type (called Unit-based sectioning). A total of 6 and 3 sections were realised respectively. For the LNG plant, 3 sections were adopted according the functions groups of units performed in the plant and as proposed by the original authors.

All models obtained the globally optimal solution for each of the examples in less than 3mins, with model A.4_PS taking the shortest CPU time in all cases. Layout results showed that the site and plot layouts were obtained in all cases with valid equipment-section allocation. The optimal number of floors were determined for each section, and floors where items had not been allocated were not constructed, saving cost. The proposed models also determined the base floor area as well as the area of each section. Although, an increased total cost was observed in all the example when compared with the cases without production sections, the reduction in computational effort in the revised model, long-run operating costs benefits, and the advantages attributed to sectioning, proved a worthwhile adoption of this feature.

In the following chapters, safety factors are incorporated to the proposed layout models without production section. In Chapter 5, using the Dow's Fire & Explosion Index, the financial risk is quantified for fire and explosion events with the availability of protection devices.

CHAPTER 5

SAFE MULTI-FLOOR PROCESS PLANT LAYOUT USING THE DOW'S FIRE & EXPLOSION INDEX

In the previous chapters (3 and 4), novel MILP models were proposed for the solution of the multi-floor process plant layout problem having a range of features with and without production sections. However, safety factors were not considered. In this chapter, such considerations are introduced. Using the Dow's fire & explosion hazard classification guide, the proposed model considers the financial risk in the event of fire and explosion events, the choice of protection device configurations on each equipment items as well as all other layout features previously considered. A previous case study is revisited to show the benefits of such safety considerations and the performance of the model.

5.1 Introduction

It has been proven that the layout of a chemical process plant is important in defining the overall level of safety within the plant and its environment (Tugnoli et al., 2008a). Although safety is an issue of vital importance not just at the layout design stage, but at every stage of chemical process design (Khan and Amyotte, 2004), a study has shown that 79% of process plant accidents have been attributed to design errors, the most critical being poor layout (Kidam and Hurme, 2012). These accidents can result in fatalities, injuries, disruption

of production activities, major financial losses, and also impact the plant environment and neighbouring areas. Hence, it is important to incorporate safety features to the multi-floor process plant layout problem.

Roy et al. (2016) presented a review of safety indices applicable to process design in which a brief description of 25 representative indices was given with their level of application and inputs required. Two key indices were identified as having a direct relation to the layout of a process plant - the Dow's Fire and Explosion index (F&EI) (American Institute of Chemical Engineers, 1994) and the Domino Hazard Index (DHI) (Tugnoli et al., 2008a). This chapter addresses the multi-floor process plant layout problem with safety features using the Dow's F&EI as a basis to quantify risk; the DHI is adopted in Chapter 6.

The Dow F&EI is a widely applied method for hazard evaluation of chemical and industrial processes developed by American Dow Chemical Company (American Institute of Chemical Engineers, 1994; Wang and Song, 2013). It estimates the hazards of a single unit based on the chemical properties of the material(s) within it, and the potential economic risk such equipment poses to itself and neighbouring structures with or without the installation of protection devices. Specific units (called pertinent equipment items), susceptible to hazardous events, are identified and this information is incorporated into existing MILP models (Chapter 3) to estimate the probability and magnitude of damage within the plant with respect to the distances between such items and other neighbouring items. The final MILP model proposed estimates the optimal multi-floor layout configuration with minimal costs attributed to the installation of connecting pipes, pumping process fluids, area-dependent construction of floors, land purchase, and the risk associated with fire and explosion events, with decisions being made on the installation of passive protection devices.

In the next Section 5.2, the problem is explained in detail. Section 5.3 highlights the mathematical formulation. The formulation is an extension of model A.4^{+}_IC. The ethylene oxide plant example is re-investigated in Section 5.4 to show the proposed model capabilities and changes to the layout results, with key observations summarised in Section 5.5.

5.2 Problem description

The problem description is given as follows.

Given:

- a set of equipment items and their dimensions (length, breadth and height);
- a subset of pertinent equipment items ($I^{pe} \subset I$);
- distance of exposure and damage factors of pertinent equipment items;
- connectivity network amongst equipment items;
- a set of potential floors for layout with known floor height;
- a set of protection device configurations for each pertinent equipment item and its corresponding loss control credit factor if installed on such item;
- cost data (connection, protection device purchase, equipment purchase, pumping, land, and construction);
- space and equipment item allocation limitations;

to determine:

- total number of required floors for the layout;
- protection device configuration to be installed on each pertinent equipment item;
- floor area;
- plot layout;

so as to: minimise the total plant layout and safety costs evaluated using the Dow's Fire & Explosion Index (F&EI).

The total plant layout cost is the sum of the cost of connecting equipment items by pipes, pumping process fluids through pipes, purchasing the land for the layout based on its area, constructing each floor, installing selected protection devices as well as the financial risk in the event of a fire and/or explosion event.

The following assumptions are made:

- each equipment item is approximated with a rectangular geometry;
- every item is connected to the other from its geometrical centre in the x-y plane, and from a predefined height along the z-plane, based on design calculations;

- for safety considerations, all rectilinear distances between items of concern as measured from the equipment item boundaries to evaluate the probability, magnitude and impact of an incident on a pertinent item;
- an item is allowed to rotate through 90° angles about the x-y plane as deemed optimal but it must start at the base point of the floor it has been assigned to;
- floors are numbered from bottom to top with a fixed floor height;
- equipment items tall enough to exceed the fixed floor height are allowed to extend through successive floors.

5.3 Mathematical formulation

Nomenclature

The following symbols are re-defined as follows:

Indices

i, j, n	equipment item
k, k'	floor number
p	protection device configuration
s	rectangular area sizes

Sets

ζ	set of ordered pairs of pertinent equipment items and other items; $\zeta = \{(i,j) : i \in I^{pe}, j \neq i\}$
I	set of equipment items
I^{pe}	set of pertinent equipment items
P_i	set of protection device configurations suitable for installation on item i
MF	set of multi-floor equipment items

Parameters

$\alpha_i, \beta_i, \gamma_i$	dimensions of item i
BM	a large number
C^c_{ij}	connection/piping costs
C^e_i	purchase cost of item i
C^h_{ij}	horizontal pumping costs
C^p_{ip}	purchase and installation cost of protection device configuration p for item i
C^v_{ij}	vertical pumping costs
CF_{ip}	loss control credit factor of protection device configuration p for item i
D^e_i	distance of exposure of item i
DF_i	damage factor of pertinent item i
f_{ij}	1 if flow direction between i and j is positive; 0, otherwise
$FC1$	fixed floor construction cost
$FC2$	area-dependent floor construction cost
FH	floor height
IP_{ij}	distance between the base and input point on equipment j
LC	land cost
M_i	number of floors required by item i
OP_{ij}	distance between the base and output point on equipment i
$\overline{X}_s, \overline{Y}_s$	x-y dimensions of pre-defined rectangular area sizes s

Integer variables

NF	number of floors required for layout

Binary variables

$\psi_{i,j}$	1 if item j is within the distance of exposure of pertinent item i, 0 otherwise
μ_{ip}	1 if protection device configuration p is installed on pertinent item i, 0 otherwise
$E1_{ij}, E2_{ij}$	non-overlapping binaries, a set of values which prevents equipment
N_{ij}	1 if items i and j are assigned to the same floor; 0, otherwise
O_i	1 if length of item i is equal to α_i; 0, otherwise
Q_s	1 if rectangular area s is selected for the layout; 0, otherwise
S^s_{ik}	1 if item i begins at floor k; 0, otherwise
S^f_{ik}	1 if item i terminates at floor k; 0, otherwise
Up^b_{ij}	1 if item i is located on a floor above item j, 0 otherwise or if items i and j are on the same floor
Dn^b_{ij}	1 if item i is located on a floor below item j, 0 otherwise or if items i and j are on the same floor
V_{ik}	1 if item i is assigned to floor k
W_k	1 if floor k is occupied; 0, otherwise
W^x_{ij}	1 if item i is to the right of item j in the x plane; 0 otherwise
W^{xo}_{ij}	1 if the boundary of item i is strictly to the right or left of item j in the x plane; 0 otherwise
W^y_{ij}	1 if item i is above item j in the y plane; 0 otherwise
W^{yo}_{ij}	1 if the boundary of item i is strictly above or below item j in the y plane; 0 otherwise
W^z_{ij}	1 if item i is on a higher floor than item j; 0 otherwise

Continuous variables

η^u_{ij}, η^d_{ij}	positive continuous variables to determine vertical safety distance between items i and j

Ω_i^0	base maximum probable property damage cost for pertinent equipment item i
Ω_i	actual maximum probable property damage cost for pertinent equipment item i
$\Omega_{ip}^{'}$	linearization variable denoting the the product of Ω_i and μ_{ip}
A_{ij}	distance in the y plane between items i and j in the x-y plane, if i is above j
AR_s	predefined rectangular floor area s
B_{ij}	distance in the y plane between items i and j in the x-y plane, if i is below j
d_i	breadth of item i
D_{ij}	connection distance in the z plane between items i and j, if i is lower than j
Dn_{ij}	vertical separation distance between items i and j, if i is on a lower floor than j
FA	floor area
h_i	height of item i
l_i	length of item i
L_{ij}	distance in the x plane between items i and j, if i is to the left of j
NQ_s	linearisation variable expressing the product of NF and Q_s
R_{ij}	distance in the x plane between items i and j, if i is to the right of j
TD_{ij}	total rectilinear connection distance between items i and j
TD_{ij}^{in}	total rectilinear safety distance between items i and j, if j is within the distance of exposure of item i
TD_{ij}^{out}	total rectilinear safety distance between items i and j, if j is outside of the distance of exposure of item i
TD_{ij}^{s}	total rectilinear safety distance between items i and j
U_{ij}	connection distance in the z plane between items i and j, if i is higher than j

Up_{ij}	vertical separation distance between items i and j, if i is on a higher floor than j
V_i^e	value of area of exposure of item i
VD_{ij}	total vertical distance between items i and j
x_i, y_i	coordinates of the geometrical centre of item i
X^{max}, Y^{max}	dimensions of floor area

For the mathematical formulation, model A.4$^+$_IC is extended to include safety considerations using the Dow's F&EI. Model A.4$^+$_IC was chosen as its base case (model A.4) proved to be more computationally efficient when compared to other proposed models in the examples considered in Chapters 3 and 4, as well as having the additional feature that tall equipment items could extend well beyond the topmost available floor. However, all constraints are also applicable to the other models proposed. The constraints for the safety considerations are an extension of the single-floor layout model of Patsiatzis et al. (2004). The following constraints are then modified/included:

5.3.1 Floor constraints

First, the floor constraint of equation (3.2), defining if two items i and j are allocated to the same floor is modified to included all possible equipment item pairs ($j \neq i$):

$$N_{ij} \geq V_{ik} + V_{jk} - 1 \qquad \forall\, i, j \neq i \tag{5.1}$$

5.3.2 Distance constraints

Distance constraints described by equations (3.17) - (3.20) are modified as follows to determine the distances between equipment items.

Connection distance

To evaluate the total connection distance, rectilinear distances from equipment item midpoints are estimated. Horizontal distances between items are evaluated using equations (5.2) and

(5.3). These are written not only for connected equipment items ($f_{ij} = 1$), but for all possible combinations between pertinent items and other items ($(i, j) \in \zeta$). These determine the distances in the x and y plane respectively, between items i and j.

$$R_{ij} - L_{ij} = x_i - x_j \qquad \forall\, i, j : f_{ij} = 1, (i, j) \in \zeta \tag{5.2}$$

$$A_{ij} - B_{ij} = y_i - y_j \qquad \forall\, i, j : f_{ij} = 1, (i, j) \in \zeta \tag{5.3}$$

R_{ij} or L_{ij} determine the distance between items i and j if item i is the right or left of item j in the x plane respectively. To force one of R_{ij} or L_{ij} to zero, equations (5.4) - (5.5) is introduced. When the binary variable $W^x_{ij} = 1$, R_{ij} is forced to zero and L_{ij} takes a positive value equal to $\mid x_i - x_j \mid$. When $W^x_{ij} = 0$, only R_{ij} takes a positive non-zero value.

$$R_{ij} \leq BM \cdot W^x_{ij} \qquad \forall\, i, j : f_{ij} = 1, (i, j) \in \zeta \tag{5.4}$$

$$L_{ij} \leq BM \cdot (1 - W^x_{ij}) \qquad \forall\, i, j : f_{ij} = 1, (i, j) \in \zeta \tag{5.5}$$

The same condition applies to the variables A_{ij} or B_{ij} when item i is above or below item j in the y plane respectively, using equations (5.6) - (5.7) and the binary variable W^y_{ij}:

$$A_{ij} \leq BM \cdot W^y_{ij} \qquad \forall\, i, j : f_{ij} = 1, (i, j) \in \zeta \tag{5.6}$$

$$B_{ij} \leq BM \cdot (1 - W^y_{ij}) \qquad \forall\, i, j : f_{ij} = 1, (i, j) \in \zeta \tag{5.7}$$

The vertical distances between connected items ($f_{ij} = 1$) are evaluated using equation (5.8) and are taken from the design specified connection points along the height of such items:

$$U_{ij} - D_{ij} = FH \sum_k (k-1)(S^s_{ik} - S^s_{jk}) + OP_{ij} - IP_{ij} \qquad \forall\, i, j : f_{ij} = 1 \tag{5.8}$$

where OP_{ij} represents the vertical distance from the base of equipment i to its output point, and IP_{ij} represents the vertical distance from the base of equipment j to its input point for connection i-j.

The total connection distance (TD_{ij}) is then evaluated by equation (5.9) to determine the

connection cost:

$$TD_{ij} = R_{ij} + L_{ij} + A_{ij} + B_{ij} + U_{ij} + D_{ij} \qquad \forall i, j : \ f_{ij} = 1 \tag{5.9}$$

Safety distance

For the safety distance between equipment items, separation distances between equipment item boundaries are adopted. As such, the vertical and horizontal distances earlier estimated for connection costs need to be re-evaluated. For the vertical safety distance, the following conditions should be satisfied as illustrated in Fig. 5.1:

- if i and j are on the same floor, the vertical distance is zero;
- if i is on a higher floor than j, the vertical distance is taken from the top of j to the bottom of i; *and*
- if i is on a lower floor than j, the vertical distance is taken from the top of i to the bottom of j.

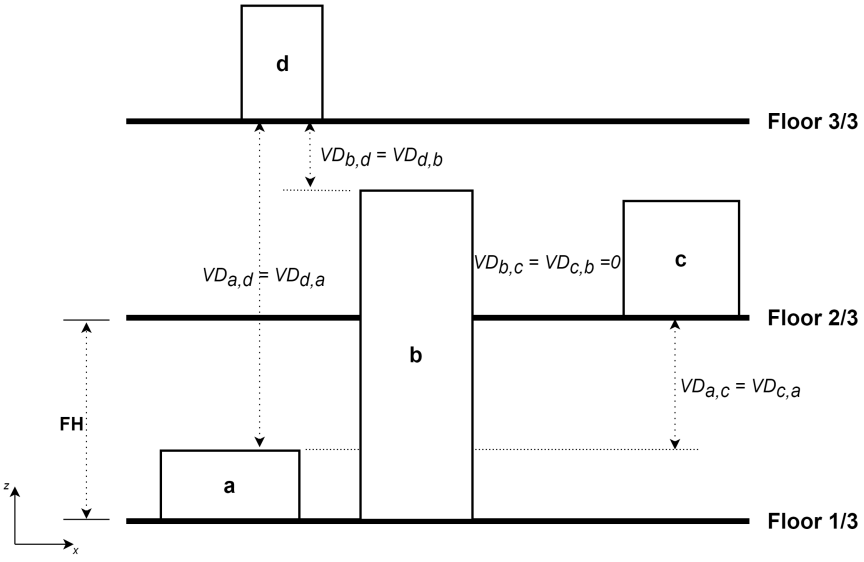

Fig. 5.1 Vertical safety distance between equipment items

This represents a more accurate assumption for safety considerations compared to the distances taken from the midpoint of equipment items used for the connection distances. This is especially true for large and/or tall equipment which can have large distances between

the mid-points but be physically close to each other. As accidents may occur at any point on a pertinent equipment item, a more valid assumption is to calculate separation distances from equipment boundaries.

The conditions stated above are represented mathematically by equation (5.10) to obtain the vertical separation distance, VD_{ij}, between any two items i and j.

$$VD_{ij}\begin{cases}\geq 0, & \text{when } N_{ij}=0\\ = 0, & \text{when } N_{ij}=1\end{cases} \tag{5.10}$$

For cases were items i and j are on different floors ($N_{ij}=0$), the vertical distance is determined as follows. First, equations (5.11) or (5.12) determine the separation distances between items i and j if i is above or below j respectively (Fig. 5.1).

$$Up_{ij} = FH\sum_{k}(k-1)(S^s_{ik}-S^s_{jk})-\gamma_j \qquad \forall\,(i,j)\in\zeta, N_{ij}=0 \tag{5.11}$$

$$Dn_{ij} = FH\sum_{k}(k-1)(S^s_{jk}-S^s_{ik})-\gamma_i \qquad \forall\,(i,j)\in\zeta, N_{ij}=0 \tag{5.12}$$

The vertical separation distance between the two items i and j will be the maximum value of Up_{ij} and Dn_{ij}:

$$VD_{ij} = \max\left(Up_{ij}, Dn_{ij}\right) = Dn_{ij} + \max\left(Up_{ij}-Dn_{ij}, 0\right) \qquad \forall\,(i,j)\in\zeta, N_{ij}=0 \tag{5.13}$$

As equations (5.11) - (5.13) cannot be implemented directly, linear equivalents are expressed as follows. Equation (5.14) helps to determine $\max\left(Up_{ij}-Dn_{ij},0\right)$ where η^u_{ij} and η^d_{ij} are positive variables:

$$\eta^u_{ij}-\eta^d_{ij} = 2FH\sum_{k}(k-1)(S^s_{ik}-S^s_{jk})+\gamma_i-\gamma_j \qquad \forall\,(i,j)\in\zeta \tag{5.14}$$

$$\eta^u_{ij} \leq BM\cdot W^z_{ij} \qquad \forall\,(i,j)\in\zeta \tag{5.15}$$

$$\eta^d_{ij} \leq BM\cdot(1-W^z_{ij}) \qquad \forall\,(i,j)\in\zeta \tag{5.16}$$

Equations (5.15) and (5.16) force only one of η^u_{ij} and η^d_{ij} to zero. The total vertical distance from equation (5.13) then becomes:

$$VD_{ij} = FH\sum_k (k-1)(S^s_{jk} - S^s_{ik}) - \gamma_i + \eta^u_{ij} \qquad \forall\,(i,j) \in \zeta \tag{5.17}$$

To further account for cases where $N_{ij} = 1$, equation (5.17) is rewritten as:

$$VD_{ij} \leq FH\sum_k (k-1)(S^s_{jk} - S^s_{ik}) - \gamma_i + \eta^u_{ij} + BM \cdot N_{ij} \qquad \forall\,(i,j) \in \zeta \tag{5.18}$$

$$VD_{ij} \geq FH\sum_k (k-1)(S^s_{jk} - S^s_{ik}) - \gamma_i + \eta^u_{ij} - BM \cdot N_{ij} \qquad \forall\,(i,j) \in \zeta \tag{5.19}$$

$$VD_{ij} \leq BM \cdot (1 - N_{ij}) \qquad \forall\,(i,j) \in \zeta \tag{5.20}$$

Equations (5.18) - (5.20) ensure VD_{ij} only takes a non-zero value when items i and j are on different floors.

This separation distance calculation is also extended to the x and y plane to obtain the horizontal distances from the boundaries of each equipment item, as opposed to their geometrical centres (equations (3.17) and (3.18)). A value of zero is assigned to this distance if the boundaries of an item i is not strictly to the right or left (in the x plane), or above or below (in the y plane) of j (Fig. 5.2). That is, items i and j overlap at any region on either the x or y plane.

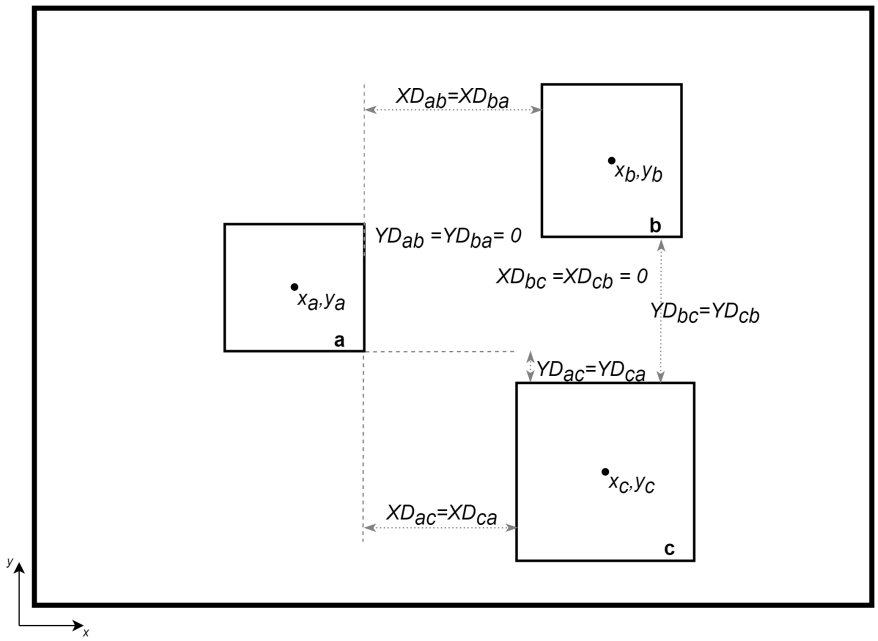

Fig. 5.2 Horizontal safety distance between equipment items

These are calculated by the following constraints:

$$y_i - y_j + 2B_{ij} \geq \left(\frac{d_i + d_j}{2}\right) - BM(1 - W_{ij}^{yo}) \qquad \forall\,(i,j) \in \zeta \tag{5.21}$$

$$YD_{ij} \leq A_{ij} + B_{ij} - \left(\frac{d_i + d_j}{2}\right) + BM(1 - W_{ij}^{yo}) \qquad \forall\,(i,j) \in \zeta \tag{5.22}$$

$$YD_{ij} \geq A_{ij} + B_{ij} - \left(\frac{d_i + d_j}{2}\right) - BM(1 - W_{ij}^{yo}) \qquad \forall\,(i,j) \in \zeta \tag{5.23}$$

$$YD_{ij} \leq BM \cdot W_{ij}^{yo} \qquad \forall\,(i,j) \in \zeta \tag{5.24}$$

Equation (5.21) establishes that if the opposing boundaries of item i is strictly above or below item j and not overlapping in any region along the y plane, W_{ij}^{yo} takes a value of 1. Equations (5.22) - (5.24) ensure that the distance between the boundaries of items i and j (YD_{ij}) in the y plane only takes a positive value if both items do not overlap along any region of the y plane, else, a value of zero is assigned. As $E2_{ij} = 1$ for all $j > i$ only if i is strictly above or below j (equations (3.15) and (3.16)), equation (5.25) is introduced for a

more efficient evaluation of W_{ij}^{yo}.

$$W_{ij}^{yo} \geq \begin{cases} E2_{ij}, & \forall\, i,j > i \\ E2_{ji}, & \forall\, i,i > j \end{cases} \tag{5.25}$$

The same set of constraints are included for the x plane ((5.26) - (5.29)).

$$x_i - x_j + 2L_{ij} \geq \left(\frac{l_i + l_j}{2}\right) - BM(1 - W_{ij}^{xo}) \qquad \forall\,(i,j) \in \zeta \tag{5.26}$$

$$XD_{ij} \leq R_{ij} + L_{ij} - \left(\frac{l_i + l_j}{2}\right) + BM(1 - W_{ij}^{xo}) \qquad \forall\,(i,j) \in \zeta \tag{5.27}$$

$$XD_{ij} \geq R_{ij} + L_{ij} - \left(\frac{l_i + l_j}{2}\right) - BM(1 - W_{ij}^{xo}) \qquad \forall\,(i,j) \in \zeta \tag{5.28}$$

$$XD_{ij} \leq BM \cdot W_{ij}^{xo} \qquad \forall\,(i,j) \in \zeta \tag{5.29}$$

A binary variable W_{ij}^{xo} is introduced having a value of 1 if the opposing boundaries of item i is strictly to the right or left of j. Equation (5.30) tightens the constraints as $E2_{ij} = 0$ only if item i is strictly to left or right of j (equations 3.13 and 3.14).

$$W_{ij}^{xo} \geq \begin{cases} 1 - E2_{ij}, & \forall\, i,j > i \\ 1 - E2_{ji}, & \forall\, i,i > j \end{cases} \tag{5.30}$$

The total safety distances between equipment items i and j is then calculated as the sum of the horizontal and vertical separation distances:

$$TD_{ij}^{s} = XD_{ij} + YD_{ij} + VD_{ij} \qquad \forall\,(i,j) \in \zeta \tag{5.31}$$

It should be noted that this value is always greater than or equal to the actual separation distance between equipment items, which is calculated using the Euclidean metric. The Euclidean distance estimation, however, introduces non-linear terms to the model which makes it difficult and/or unpredictable in obtaining solutions. The resulting effect of this

linear approximation is that the damage level calculated will almost always be underestimated. Decision makers should be aware.

5.3.3 Area of exposure constraints

In order to calculate the value of area of exposure, it needs to be determined if an item j is within the distance of exposure of a pertinent item i (Fig. 5.3). The distance of exposure (D_i^e) is the distance within which a secondary item j will be affected by a fire and explosion incident originating from a pertinent item i.

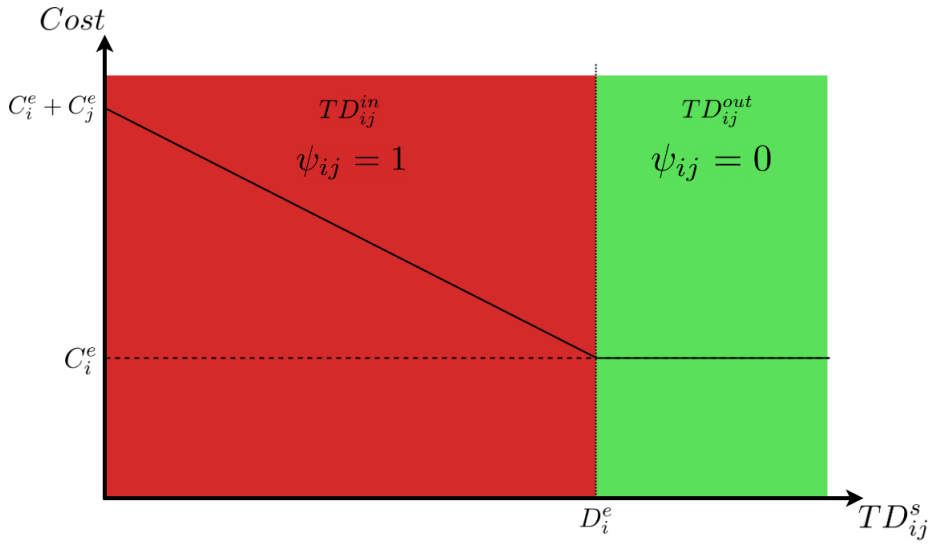

Fig. 5.3 Damage cost versus distance between items i and j

The total safety distance is then expressed as in equation (5.32), where $\psi_{i,j}$ is a binary variable denote if a secondary unit j is within the area of exposure of pertinent item i. To ensure only one of TD_{ij}^{in} and TD_{ij}^{out} is non-zero, equations (5.33) - (5.35) are introduced. TD_{ij}^{in} takes the value of the total distance if item j is within the distance of exposure (D_i^e) of item i, and TD_{ij}^{out} if not.

$$TD_{ij}^s = TD_{ij}^{in} + TD_{ij}^{out} \qquad \forall\, i \in I^{pe}, j \neq i \qquad (5.32)$$

$$TD_{ij}^{in} \leq D_i^e \cdot \psi_{i,j} \qquad \forall\, i \in I^{pe}, j \neq i \qquad (5.33)$$

$$TD_{ij}^{out} \geq D_i^e \cdot (1 - \psi_{i,j}) \qquad \forall\, i \in I^{pe}, j \neq i \qquad (5.34)$$

$$TD_{ij}^{out} \leq BM \cdot (1 - \psi_{i,j}) \qquad \forall\, i \in I^{pe}, j \neq i \tag{5.35}$$

The value of area of exposure is then determined as:

$$V_i^e = C_i^e + \sum_{j \neq i} \left(C_j^e \cdot \psi_{i,j} - \frac{C_j^e}{D_i^e} \cdot TD_{ij}^{in} \right) \qquad \forall\, i \in I^{pe} \tag{5.36}$$

5.3.4 Maximum probable property damage constraints

The base maximum probable property damage is calculated by equation (5.37). This represents the financial losses incurred as a result of an accident occurring at pertinent item i and propagating to all neighbouring items j within its distance of exposure.

$$\Omega_i^0 = DF_i \cdot V_i^e \qquad \forall\, i \in I^{pe} \tag{5.37}$$

However, if a protective device is installed on a pertinent item i, the probability and magnitude of such accident is reduced. Each configuration for the protective devices (P_i) is thus characterised by a loss control credit factor expressing such reduction. In cost terms, this is determined by the actual maximum probable property damage cost (Ω_i) given as:

$$\Omega_i = \sum_{p \in P_i} CF_{ip} \cdot \Omega_i^0 \cdot \mu_{ip} \qquad \forall\, i \in I^{pe} \tag{5.38}$$

Equation (5.38) is linearised by equations (5.39) - (5.42) below:

$$\Omega_i = \sum_{p \in P_i} CF_{ip} \cdot \Omega_{ip}^{'} \qquad \forall\, i \in I^{pe} \tag{5.39}$$

$$\Omega_{ip}^{'} \leq BM \cdot \mu_{ip} \qquad \forall\, i \in I^{pe}; p \in P_i \tag{5.40}$$

$$\sum_{p \in P_i} \Omega_{ip}^{'} = \Omega_i^0 \qquad \forall\, i \in I^{pe} \tag{5.41}$$

$$\sum_{p \in P_i} \mu_{ip} = 1; \qquad \forall\, i \in I^{pe} \tag{5.42}$$

5.3.5 Objective function

The objective function is the total cost associated with the connection cost, pumping cost, land area cost, floor construction and floor-area dependent cost, purchase and installation of protective devices and the maximum probable property damage cost. This is given as:

$$\begin{aligned} min \sum_{i,j:f_{ij}=1} \left(C^c_{ij} TD_{ij} + C^v_{ij} D_{ij} + C^h_{ij}(R_{ij} + L_{ij} + A_{ij} + B_{ij})\right) \\ + FC1 \cdot NF + FC2 \sum_s AR_s \cdot NQ_s + LC \cdot FA \\ + \sum_i \Omega_i + \sum_{i,p \in P_i} C^p_{ip} \cdot \mu_{ip} \end{aligned} \tag{5.43}$$

subject to (3.3) - (3.7), (3.13) - (3.16), (3.21) - (3.30), (3.34) - (3.36), (3.54) - (3.58), (5.1) - (5.9), (5.14) - (5.37), and (5.39) - (5.42). This constitutes model A.4$^+$_IC_FEI.

5.4 Case study of an ethylene oxide plant

The model proposed was applied to the ethylene oxide plant. Fig. 5.4 shows the process flow diagram of the plant, identifying the pertinent equipment items: 1 - Reactor, 3 - ethylene oxide absorber and 5 - CO_2 absorber. Data on equipment dimensions, connectivity, purchase and layout costs, e.t.c., are given in Section B.1.

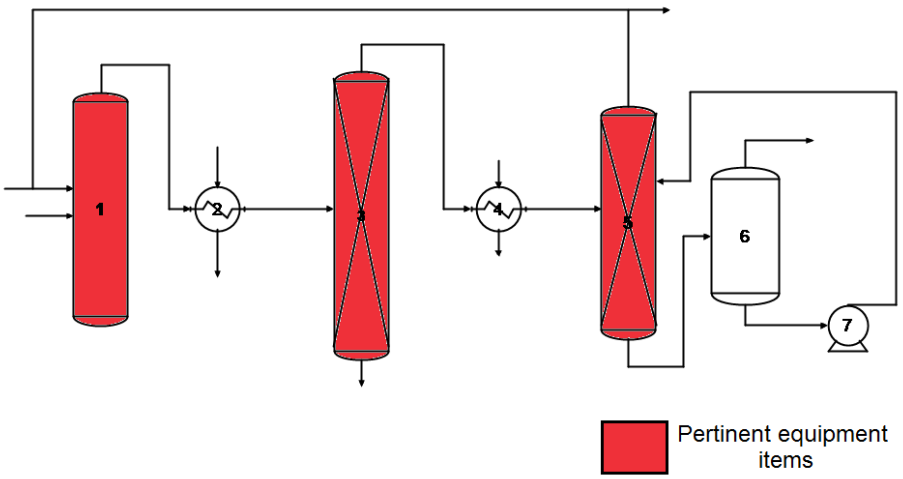

Fig. 5.4 Flow diagram of ethylene oxide plant (See Table B.1 in Appendix B for a description of the equipment item labels)

Table 5.1 Protection device configurations (Patsiatzis et al., 2004)

Device	Configuration type
1	Additional cooling water
2	Additional overpressure relief devices
3	Additional fire relief devices
4	Second skin on reactor
5	Explosion protection system of reactor
6	Duplicate control system with interlocking flow on reactor
7	Duplicate control shutdown system on absorption tower

Seven protection devices were made available as shown in Table 5.1 from which six configuration types were created for each pertinent item. Each configuration type consisted of a combination of the listed protection devices, with the first type having no protection device selected. Full details for the configurations, the protection devices in each, and the associated cost and loss control credit factor can be found in Section B.1.

Table 5.2 shows the model statistics and computational results for the EO plant with and without safety considerations. The optimal solution was obtained in 9.3s having 2 floors with

a floor area of 50m× 20m and a total cost of 424,568.2 rmu. Protection devices were selected for each pertinent item with a total cost of 70,000.0 rmu. For the reactor (item 1), the model selected the use of additional cooling water (1), overpressure relief devices (3), explosion protection system(5) and duplicate control system with interlocking flow (6); corresponding to configuration 5 (Table B.3). For both the ethylene oxide (item 3) and CO_2 absorbers, the additional cooling water (1) was selected (configuration 2). Each of these devices served to reduce the probability, magnitude and impact of a fire and explosion event on each of these items. These risks still exist as quantified by the financial risk value of 232,241.2 rmu.

Table 5.2 Model Statistics & computational performance

	Without safety (Model A.4$^+$_IC)	With safety (Model A.4$^+$_IC_FEI)
Layout cost (rmu)	66,262.0	122,327.0
Safety device cost (rmu)	0.0	70,000.0
Financial risk (rmu)	935,820.9	232,241.2
Total cost (rmu)	**1,002,082.9**	**424,568.2**
CPU (s)	0.8	9.3
Number of discrete variables	92	260
Number of continuous variables	157	376
Number of equations	392	936

Fig. 5.5 shows the optimal layout plot with and without safety considerations. With the inclusion of fire and explosion factors, the same number of floors is required for the layout compared to the layout results without safety considerations, but with a larger area and greater inter-equipment spacing for most of the equipment items. Out of the total cost of 424,568.2 rmu, 70,000.0 rmu was attributed to the installation of protection devices, 232,241.2 to financial risks and 122,327.0 rmu to connection, pumping and construction costs. The latter cost quota is much larger when compared to the case without safety considerations, 66,262 rmu, owing to additional separation distances between equipment items and a larger floor area (30m× 30m compared to 20m× 20m).

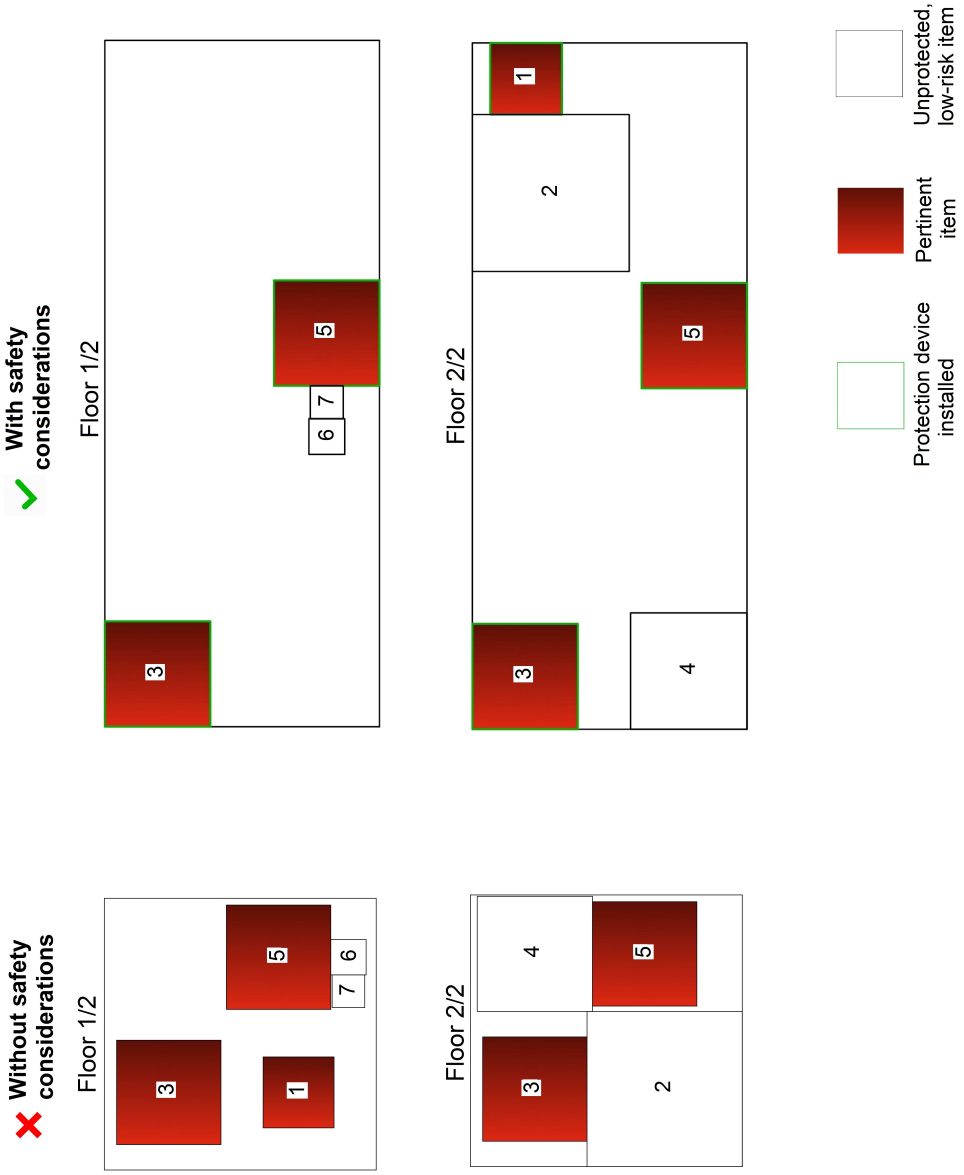

Fig. 5.5 Optimal layout results

For the case where safety was not considered and no protection device was installed, the total cost was re-calculated using the information from the layout results obtained and steps outlined for risk quantification. A total cost of 1,002,082.9 rmu was obtained with a financial risk of 935,820.9 rmu. This is about three times more than the financial risk evaluated with safety factors considered, with the cost difference (703,579.7 rmu) being almost 10x the total layout cost without safety considerations (66,262.0 rmu). As such, the cost of protection devices, financial risk, and other layout costs combined is much less for the case where safety is considered and protection devices are installed than if they were not. This provides for a more informed balance between cost savings and financial risks.

5.5 Concluding remarks

In this chapter, the MILP model earlier proposed to address the multi-floor process plant layout problem was extended to account for safety considerations, particularly, fire and explosion hazards. The probability, magnitude and impact of fire and explosion events were quantified using the Dow's fire and explosion index, where the risk of equipment items identified as highly susceptible to such events are estimated based on the chemical properties of the material it processes and the potential financial risk it poses to neighbouring items. More accurate distance measurements from the boundaries of equipment items were introduced to capture the actual separation distance for risk calculations in an MILP model. The final model considered connection, pumping, construction, financial risk and protection device installation costs to obtain an optimal multi-floor plot layout.

Model capabilities and performance were demonstrated using the ethylene oxide plant case study first introduced in Chapter 3. The 7-unit plant had 3 pertinent equipment items and 6 protection device configurations. The model successfully obtained the globally optimal solution in a modest time with the same number of floors as previous recorded without safety considerations but having a larger area and increased total cost. The best selection of protection devices were obtained to provide a balance of minimal financial risk, protection device purchase and layout costs. Although a much higher cost was attributed to layout and

protection device purchase when considering safety, it was shown that such increased cost was negligible when compared with the financial risk if not considered.

In the next chapter (Chapter 6), a more detailed index - Domino Hazard Index - is adopted to capture a broader range of hazardous events in process plants. The proposed MILP model is an extension of model A.4^{+}_IC which considers the domino effects hazardous events have on neighbouring equipment items and plant infrastructure.

CHAPTER 6

SAFE MULTI-FLOOR PROCESS PLANT LAYOUT USING THE DOMINO HAZARD INDEX

In chapter 5, safety considerations were introduced to the previously proposed mixed integer linear programming models for the multi-floor process plant layout problem using the Dow's Fire & Explosion Index. In the current chapter, the Domino Hazard Index (DHI) is adopted to quantify risk. A more detailed quantification of the escalation vectors of different fire and explosion events are considered using this index to estimate the domino effects of such events on other equipment items. Using an acrylic acid plant, the benefits of these safety considerations in the proposed model are highlighted, as is its computational performance.

6.1 Introduction

In the previous chapter, the probability and impact of hazards within chemical process plants were quantified using the Dow's Fire and explosion index (F&EI) (American Institute of Chemical Engineers, 1994) - one of the safety indices adopted in process plant design, and being directly affected by layout configurations (Roy et al., 2016). The Dow's fire and explosion risk analysis system accounted for fire, explosion and reactivity potentials of equipment items in a bid to proffer preventive and protective features (American Institute of Chemical Engineers, 1994).

Although the Dow's F&EI is a leading safety index in practice, a key metric of the system (the material factor) has been identified as being independent of process operating conditions and more on expert opinions (Roy et al., 2016). The index has also been shown not to correlate well with known plant disasters and is not scenario-driven. Chemical process plants are also susceptible to other forms of hazardous events other than fires and explosions, e.g. toxic release of gases. Fire and explosion events also exist in different forms, each having different prediction models and impact on the chemical plant. There is therefore the need for a more detailed risk estimation/ranking system for each of these events applicable to layout designs.

The Domino Hazard Index (DHI) (Tugnoli et al., 2008a) provides such added merits. Using a hazard ranking system each process plant equipment item is scored on the basis of a set of scenarios, its distance to other equipment items, and its physical and chemical properties. The DHI is a sub-index of the Integrated Inherent Safety Index (I2SI) (Khan and Amyotte, 2005) which accounts for the hazard potential, inherent safety potential and add-on control requirements of a process. The effects hazardous events originating on a particular unit have on a chemical plant are assessed considering both inherent and passive measures, and their effect on the domino escalation potential. Fire, explosion, toxic release and other closely related scenarios can all be considered.

In this chapter, an MILP model is proposed to obtain the optimal multi-floor layout of chemical process plants with risk quantification estimated using the DHI ranking system. The previously proposed MILP models are modified to account for a range of potential hazardous events, their effect on neighbouring equipment items and the installation of protection devices. The rest of the chapter is structured as follows. In the next section (6.2), the problem is described. The step-by-step procedure in calculating the DHI is explained in section 6.3 and the complete mathematical model is given in section 6.4. A case study is solved in section 6.5 showing model efficiency and capabilities, and a summary of the chapter is given in section 6.6.

6.2 Problem description

The problem description is given as follows.

Given:

- a set of process units, their type, dimensions, damage index values and process conditions;
- a set of likely primary events for each equipment item *i*;
- a set of potential floors;
- connectivity network amongst process units;
- cost data (connection, pumping, land, construction, protection devices, equipment purchase);
- space and unit allocation limitations;

to determine:

- total number of floors required;
- base land area;
- area of floors;
- plot layout;
- type and number of protective devices required;
- Domino Hazard Index for each unit;

so as to: minimise the total cost attributed to construction, pumping, connection, protection device installation and domino escalation.

The following assumptions are also made:

- each equipment item is approximated with a rectangular geometry;
- every item is connected to the other from its geometrical centre in the x-y plane, and from a predefined height along the z-plane, based on design calculations;
- for safety considerations, all distances between items of concern are measured from the equipment item boundaries and taken as the Tchebychev distance in all x,y and z planes;
- an item is allowed to rotate through 90° angles about the x-y plane as deemed optimal but must start at the base point of the floor it has been assigned to;

- floors are numbered from bottom to top with a fixed floor height;
- equipment items tall enough to exceed the fixed floor height are allowed to extend through successive floors;
- separating floor structures can act as protection devices against fires and blast wave events.

Nomenclature

The symbols used are defined as follows:

Indices

e	primary events/scenarios
h	potential hazard scenarios
i, j, n	equipment item
k	floor number
p	protection devices
s	rectangular area sizes
$\hat{k}$	piecewise linearisation sample points for Cr_{ij} variable
$\hat{q}$	piecewise linearisation sample points for pool and jet fire DHS_{ij} variable

Sets

Γ^C	set of ordered pairs of connected items i and j
Γ^H	set of ordered pairs of items i and j regarded as highly hazardous
Γ^θ	set of ordered pairs of items i and j regarded as highly hazardous or connected to each other. $\Gamma^\theta = \Gamma^H \cup \Gamma^C$
E	set of primary events/scenarios
H_e	set of potential hazard scenarios for primary event e

I	set of equipment items
I^A	set of atmospheric equipment items
I^T	set of tall equipment items
I^P	set of pressurised equipment items
I^V	set of equipment items likely to release flammable vapours
K	set of potential floors

Parameters

$\alpha_i, \beta_i, \gamma_i$	dimensions of equipment item i
$\delta_{i\theta}$	1 for equipment item i if $\theta \leq I^T$; 0 otherwise
ε	a very small positive number
$\kappa_{ei}^{BW}, \lambda_{ei}^{BW}$	parameter for DHS_{ij} evaluation for blast wave scenario
$\kappa_{ihe\hat{q}}^{A}, \lambda_{ihe\hat{q}}^{A}$	piecewise parameters to evaluate the radiation effects by pool and jet fire events for atmospheric equipment
$\kappa_{ihe\hat{q}}^{P}, \lambda_{ihe\hat{q}}^{P}$	piecewise parameters to evaluate the radiation effects by pool and jet fire events for pressurized equipment
ζ	threshold value for DI for units
BM	a large number
C_i^P	purchase cost of item i
C_{ij}^c	connection costs between items i and j
C_{ij}^H	horizontal pumping costs between items i and j
C_{ij}^v	vertical pumping costs between items i and j
C_{ip}	cost of protection device p on unit i
d_{ei}^F	distance from the surface of item i to the source of primary event e
d_{ei}^S	proposed minimum safety distance from item i for primary event $e \in \{PF, JF\}$
D_{ij}^{min}	minimum distance between items i and j to prevent overlap
De_{ij}^{min}	minimum specified distance between items i and j
DI_i	damage index for equipment item i

f_{ij}	1 if flow direction between equipment items i and j is positive; 0, otherwise
$FC1$	fixed floor construction cost
$FC2$	area-dependent floor construction cost
FH	floor height
IP_{ij}	distance between the base and input point on item j for the connection between items i and j
LC	area-dependent land purchase cost
M_i	number of floors required by equipment item i
OP_{ij}	distance between the base and output point on equipment i for the connection between items i and j
P_i^{lo}, P_i^{up}	static peak overpressure distance limits for blast wave primary event
$\overline{X}_s, \overline{Y}_s$	x-y dimensions of pre-defined rectangular area sizes s

Integer variables

NF	number of floors

Binary variables

$\xi_{ij\hat{k}}$	1 if interval $\hat{k}$, $\hat{k}+1$ is selected during piecewise linearisation of Cr_{ij}; 0 otherwise
B_{ip}	1 if protective device p is installed on equipment item i 0, otherwise
$B^F_{ijhe\hat{q}}$	1 interval $\hat{q}$ is selected to evaluate the radiation effects by pool and jet fire events; 0, otherwise
B^L_{ijhe}	1 if secondary unit j is located within the boundaries for hazard scenario h owing to an event e emanating from item i
$E1_{ij}$, $E2_{ij}$	non-overlapping binary, a set of values which prevents equipment overlap in one direction in the x-y plane
MB^{xy}_{ij}	1 if $XD_{ij} \geq YD_{ij}$; 0 otherwise

MB_{ij}^{z}	1 if $XY_{ij}^{max} \geq VD_{ij}$; 0 otherwise
N_{ij}	1 if items i and j are assigned to the same floor; 0, otherwise
$N_{ijk}^{'}$	1 if items i and j are assigned to floor k; 0, otherwise
O_i	1 if length of item i is equal to α_i; 0, otherwise
Q_s	1 if rectangular area s is selected for the layout; 0, otherwise
S_{ik}^{S}	1 if item i begins on floor k; 0, otherwise
V_{ik}	1 if item i is assigned to floor k
W_k	1 if floor k is occupied; 0, otherwise
W_{ij}^{x}	1 if item i is to the right of item j in the x plane; 0 otherwise
W_{ij}^{xo}	1 if the boundary of item i is strictly to the right or left of item j in the x plane; 0 otherwise
W_{ij}^{y}	1 if item i is above item j in the y plane; 0 otherwise
W_{ij}^{yo}	1 if the boundary of item i is strictly above or below item j in the y plane; 0 otherwise
W_{ij}^{z}	1 if item i is on a higher floor than item j; 0 otherwise

Continuous variables

$\eta_{ij}^{u}, \eta_{ij}^{d}$	positive continuous variables to determine vertical safety distance between items i and j
$\mu_{ijhe\hat{q}}$	variable for selection of piecewise parameter to evaluate radiation effects of pool and jet fire events
ω_i	number of floors by which a multi-floor item $i \in I^T$ extends over the topmost floor
$\phi_{ij\hat{k}}$	variable for piecewise linearisation of Cr_{ij} and DHS_{ij}
A_{ij}	distance in the y plane between items i and j, if i is above j
AR_s	predefined rectangular floor area s
B_{ij}	distance in the y plane between items i and j, if i is below j
C_i^{AL}	direct asset loss of item i
C_i^{DEC}	total cost attributed to domino escalation on unit i

Cr_{ij}	credibility that the failure of unit i affects j
d_i	breadth of item i
d^H_{ijhe}	effective distance between items i and j for primary event e under hazard scenario h
Dn_{ij}	vertical separation distance between items i and j, if i is on a lower floor than j
dr_{ije}	distance of item j from the flame envelope produced by i due to primary event $e \in \{PF, JF\}$
DHI_i	Domino Hazard Index for item i
DHI^T	Domino Hazard Index value for the entire plant; evaluated as $\sum_i DHI_i$
DHS_{ij}	maximum Domino Hazard Score of item i with respect to j for all possible events
DHS^E_{ije}	Domino Hazard Score of item i for event e with reference to j
DHS^H_{ijhe}	Domino Hazard Score for an event e under hazard scenario h emanating from item i to j
FA	base land area
l_i	length of item i
L_{ij}	distance in the x plane between items i and j, if i is to the left of j
NQ_s	linearisation variable expressing the product of NF and Q_s
R_{ij}	distance in the x plane between items i and j, if i is to the right of j
TD_{ij}	total rectilinear distance between items i and j for connection considerations
TD^S_{ij}	total rectilinear distance between items i and j for safety considerations
Up_{ij}	vertical separation distance between items i and j, if i is on a higher floor than j
VD_{ij}	total vertical distance between items i and j
x_i, y_i	x,y coordinates of the geometrical centre of item i
X^{max}, Y^{max}	dimensions of base land area

XY_{ij}^{max}	maximum value between the horizontal separation distance between items i and j in the x- and y- planes
XD_{ij}, YD_{ij}	total horizontal distance between the boundaries of items i and j in the x, y directions respectively
Z_{ij}^{+}, Z_{ij}^{-}	positive continuous variables evaluate the difference between XY_{ij}^{max} and VD_{ij} if $XY_{ij}^{max} > VD_{ij}$ and $XY_{ij}^{max} < VD_{ij}$ respectively

6.3 Domino Hazard Index (DHI)

The steps carried out in estimating the Domino Hazard Index is shown in Fig. 6.1. A description of each step and its mathematical formulation is described below.

Step 1: Determine the separation distance (TD_{ij}^{s}) of each equipment item pair.

Step 2: For each unit i, identify the possible primary events h that can trigger domino effects:

These primary events as outlined by Cozzani et al. (2006) are listed in Table 6.1. Based on the nature/type of the equipment and/or material it processes, a set of primary event can be identified for each unit.

Table 6.1 Escalation vectors and expected secondary scenarios for different primary events

Primary events	Escalation vector	Expected secondary scenarios
Pool fire	Radiation, fire impingement	Jet fire, pool fire, BLEVE, toxic release
Jet fire	Radiation, fire impingement	Jet fire, pool fire, BLEVE, toxic release
Fireball	Radiation, fire impingement	Tank fire
Flash fire	Fire impingement	Tank fire
Blast wave	Overpressure	All[1]

BLEVE - boiling liquid expanding vapour explosion

[1] All - any of the events listed under the 'Primary events' column

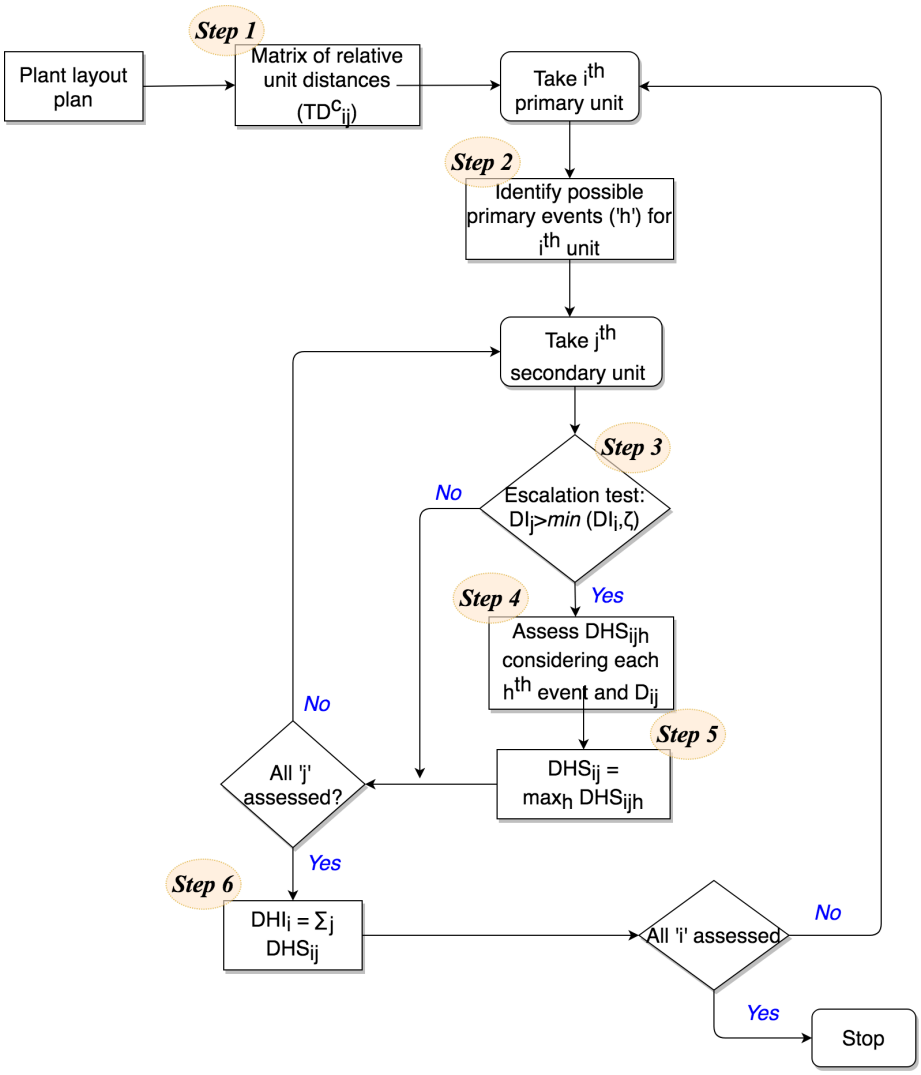

Fig. 6.1 Flow diagram of DHI assessment

Step 3: For each secondary unit j, compare the values of the Damage Index (DI) for both units i and j to take into account only units having significant potential to increase adverse scenarios.

The Damage Index is calculated as described by Khan and Amyotte (2004). The secondary units are selected based on the following condition:

$$\Gamma^H = \{(i,j) : DI_j > min(DI_i, \zeta)\} \tag{6.1}$$

where the value of ζ defines the lower limit of *DI* for units considered as highly hazardous. The set Γ^H defines the pairs of equipment items (i, j) where i is the primary item and hazardous event source, and j is the secondary item susceptible to the domino effects of the event on i.

Step 4: Evaluate the Domino Hazard Score (DHS^E_{ije}) for every identified event e from unit i to unit j.

The Domino Hazard Score (DHS^E_{ije}) is assigned a value of 10 for a highly probably escalation of event e and 0 for the inherently "safest" level for domino escalation. This score is evaluated for every identified primary event's escalation vector. A list of rules for events listed in Table 6.1 are outlined below. These rules help to estimate the values of DHS^E_{ije} where both inherent and passive measures are made available.

Flash fire (FF): For FF events, the score DHS^E_{ije} is 0 or 10 depending on whether the secondary unit j is within direct reach of the flame envelope (d^F_{ei}). No passive protection devices are considered, and assuming the flame originates from the outer surface of unit i:

$$DHS^E_{ije} = \begin{cases} 0, & TD^s_{ij} > d^F_{ei} \\ 10, & TD^s_{ij} \leq d^F_{ei} \end{cases} \quad \forall\,(i,j) \in \Gamma^H, j \in I^V, e \in \{FF\} \tag{6.2}$$

where I^V is the set of units likely to release flammable vapours.

Fire ball (FB): For fire ball events, fire impingement is likely to affect only atmospheric units ($i \in I^A$) (de Lira-Flores et al., 2014) within the fireball radius d^F_{ei}. The presence of passive devices, such as fire insulation (FI), reduce the hazard score:

$$DHS^E_{ije} = \begin{cases} 0, & TD^s_{ij} > d^F_{ei} \\ 5, & TD^s_{ij} \leq d^F_{ei} \text{ FI installed} \\ 10, & TD^s_{ij} \leq d^F_{ei} \text{ FI not installed} \end{cases} \quad \forall\,(i,j) \in \Gamma^H, j \in I^A, e \in \{FB\} \tag{6.3}$$

Pool fire (PF) and Jet fire (JF): From Table 6.1, escalations vectors due to pool and jet fires are by fire impingement and heat radiation. In the case of fire impingement, no passive protection device is considered adequate to reduce the DHS for a unit within the flame envelope (d_{ei}^{F}), as small defects can nullify the protective behaviour (Tugnoli et al., 2008a). For escalation events due to heat radiation, the value of the DHS is influenced by the secondary unit's distance from the flame envelope dr_{ije}, the scenario (jet or pool fire) and the characteristics of the unit (atmospheric or pressurised equipment) (Fig. 6.2). This relationship has been represented as a graph by Tugnoli et al. (2008a) as shown in Figs. 6.3 and 6.4.

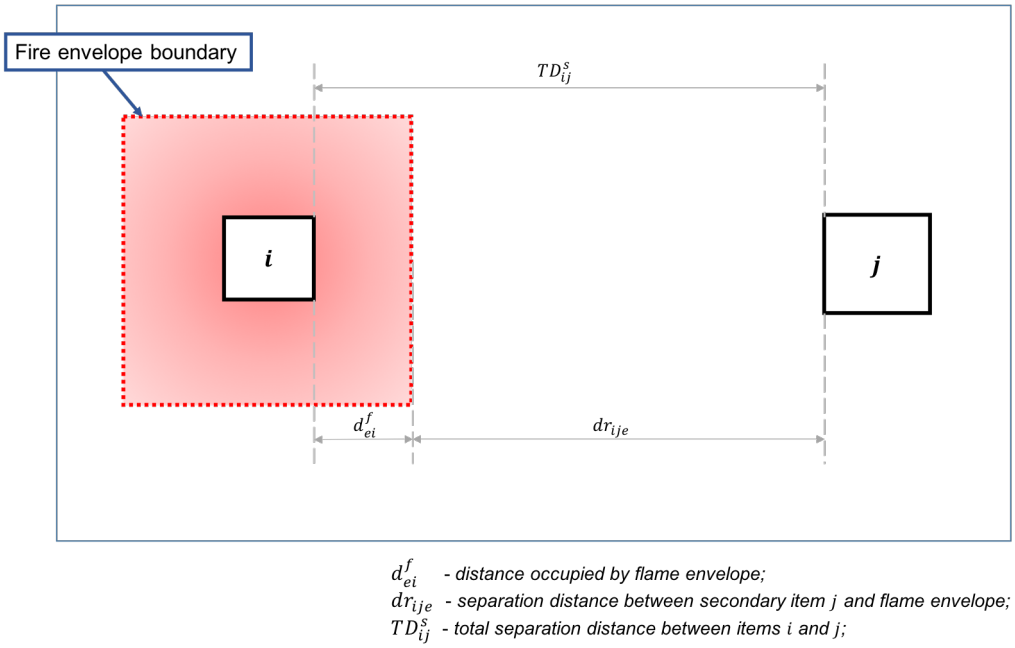

Fig. 6.2 Distance calculations for Pool/Jet fire events

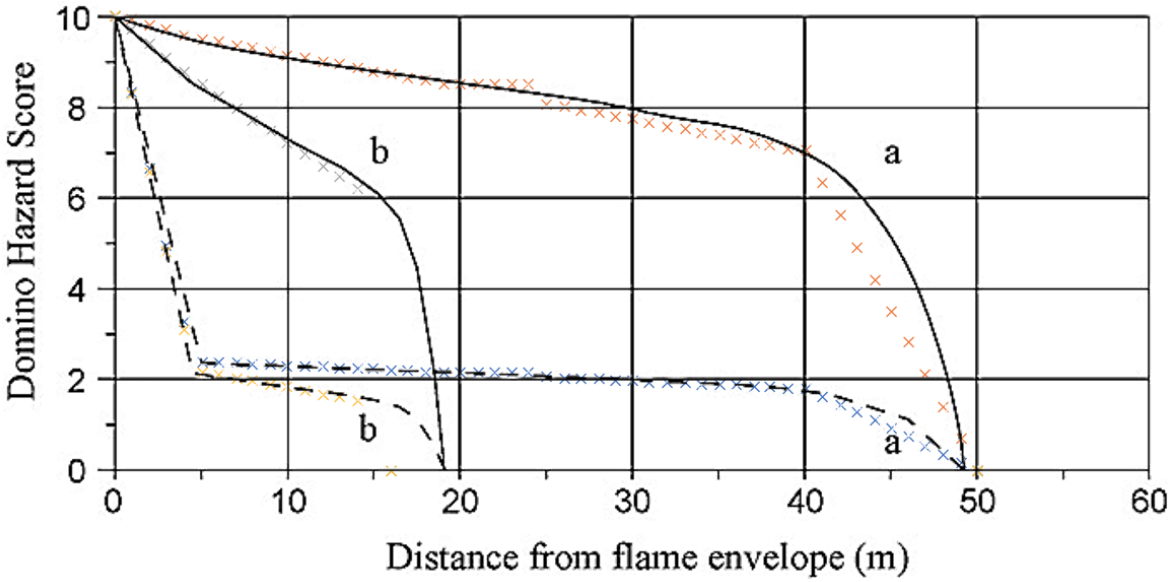

Fig. 6.3 DHS vs distance from flame envelope for pool fire scenarios
Solid line: unprotected items | Dashed line: fire-insulated items | a: atmospheric items | b: pressurized items; X - piecewise linear approximations

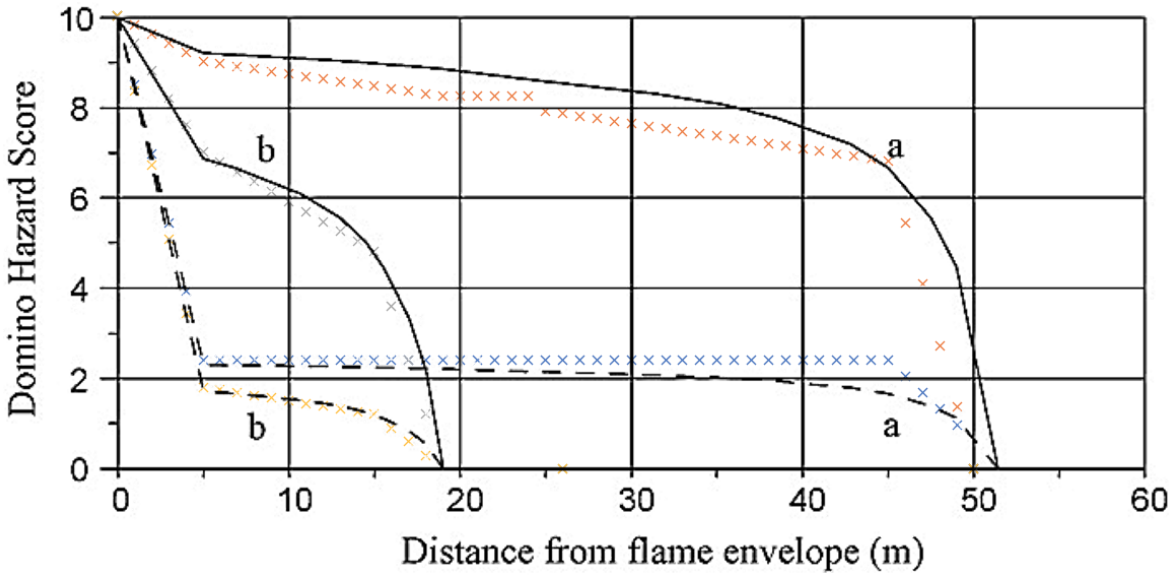

Fig. 6.4 DHS vs distance from flame envelope for jet fire scenarios
Solid line: unprotected items | Dashed line: fire-insulated items | a: atmospheric items | b: pressurized items; X - piecewise linear approximations

A piece-wise linear approximation is given in de Lira-Flores et al. (2014) as follows. For atmospheric equipment items:

$$DHS^{E}_{ije} = \begin{cases} 0, & dr_{ije} > d^{S}_{ej} \\ 1, & dr_{ije} \leq d^{S}_{ej} \text{ FW installed} \\ 10 - \sum_{\hat{q}=1}^{4} \kappa^{A}_{ihe\hat{q}} \cdot \mu_{ijhe\hat{q}}, & 0 < dr_{ije} \leq d^{S}_{ej} \quad \forall\,(i,j) \in \Gamma^{H} \\ & \quad \& \; dr_{ije} = \sum_{q=1}^{4} \lambda^{A}_{ihe\hat{q}} \cdot \mu_{ijhe\hat{q}} \\ 10, & dr_{ije} \leq 0 \end{cases} \tag{6.4}$$

and for pressured equipment items:

$$DHS^{E}_{ije} = \begin{cases} 0, & dr_{ije} > d^{S}_{ej} \\ 1, & dr_{ije} \leq d^{S}_{ej} \text{ FW installed} \\ 10 - \sum_{\hat{q}=1}^{4} \kappa^{P}_{ihe\hat{q}} \cdot \mu_{ijhe\hat{q}}, & 0 < dr_{ije} \leq d^{S}_{ej} \quad \forall\,(i,j) \in \Gamma^{H} \\ & \quad \& \; dr_{ije} = \sum_{q=1}^{4} \lambda^{P}_{ihe\hat{q}} \cdot \mu_{ijhe\hat{q}} \\ 10, & dr_{ije} \leq 0 \end{cases} \tag{6.5}$$

where the values of the parameters $\kappa^{A}_{ihe\hat{q}}$, $\lambda^{A}_{ihe\hat{q}}$ and $\kappa^{P}_{ihe\hat{q}}$, $\lambda^{P}_{ihe\hat{q}}$ are available in de Lira-Flores et al. (2014) as presented in Table 6.2 for pressurised and atmospheric equipment respectively for both unprotected (HZ2) and fire-insulated scenarios; d^{S}_{ei} is the safety distance given by Cozzani et al. (2006) for pool fires (15m - pressurised equipment, 50m - atmospheric equipment) and jet fires (25m - pressurised equipment, 50m - atmospheric equipment); and $\mu_{ijhe\hat{q}}$ are variables satisfying:

- $\mu_{ijhe,1} \leq 1$,
- $\mu_{ijhe,4} \geq 0$ and
- $\mu_{ijhe,\hat{q}+1} \leq B^{F}_{ijhe\hat{q}} \leq \mu_{ijhe\hat{q}}$.

When the distance from the flame source (dr_{ije}) is between a value of 0 and d^{S}_{ei}, and a FW is not installed, the values of $\kappa^{A}_{ihe\hat{q}}$ and $\lambda^{A}_{ihe\hat{q}}$ are appropriately evaluated from dr_{ije} (for

atmospheric items), which is used to obtain the DHS as shown in the third disjunction in equations (6.4) and (6.5). The fits of these linear approximations, using the aforementioned safety distances, are shown in Figs 6.3 and 6.4.

The distance from the secondary unit to the flame source is calculated as:

$$dr_{ije} = TD^{S}_{ij} - d^{F}_{ei} \quad \forall\,(i,j) \in \Gamma^{H}, e \in \{PF, JF\} \tag{6.6}$$

Table 6.2 Piecewise parameters for evaluation of DHS for Pool/Jet fire scenarios

		Atmospheric equipment				**Pressurized equipment**			
		Unprotected		**FI**		**Unprotected**		**FI**	
	$\hat{q}$	$\kappa^{A}_{ihe\hat{q}}$	$\lambda^{A}_{ihe\hat{q}}$	$\kappa^{A}_{ihe\hat{q}}$	$\lambda^{A}_{ihe\hat{q}}$	$\kappa^{P}_{ihe\hat{q}}$	$\lambda^{P}_{ihe\hat{q}}$	$\kappa^{P}_{ihe\hat{q}}$	$\lambda^{P}_{ihe\hat{q}}$
	1	0	0	0	0	0	0	0	0
Pool fire	2	0.5	4.5	7.6	4.5	1.4	4.5	7.8	4.5
scenario	3	2.5	35.5	0.6	35.5	3	11.7	0.8	11.7
	4	7	10	1.8	10	5.6	2.8	1.4	2.8
	1	0	0	0	0	0	0	0	0
Jet fire	2	1	5	7.6	5	3	5	8.2	5
scenario	3	2.2	40	0	40	2.2	10	0.6	10
	4	6.8	5	1.8	5	4.8	4	1.2	4

Source: de Lira-Flores et al. (2014)

Blast wave (BW): Blast wave events encompass all primary events that result in an explosion - mechanical explosion, confined explosion, boiling liquid expanding vapour explosion (BLEVE), vapour cloud explosion (VCE) - with overpressure being the resulting escalation vector. Overpressure is the pressure, over and above the atmospheric pressure, caused by a shock wave from an explosion. The Domino Hazard Scores for blast wave events (DHS^{E}_{ije}) are calculated as a function of the static peak overpressure, which is a function of the distance

from the explosion source (dr_{ije}):

$$DHS^{E}_{ije} = \begin{cases} 0, & dr_{ije} > u^{BW}_{i} \\ 1, & dr_{ije} \leq u^{BW}_{i} \text{ BWl installed} \\ \alpha^{BW}_{i} dr_{ije} + \beta^{BW}_{i} & l^{BW}_{i} \leq dr_{ije} \leq u^{BW}_{i} \\ 10, & dr_{ije} < l^{BW}_{i} \end{cases} \forall\, (i,j) \in \Gamma^{H}, e \in \{BW\} \quad (6.7)$$

where:

$$\alpha^{BW}_{i} = \frac{10}{l^{BW}_{i} - u^{BW}_{i}} \quad (6.8)$$

$$\beta^{BW}_{i} = -\alpha^{BW}_{i} u^{BW}_{i} \quad (6.9)$$

The distance between equipment items is thus given by:

$$dr_{ije} = TD^{S}_{ij} \quad \forall\, (i,j) \in \Gamma^{H}, e \in \{BW\} \quad (6.10)$$

as it is assumed that the explosion source is at the surface of the primary equipment item.

For pressurized items j, DHS is calculated as follows:

$$DHS^{E}_{ije} = \begin{cases} 0, & dr_{ije} > u^{BW}_{i} \\ 1, & dr_{ije} \leq u^{BW}_{i} \text{ BWl installed} \\ 10, & dr_{ije} \leq u^{BW}_{i} \end{cases} \forall\, (i,j) \in \Gamma^{H}, e \in \{BW\} \quad (6.11)$$

Another primary event worthy of mention is toxic release, however this will not be considered in this thesis.

Step 5: *Evaluate the Domino Hazard Score for every unit pair (i, j).*

This value is taken as the highest value amongst all evaluated events:

$$DHS_{ij} \geq DHS^{E}_{ije} \quad \forall\, (i,j) \in \Gamma^{H} \tag{6.12}$$

Step 6: Evaluate the Domino Hazard Index for each unit i.

This is evaluated as follows:

$$DHI_i = \sum_{j:(i,j)\in\Gamma^{H}} DHS_{ij} \quad \forall\, i \tag{6.13}$$

These steps are taken for all available units.

To incorporate these steps within an optimisation problem, additional constraints are included to describe the costs associated with passive measures to reduce domino effects, as well as the damage costs owing to the domino escalation of an event.

6.4 Mathematical formulation

6.4.1 Safety distance constraints

The safety distance estimation method for the Dow's F&EI is also adopted for the DHI (equations (5.2) - (5.30)) where the safety distances between equipment items are calculated as the distance between equipment item boundaries (Fig. 6.5).

Equations (5.2) and (5.3) are re-written for hazardous pairs of equipment items as well as those connected to each other ($(i, j) \in \Gamma^{\theta}$):

$$R_{ij} - L_{ij} = x_i - x_j \qquad \forall\, (i,j) \in \Gamma^{\theta} \tag{6.14}$$

$$A_{ij} - B_{ij} = y_i - y_j \qquad \forall\, (i,j) \in \Gamma^{\theta} \tag{6.15}$$

As previously stated, binary variables W_{ij}^{x} and W_{ij}^{y} force one of R_{ij} or L_{ij} (equation (6.14)), and A_{ij} or B_{ij} (equation (6.15)) to zero respectively by equations (6.16) - (6.19).

$$R_{ij} \leq BM \cdot W_{ij}^{x} \qquad \forall\,(i,j) \in \Gamma^{H} \tag{6.16}$$

$$L_{ij} \leq BM \cdot (1 - W_{ij}^{x}) \qquad \forall\,(i,j) \in \Gamma^{H} \tag{6.17}$$

$$A_{ij} \leq BM \cdot W_{ij}^{y} \qquad \forall\,(i,j) \in \Gamma^{H} \tag{6.18}$$

$$B_{ij} \leq BM \cdot (1 - W_{ij}^{y}) \qquad \forall\,(i,j) \in \Gamma^{H} \tag{6.19}$$

The vertical connection distances for connected items ($(i,j) \in \Gamma^{C}$) is calculated as:

$$U_{ij} - D_{ij} = FH \sum_{k} (k-1)(S_{ik}^{S} - S_{jk}^{S}) + OP_{ij} - IP_{ij} \qquad \forall\,(i,j) \in \Gamma^{C} \tag{6.20}$$

and the total connection distance (TD_{ij}):

$$TD_{ij} = R_{ij} + L_{ij} + A_{ij} + B_{ij} + U_{ij} + D_{ij} \qquad \forall (i,j) \in \Gamma^{C} \tag{6.21}$$

The separation distances between equipment items for safety considerations are calculated as in section 5.3.2 (Fig. 6.5).

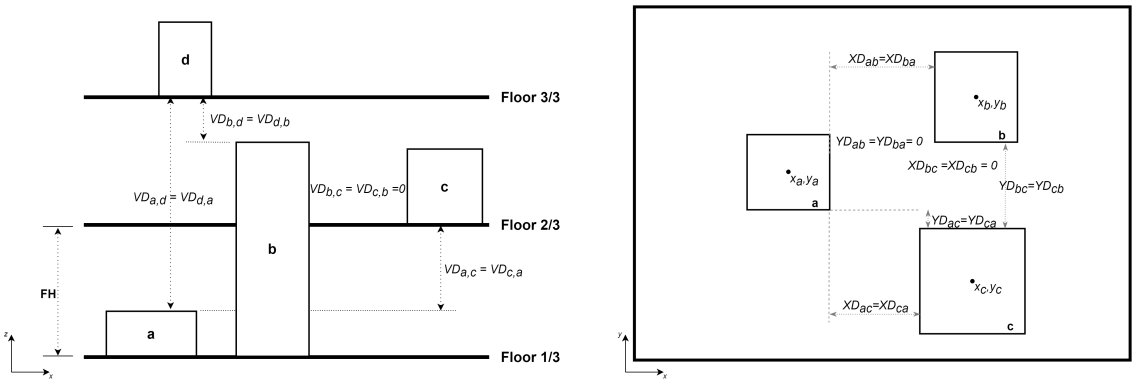

Fig. 6.5 Vertical & Horizontal safety distance estimation

The vertical separation distance between two items is calculated using equations (6.22) - (6.28):

$$\eta^u_{ij} - \eta^d_{ij} = 2FH\sum_k (k-1)(S^S_{ik} - S^S_{jk}) + \gamma_i - \gamma_j \qquad \forall\,(i,j) \in \Gamma^H \tag{6.22}$$

$$\eta^u_{ij} \leq BM \cdot W^z_{ij} \qquad \forall\,(i,j) \in \Gamma^H \tag{6.23}$$

$$\eta^d_{ij} \leq BM \cdot (1 - W^z_{ij}) \qquad \forall\,(i,j) \in \Gamma^H \tag{6.24}$$

$$VD_{ij} = FH\sum_k (k-1)(S^S_{jk} - S^S_{ik}) - \gamma_i + \eta^u_{ij} \qquad \forall\,(i,j) \in \Gamma^H \tag{6.25}$$

$$VD_{ij} \leq FH\sum_k (k-1)(S^S_{jk} - S^S_{ik}) - \gamma_i + \eta^u_{ij} + BM \cdot N_{ij} \qquad \forall\,(i,j) \in \Gamma^H \tag{6.26}$$

$$VD_{ij} \geq FH\sum_k (k-1)(S^S_{jk} - S^S_{ik}) - \gamma_i + \eta^u_{ij} - BM \cdot N_{ij} \qquad \forall\,(i,j) \in \Gamma^H \tag{6.27}$$

$$VD_{ij} \leq BM \cdot (1 - N_{ij}) \qquad \forall\,(i,j) \in \Gamma^H \tag{6.28}$$

Separation distance on the y-plane between equipment items are evaluated using equations (6.29) - (6.32):

$$y_i - y_j + 2B_{ij} \geq \left(\frac{d_i + d_j}{2}\right) - BM \cdot (1 - W^{yo}_{ij}) \qquad \forall\,(i,j) \in \Gamma^H \tag{6.29}$$

$$YD_{ij} \leq A_{ij} + B_{ij} - \left(\frac{d_i + d_j}{2}\right) + BM \cdot (1 - W^{yo}_{ij}) \qquad \forall\,(i,j) \in \Gamma^H \tag{6.30}$$

$$YD_{ij} \geq A_{ij} + B_{ij} - \left(\frac{d_i + d_j}{2}\right) - BM \cdot (1 - W^{yo}_{ij}) \qquad \forall\,(i,j) \in \Gamma^H \tag{6.31}$$

$$YD_{ij} \leq BM \cdot W^{yo}_{ij} \qquad \forall\,(i,j) \in \Gamma^H \tag{6.32}$$

and for the x-plane, equations (6.33) - (6.36) are used:

$$x_i - x_j + 2L_{ij} \geq \left(\frac{l_i + l_j}{2}\right) - BM \cdot (1 - W^{xo}_{ij}) \qquad \forall\,(i,j) \in \Gamma^H \tag{6.33}$$

$$XD_{ij} \leq R_{ij} + L_{ij} - \left(\frac{l_i + l_j}{2}\right) + BM \cdot (1 - W^{xo}_{ij}) \qquad \forall\,(i,j) \in \Gamma^H \tag{6.34}$$

$$XD_{ij} \geq R_{ij} + L_{ij} - \left(\frac{l_i + l_j}{2}\right) - BM \cdot (1 - W^{xo}_{ij}) \qquad \forall\,(i,j) \in \Gamma^H \tag{6.35}$$

$$XD_{ij} \leq BM \cdot W^{xo}_{ij} \qquad \forall\,(i,j) \in \Gamma^H \tag{6.36}$$

The total safety distances between equipment items i and j, however, is calculated as the Tchebychev distance between the equipment boundaries of such items in all x-, y- and z-planes. The Tchebychev distance between any two points in a vector space is the maximum of the differences along any coordinate dimension (Khani and Beigi, 2015). This distance metric is selected as it is a closer estimate to the Euclidean distance between equipment item boundaries than the rectilinear distance. It is also always less than or equal to the Euclidean distance, which ensures than hazard levels within the plant are overestimated, rather than underestimated as is the case with rectilinear distances. The total safety distance is then calculated as:

$$TD_{ij}^{s} = max(XD_{ij}, YD_{ij}, VD_{ij}) \qquad \forall\,(i,j) \in \Gamma^{H} \tag{6.37}$$

Equation (6.37) may also be expressed as $max(max(XD_{ij}, YD_{ij}), VD_{ij})$ which is linearised as follows.

The first part $XY_{ij}^{max} = max(XD_{ij}, YD_{ij})$ is linearised using equations (6.38) - (6.44):

$$XY_{ij}^{max} \leq XD_{ij} + BM \cdot (1 - MB_{ij}^{XY}) \qquad \forall\,(i,j) \in \Gamma^{H} \tag{6.38}$$

$$XY_{ij}^{max} \geq XD_{ij} - BM \cdot (1 - MB_{ij}^{XY}) \qquad \forall\,(i,j) \in \Gamma^{H} \tag{6.39}$$

$$XY_{ij}^{max} \leq YD_{ij} + BM \cdot MB_{ij}^{XY} \qquad \forall\,(i,j) \in \Gamma^{H} \tag{6.40}$$

$$XY_{ij}^{max} \geq YD_{ij} - BM \cdot MB_{ij}^{XY} \qquad \forall\,(i,j) \in \Gamma^{H} \tag{6.41}$$

$$XD_{ij} \geq YD_{ij} - BM \cdot (1 - MB_{ij}^{XY}) \qquad \forall\,(i,j) \in \Gamma^{H} \tag{6.42}$$

$$YD_{ij} \geq XD_{ij} - BM \cdot MB_{ij}^{XY} \qquad \forall\,(i,j) \in \Gamma^{H} \tag{6.43}$$

$$XY_{ij}^{max} \leq BM \cdot (W_{ij}^{XO} + W_{ij}^{YO}) \qquad \forall\,(i,j) \in \Gamma^{H} \tag{6.44}$$

where MB_{ij}^{XY} is a binary variable with a value equal to 1 when XD_{ij} is greater than YD_{ij}. Additional constraints are included to select YD_{ij} if XD_{ij} is zero (equations (6.45)), and XD_{ij} if both XD_{ij} and YD_{ij} are zero (equations (6.46)):

$$MB_{ij}^{XY} \leq W_{ij}^{XO} + W_{ij}^{YO} \qquad \forall\,(i,j) \in \Gamma^{H} \tag{6.45}$$

$$W_{ij}^{XO} \geq MB_{ij}^{XY} \qquad \forall\,(i,j) \in \Gamma^H \tag{6.46}$$

The second part of equation (6.37), $max(XY_{ij}^{max}, VD_{ij})$ is linearised as:

$$TD_{ij}^{s} = XY_{ij}^{max} + ZD_{ij}^{+} \qquad \forall\,(i,j) \in \Gamma^H \tag{6.47}$$

$$ZD_{ij}^{+} - ZD_{ij}^{-} = VD_{ij} - XY_{ij}^{max} \qquad \forall\,(i,j) \in \Gamma^H \tag{6.48}$$

$$ZD_{ij}^{+} \leq BM \cdot MB_{ij}^{z} \qquad \forall\,(i,j) \in \Gamma^H \tag{6.49}$$

$$ZD_{ij}^{-} \leq BM \cdot (1 - MB_{ij}^{z}) \qquad \forall\,(i,j) \in \Gamma^H \tag{6.50}$$

$$MB_{ij}^{z} \leq 1 - N_{ij} \qquad \forall\,(i,j) \in \Gamma^H \tag{6.51}$$

where MB_{ij}^{Z} is a binary variable equal to 1 when $VD_{ij} \geq XY_{ij}^{max}$.

6.4.2 Floor constraints

In addition to the floor constraints in equations (3.1) - (3.5), the following constraints are included.

To accurately estimate if two items are assigned to the same floor ($N_{ij} = 1$), equation (3.2) is replaced by equations (6.52) - (6.58). For equipment item pairs that do not span multiple floors:

$$N_{ij} \geq V_{ik} + V_{jk} - 1 \qquad \forall\, i \notin I^T, j \notin I^T,\ j > i,k \tag{6.52}$$

$$N_{ij} \leq 1 - V_{ik} + V_{jk} \qquad \forall\, i \notin I^T, j \notin I^T,\ j > i,k \tag{6.53}$$

$$N_{ij} \leq 1 + V_{ik} - V_{jk} \qquad \forall\, i \notin I^T, j \notin I^T,\ j > i,k \tag{6.54}$$

As tall equipment items span through more than one floor, the above constraints will be infeasible for such items. A binary variable, $N_{ijk}^{'}$, is thus introduced for a floor by floor consideration to determine the value of N_{ij} for tall equipment items:

$$N_{ijk}^{'} \geq V_{ik} + V_{jk} - 1 \qquad \forall\,(i \in I^T \ or\ j \in I^T),\ j > i,k \tag{6.55}$$

$$N'_{ijk} \leq \frac{V_{ik} + V_{jk}}{2} \qquad \forall\, (i \in I^T \; or \; j \in I^T),\; j > i,k \tag{6.56}$$

The variable N_{ij} is then determined as:

$$N'_{ijk} \leq N_{ij} \qquad \forall\, (i \in I^T \; or \; j \in I^T),\; j > i,k \tag{6.57}$$

$$N_{ij} \leq \sum_k N'_{ijk} \qquad \forall\, (i \in I^T \; or \; j \in I^T),\; j > i \tag{6.58}$$

Equation (6.59) is also written to account for all possible equipment item pairs:

$$N_{ij} = N_{ji} \qquad \forall\, i, j > i \tag{6.59}$$

Equation (6.60) is included to guarantee that existing floors have at least one equipment item assigned to them:

$$W_k \leq \frac{\left(\sum_i S^S_{ik}\right) - 1}{|I|} + 1 \quad \forall\, k \tag{6.60}$$

6.4.3 Flash fire (FF)

For all possible events, a new variable d^H_{ijhe} is introduced expressing the distance between i and j if j is within the distance that defines a hazard scenario h for an event e. For every event e relating to an equipment item pair i, j, only one non-zero value of d^H_{ijhe} is permitted corresponding to a selected hazard scenario from H_e.

For flash fire events, two potential hazard scenarios can occur: HZ1 - corresponding to unit j being within direct reach of the flame envelope and SF - a safe condition where j is outside of the flame envelope produced by unit i. To obtain the correct Domino Hazard Score (DHS) based on the separation distance TD^S_{ij} between two items, the disjunctions in equation (6.2) are reformulated as equations (6.61) - (6.66). Equation (6.61) ensures that non-zero values are obtainable only for the distances between items i and j for scenarios associated

with flash fires ($h \in H_{FF}$, where $H_{FF} = \{HZ1, SF\}$):

$$TD^{S}_{ij} = \sum_{h \in H_{FF}} d^{H}_{ijh,FF} \quad \forall\,(i,j) \in \Gamma^{H}, j \in I^{V} \tag{6.61}$$

The DHS for flash fire events takes a value of 0 or 10 for a SF and HZ1 scenario respectively, as described in equation (6.62):

$$DHS^{E}_{ij,FF} = 10 \cdot B^{L}_{ij,HZ1,FF} \quad \forall\,(i,j) \in \Gamma^{H}, j \in I^{V} \tag{6.62}$$

The distances for each scenario must correspond to the permitted range as described in equation (6.2):

$$d^{H}_{ij,HZ1,FF} \leq d^{F}_{FF,i} \cdot B^{L}_{ij,HZ1,FF} \quad \forall\,(i,j) \in \Gamma^{H}, j \in I^{V} \tag{6.63}$$

$$d^{H}_{ij,SF,FF} \geq (d^{F}_{FF,i} + \varepsilon) \cdot B^{L}_{ij,SF,FF} \quad \forall\,(i,j) \in \Gamma^{H}, j \in I^{V} \tag{6.64}$$

$$d^{H}_{ij,SF,FF} \leq BM \cdot B^{L}_{ij,SF,FF} \quad \forall\,(i,j) \in \Gamma^{H}, j \in I^{V} \tag{6.65}$$

Finally, only one of HZ1 or SF scenario can occur:

$$\sum_{h \in H_{FF}} B^{L}_{ijh,FF} = 1 \quad \forall\,(i,j) \in \Gamma^{H}, j \in I^{V} \tag{6.66}$$

6.4.4 Fireball (FB)

For fireball events, three potential hazard scenarios can occur: HZ1 - corresponding to unit j being within direct reach of the flame envelope, FI - corresponding to a HZ1 scenario with a fire insulation installed on the secondary unit and SF - a safe condition where unit j is outside of the exposure distance of i. Thus, the total separation distance must equal the sum of effective distances of each potential hazard scenario:

$$TD^{S}_{ij} = \sum_{h \in H_{FB}} d^{H}_{ijh,FB} \quad \forall\,(i,j) \in \Gamma^{H}, j \in I^{A} \tag{6.67}$$

where $H_{FB} = \{HZ1, FI, SF\}$. The total DHS for each unit pair i, j is the sum of the DHS for each potential hazard scenario based on the separation distance:

$$DHS^{E}_{ij,FB} = \sum_{h \in H_{FB}} DHS^{H}_{ijh,FB} \quad \forall\, (i,j) \in \Gamma^{H}, j \in I^{A} \tag{6.68}$$

The DHS of each potential hazard scenario for a fireball event, $DHS^{H}_{ijh,FB}$, will only take its corresponding value as stated in equation (6.3) if the separation distance and hazard conditions fall within the allowable limits. Else, a zero value is assigned. This is modelled using equations (6.69) - (6.74).

$$DHS^{H}_{ij,HZ1,FB} = 10 \cdot B^{L}_{ij,HZ1,FB} \quad \forall\, (i,j) \in \Gamma^{H}, j \in I^{A} \tag{6.69}$$

$$d^{H}_{ij,HZ1,FB} \leq d^{F}_{FB,i} \cdot B^{L}_{ij,HZ1,FB} \quad \forall\, (i,j) \in \Gamma^{H}, j \in I^{A} \tag{6.70}$$

$$DHS^{H}_{ij,FI,FB} = 5 \cdot B^{L}_{ij,FI,FB} \quad \forall\, (i,j) \in \Gamma^{H}, j \in I^{A} \tag{6.71}$$

$$d^{H}_{ij,FI,FB} \leq d^{F}_{FB,i} \cdot B^{L}_{ij,FI,FB} \quad \forall\, (i,j) \in \Gamma^{H}, j \in I^{A} \tag{6.72}$$

$$d^{H}_{ij,SF,FB} \geq (d^{F}_{FB,i} + \varepsilon) \cdot B^{L}_{ij,SF,FB} \quad \forall\, (i,j) \in \Gamma^{H}, j \in I^{A} \tag{6.73}$$

$$d^{H}_{ij,SF,FB} \leq BM \cdot B^{L}_{ij,SF,FB} \quad \forall\, (i,j) \in \Gamma^{H}, j \in I^{A} \tag{6.74}$$

where ε is a very small number included to force a strict inequality. Finally, only one potential scenario can occur per time:

$$\sum_{h \in H_{FB}} B^{L}_{ij,h,FB} = 1 \quad \forall\, (i,j) \in \Gamma^{H}, j \in I^{A} \tag{6.75}$$

If a secondary unit j is on a different floor than i, the separating floor structure(s) can be assumed to act as a fire insulating material. Thus:

$$B^{L}_{ij,FI,FB} + B^{L}_{ij,SF,FB} \geq 1 - N_{ij} \quad \forall\, (i,j) \in \Gamma^{H}, j \in I^{A} \tag{6.76}$$

6.4.5 Pool fire (PF) and Jet fire (JF)

For pool and jet fire events, five potential hazard scenarios can occur: HZ1 - corresponding to unit j being within direct reach of the flame envelope, HZ2 - corresponding to unit j being within reach of the effect of heat radiation from the flame envelope, FI - corresponding to a HZ2 scenario with a fire insulation installed on the secondary unit, FW - corresponding to a HZ2 scenario with a firewall installed and SF - a safe condition where unit j is outside of the exposure distance of both the direct flame and radiation effects of i.

For a pool fire event, the separation distance, $dr_{ij,PF}$, between an item j and the flame envelope produced from i is given by:

$$dr_{ij,PF} = TD^{S}_{ij} - d^{F}_{PF,i} \quad \forall\, i \in I^{V}, (i,j) \in \Gamma^{H} \tag{6.77}$$

This distance is equal to the sum of the effective distances for each potential hazard scenario in a pool fire event:

$$dr_{ij,PF} = \sum_{h \in H_{PF}} d^{H}_{ijh,PF} \quad \forall\, i \in I^{V}, (i,j) \in \Gamma^{H} \tag{6.78}$$

where $H_{PF} = \{HZ1, HZ2, FI, FW, SF\}$. The DHS for each potential hazard scenario h in a pool fire event, $DHS^{H}_{ijh,PF}$, is then calculated using equations (6.79) - (6.99). Each score is evaluated based on the separation distance, $dr_{ij,PF}$, between the flame envelope and item j, and other conditions as outlined in equations (6.4) and (6.5). Thus, the DHS for the pool fire event is evaluated as:

$$DHS^{E}_{ij,PF} = \sum_{h \in H_{PF}} DHS^{H}_{ijh,PF} \quad \forall\, i \in I^{V}, (i,j) \in \Gamma^{H} \tag{6.79}$$

For HZ1 scenario to occur, the secondary item j has to be within direct reach of the flame envelope:

$$DHS^{H}_{ij,HZ1,PF} = 10 \cdot B^{L}_{ij,HZ1,PF} \quad \forall\, i \in I^{V}, (i,j) \in \Gamma^{H} \tag{6.80}$$

$$d^H_{ij,HZ1,PF} \leq 0 \quad \forall\, i \in I^V, (i,j) \in \Gamma^H \tag{6.81}$$

HZ2 and FI scenarios corresponds to item j being within reach of the effect of heat radiation ($0 < dr_{ije} \leq d^S_{ej}$) and having no device protection or a fire insulation installed respectively. The trend in values for the DHS is shown in Fig. 6.3 and a linear representation is given in equations (6.82) - (6.90) where $HI = \{HZ2, FI\}$. For atmospheric secondary item j:

$$DHS^H_{ijhPF} = 10 \cdot B^L_{ijhPF} - \sum_{\hat{q}} \kappa^A_{ihe\hat{q}} \mu_{ijhe\hat{q}} \quad \forall\, i \in I^V, (i,j) \in \Gamma^H, j \in I^A, h \in \{HZ2, FI\} \tag{6.82}$$

$$d^H_{ijh,PF} = \sum_{\hat{q}} \lambda^A_{ihe\hat{q}} \mu_{ijhe\hat{q}} \quad \forall\, i \in I^V, (i,j) \in \Gamma^H, j \in I^A, h \in \{HZ2, FI\} \tag{6.83}$$

$$\mu_{ijh,PF,1} \leq 1 \quad \forall\, i \in I^V, (i,j) \in \Gamma^H, h \in \{HZ2, FI\} \tag{6.84}$$

$$\mu_{ijh,PF,4} \geq 0 \quad \forall\, i \in I^V, (i,j) \in \Gamma^H, h \in \{HZ2, FI\} \tag{6.85}$$

$$\mu_{ijh,PF,\hat{q}+1} \leq B^F_{ijh,PF,\hat{q}} \quad \forall\, i \in I^V, (i,j) \in \Gamma^H, h \in \{HZ2, FI\} \tag{6.86}$$

$$B^F_{ijh,PF,\hat{q}} \leq \mu_{ijh,PF,1} \quad \forall\, i \in I^V, (i,j) \in \Gamma^H, h \in \{HZ2, FI\} \tag{6.87}$$

$$B^F_{ijh,PF,\hat{q}} \leq B^L_{ijh,PF} \quad \forall\, i \in I^V, (i,j) \in \Gamma^H, h \in \{HZ2, FI\} \tag{6.88}$$

$$\varepsilon \cdot B^L_{ijhPF} \leq d^H_{ijh,PF} \quad \forall\, i \in I^V, (i,j) \in \Gamma^H, h \in \{HZ2, FI\} \tag{6.89}$$

$$d^H_{ijh,PF} \leq d^S_{PF,j} B^L_{ijh,PF} \quad \forall\, i \in I^V, (i,j) \in \Gamma^H, h \in \{HZ2, FI\} \tag{6.90}$$

For pressurized secondary items, equations (6.82) and (6.83) are replaced with (6.91) and (6.92) below:

$$DHS^H_{ijh,PF} = 10 \cdot B^L_{ijh,PF} - \sum_{\hat{q}} \kappa^P_{ihe\hat{q}} \mu_{ijhe\hat{q}} \quad \forall\, i \in I^V, (i,j) \in \Gamma^H, j \in I^P, h \in \{HZ2, FI\} \tag{6.91}$$

$$d^H_{ijh,PF} = \sum_{\hat{q}} \lambda^P_{ihe\hat{q}} \mu_{ijhe\hat{q}} \quad \forall\, i \in I^V, (i,j) \in \Gamma^H, j \in I^P, h \in \{HZ2, FI\} \tag{6.92}$$

FW scenarios correspond to the same conditions as the HZ2 scenario with the addition of an installed firewall for item j. A DHS of 1 is assigned to this scenario:

$$DHS^{H}_{ij,FW,PF} = B^{L}_{ij,FW,PF} \quad \forall\, i \in I^{V}, (i,j) \in \Gamma^{H} \tag{6.93}$$

$$d^{H}_{ij,FW,PF} \leq d^{S}_{PF,i} B^{L}_{ij,FW,PF} \quad \forall\, i \in I^{V}, (i,j) \in \Gamma^{H} \tag{6.94}$$

Finally, if the secondary item is out of reach of the effects of radiation and direct flame impingement, a DHS of 0 is assigned:

$$(d^{S}_{PF,j} + \varepsilon) \cdot B^{L}_{ij,SF,PF} \leq d^{H}_{ij,SF,PF} \quad \forall\, i \in I^{V}, (i,j) \in \Gamma^{H} \tag{6.95}$$

$$d^{H}_{ij,SF,PF} \leq BM \cdot B^{L}_{ij,SF,PF} \quad \forall\, i \in I^{V}, (i,j) \in \Gamma^{H} \tag{6.96}$$

and only one hazard scenario can occur:

$$\sum_{h \in H_{PF}} B^{L}_{ijh,PF} = 1 \quad \forall\, i \in I^{V}, (i,j) \in \Gamma^{H} \tag{6.97}$$

Additional constraints ((6.98) - (6.99)) are included to ensure that separation distance values are assigned to the right hazard scenario based on equations (6.4) and (6.5).

$$d^{H}_{ijh,PF} \leq d^{S}_{PF,i}(B^{L}_{ij,HZ2,PF} + B^{L}_{ij,FI,PF} + B^{L}_{ij,FW,PF}) + BM \cdot B^{L}_{ij,SF,PF} \quad \forall\, i \in I^{V}, (i,j) \in \Gamma^{H}, h \in H_{PF} \tag{6.98}$$

$$d^{H}_{ijh,PF} \geq -d^{F}_{PF,i} \cdot (B^{L}_{ij,HZ1,PF} + B^{L}_{ij,FW,PF}) + (d^{S}_{PF,i} + \varepsilon) \cdot B^{L}_{ij,SF,PF} \quad \forall\, i \in I^{V}, (i,j) \in \Gamma^{H}, h \in H_{PF} \tag{6.99}$$

Similar to equation (6.76), if a secondary unit j is on a different floor, it is assumed that the separating floor structure acts as a fire insulator/wall. Thus:

$$B^{L}_{ij,FW,PF} + B^{L}_{ij,FI,PF} + B^{L}_{ij,SF,PF} \geq 1 - N_{ij} \quad \forall\, i \in I^{V}, (i,j) \in \Gamma^{H} \tag{6.100}$$

The same set of equations (6.77) - (6.100) apply to a jet fire event.

6.4.6 Blast wave (BW)

For blast wave events, four potential hazard scenarios can occur for atmospheric secondary equipment items based on the disjunction in equation (6.7): HZ1 - corresponding to unit j being within a distance where static peak overpressure can cause the most damage, HZ2 - corresponding to unit j being within a linearly reducing damage effect of overpressure originating from unit i, BWl - corresponding to a HZ2 scenario with a barricade such as a blast wall (BWl) installed by the secondary unit, and SF - a safe condition where unit j is well outside the distance range of the damaging effect from overpressure. For pressurized secondary equipment items, hazard scenario HZ2 does not exist.

The distance from the explosion source $dr_{ij,BW}$ is given by:

$$dr_{ij,BW} = TD^{S}_{ij} - d^{F}_{BW,i} \quad \forall\,(i,j) \in \Gamma^{H} \tag{6.101}$$

The sum of the effective distance for each hazard scenario, $d^{H}_{ijh,BW}$, must be equal to the distance from the explosion source both for atmospheric (equation (6.102) and pressurized secondary items (equation (6.103)).

$$dr_{ij,BW} = \sum_{h \in H_{BW}} d^{H}_{ijh,BW} + d^{H}_{ij,HZ2,BW} \mid_{j \in I^{A}} \quad \forall\,(i,j) \in \Gamma^{H} \tag{6.102}$$

where $H_{BW} = \{HZ1, BWl, SF\}$. The DHS for items i, j is the sum of the DHS for each scenario defined by H_{BW} plus an additional term for HZ2 scenario if the secondary item is atmospheric:

$$DHS^{E}_{ij,BW} = \sum_{h \in H_{BW}} DHS^{H}_{ijh,BW} + DHS^{H}_{ij,HZ2,BW} \mid_{j \in I^{A}} \quad \forall\,(i,j) \in \Gamma^{H} \tag{6.103}$$

For HZ1 scenario, a DHS of 10 is assigned if the secondary item is within the upper distance limit for pressurized secondary items, and the lower distance limit for atmospheric secondary items.

$$DHS^{H}_{ij,HZ1,BW} = 10 \cdot B^{L}_{ij,HZ1,BW} \quad \forall\,(i,j) \in \Gamma^{H} \tag{6.104}$$

$$d^H_{ij,HZ1,BW} \geq 0 \quad \forall\,(i,j) \in \Gamma^H \tag{6.105}$$

$$d^H_{ij,HZ1,BW} \leq \left((P^{lo}_i - \varepsilon) \mid_{j \in I^A} + P^{up}_i \mid_{j \in I^P} \right) \cdot B^L_{ij,HZ1,BW} \quad \forall\,(i,j) \in \Gamma^H \tag{6.106}$$

HZ2 scenario only occurs for atmospheric secondary equipment items where the DHS is evaluated if the distance from the explosion source is within the upper and lower distance limits (P^{up}_i, P^{lo}_i):

$$DHS^H_{ij,HZ2,BW} = \kappa^{BW}_{ei} \cdot d^H_{ij,HZ2,BW} + \lambda^{BW}_{ei} \cdot B^L_{ij,HZ2,BW} \quad \forall\,(i,j) \in \Gamma^H \cap I^A \tag{6.107}$$

$$P^{lo}_i \cdot B^L_{ij,HZ2,BW} \leq d^H_{ij,HZ2,BW} \quad \forall\,(i,j) \in \Gamma^H, j \in I^A \tag{6.108}$$

$$d^H_{ij,HZ2,BW} \leq P^{up}_i \cdot B^L_{ij,HZ2,BW} \quad \forall\,(i,j) \in \Gamma^H, j \in I^A \tag{6.109}$$

The installation of a barricade such as a blast wall acts as a passive measure and limits the effect of overpressure on the secondary item. This corresponds to scenario BWl and occurs when the separation distance from the explosion source is within the upper distance limit for overpressure:

$$DHS^H_{ij,BWl,BW} = B^L_{ij,BWl,BW} \quad \forall\,(i,j) \in \Gamma^H \tag{6.110}$$

$$d^H_{ij,BWl,BW} \geq 0 \quad \forall\,(i,j) \in \Gamma^H \tag{6.111}$$

$$d^H_{ij,BWl,BW} \leq P^{up}_i \cdot B^L_{ij,BWl,BW} \quad \forall\,(i,j) \in \Gamma^H \tag{6.112}$$

Separating floor structures can also act as barricades to reduce the effect of overpressure. Hence, if the two items are on different floors and not within the safe zone, the separating floor is considered to be a blast wall:

$$B^L_{ij,BWl,BW} + B^L_{ij,SF,PF} \geq 1 - N_{ij} \quad \forall\,(i,j) \in \Gamma^H \tag{6.113}$$

If the separating distance between the secondary item and the point of explosion is greater than the upper overpressure distance limit, such item is considered to be at a safe distance

away:

$$(P_i^{up} + \varepsilon) B_{ij,SF,BW}^L \leq d_{ij,SF,BW}^H \quad \forall\, (i,j) \in \Gamma^H \tag{6.114}$$

$$d_{ij,SF,BW}^H \leq BM \cdot B_{ij,SF,BW}^L \quad \forall\, (i,j) \in \Gamma^H \tag{6.115}$$

Finally, only one of the mentioned hazard scenarios can occur for each equipment pair i, j depending on the equipment type of the secondary item j - atmospheric or pressurized:

$$\sum_{h \in H_{BW}} B_{ijh,BW}^L + B_{ij,HZ2,BW}^L \,|_{j \in I^A} = 1 \quad \forall\, (i,j) \in \Gamma^H \tag{6.116}$$

6.4.7 Protection device cost

Passive measures to prevent or reduce domino escalation are taken by the installation of protective devices (p). Each protection device type/configuration p corresponds to a potential hazard scenario which has the possibility of reducing domino effects: fire insulation (FI), firewall (FW), blast wall (BWl). The cost associated with the purchase, installation and maintenance of such device is given as:

$$C_i^{PD} = \sum_p C_{ip} \cdot B_{ip} \quad \forall\, i \tag{6.117}$$

where:

$$B_{j,FI} \geq B_{ij,FI,e}^L + N_{ij} - 1 \quad (i,j) \in \Gamma^H, e \tag{6.118}$$

$$B_{j,FW} \geq B_{ij,FW,e}^L + N_{ij} - 1 \quad (i,j) \in \Gamma^H, e \tag{6.119}$$

$$B_{j,BWl} \geq B_{ij,BWl,e}^L + N_{ij} - 1 \quad (i,j) \in \Gamma^H, e \tag{6.120}$$

The last two terms on the RHS of equations (6.118) - (6.120) ensure that passive protection device cost are only included when an actual device is installed, as opposed to separating floors acting as firewalls, fire insulators and/or blast walls.

6.4.8 Cost of expected losses

The total cost attributed to losses caused by accidental events in a unit i is given by the Domino Escalation Cost C_i^{DEC}.

$$C_i^{DEC} = \sum_{j:(i,j)\in\Gamma^H} C_j^{AL} \cdot Cr_{ij} \quad \forall\, i \tag{6.121}$$

$$C_j^{AL} = C_j^P \quad \forall\, j \tag{6.122}$$

It accounts for the loss associated with domino escalation to secondary units, and C_j^{AL} is the direct asset loss of the unit. This direct asset loss is represented as the purchase cost of all the equipment items affected. Cr_{ij} is the parameter that represents the assurance that an event in item i affects secondary item j. It is determined as a function of the Domino Hazard Score (DHS_{ij}). This function is expressed as (de Lira-Flores et al., 2014):

$$Cr_{ij} = a \cdot DHS_{ij}^3 + b \cdot DHS_{ij}^2 + c \cdot DHS_{ij} \quad \forall\, (i,j) \in \Gamma^H \tag{6.123}$$

where $a = 6.7374 \times 10^{-4}$, $b = 4.9158 \times 10^{-4}$ and $c = 2.7498 \times 10^{-2}$.
The human health loss and environmental clean-up cost are not considered.

Equation (6.123) has non-linear terms hence a piecewise linear approximation is used to linearise the expression (D'Ambrosio et al., 2010). Samples points, $\hat{k}$, are taken for DHS_{ij} between 0 and 10 ($D\hat{H}S_{ij\hat{k}}$) and the corresponding values of Cr_{ij} evaluated ($\hat{Cr}_{ij\hat{k}}$). An SOS2 variable ($\phi_{ij\hat{k}}$) is introduced and equation (6.123) is re-written as:

$$Cr_{ij} = \sum_{\hat{k}} \hat{Cr}_{ij\hat{k}} \phi_{ij\hat{k}} \quad \forall\, (i,j) \in \Gamma^H \tag{6.124}$$

$$DHS_{ij} = \sum_{\hat{k}} D\hat{H}S_{ij\hat{k}} \phi_{ij\hat{k}} \quad \forall\, (i,j) \in \Gamma^H \tag{6.125}$$

Figure 6.6 shows a plot of the values of Cr_{ij} vs DHS_{ij} obtained from equation (6.123) and the piecewise linearisation approximation. Using 11 equidistant sample points with DHS_{ij} values ranging from 0 - 10 (inclusive) obtained a good fit.

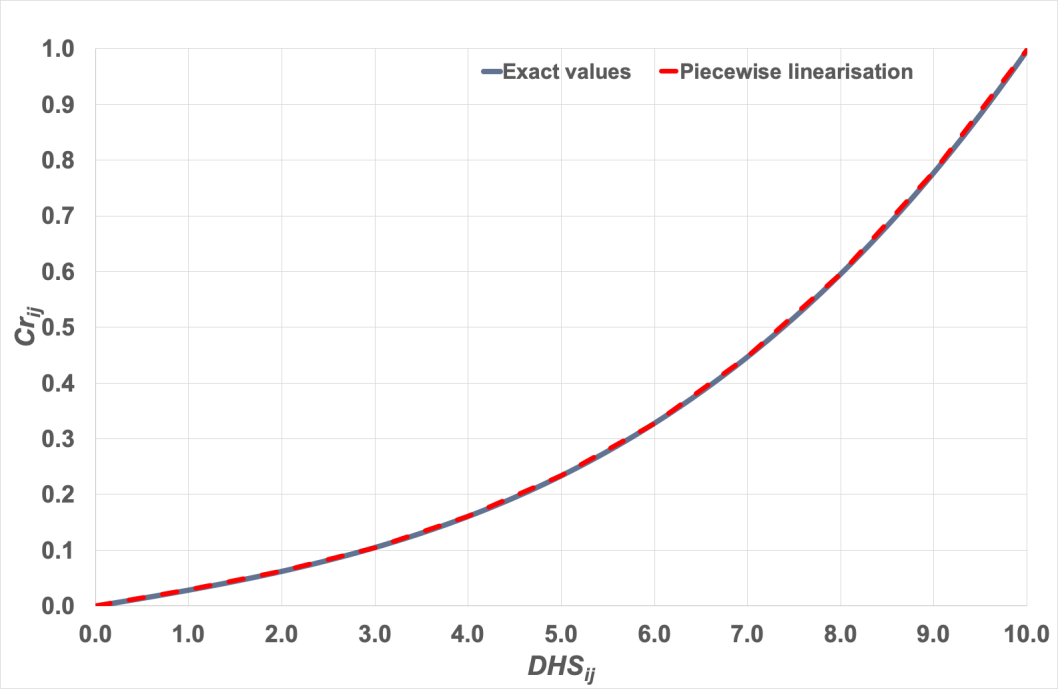

Fig. 6.6 Plots of Cr_{ij} vs DHS_{ij} using the exact values (equation (6.123)) and piecewise linear approximation

6.4.9 Objective function

The objective function is then to minimize the total cost attributed to piping, pumping, construction, protective device installation, as well as losses due to accidental events:

$$\begin{aligned} min \sum_{i,j:f_{ij}=1} \left(C^c_{ij} T D_{ij} + C^v_{ij} D_{ij} + C^H_{ij}(R_{ij} + L_{ij} + A_{ij} + B_{ij})\right) \\ + FC1 \cdot NF + FC2 \sum_s AR_s \cdot NQ_s + LC \cdot FA \\ + \sum_i C^{PD}_i + \sum_i C^{DEC}_i \end{aligned} \tag{6.126}$$

subject to layout constraints (3.1), (3.3) - (3.7), (3.13) - (3.16), (3.21) - (3.30), (3.34) - (3.36), (3.54) - (3.58), (6.52) - (6.60); and safety constraints (6.1), (6.12) - (6.36), (6.38) - (6.51), (6.61) - (6.122) and (6.124) - (6.125). This constitutes model A.4$^+$_IC_DHI.

6.5 Case study of an acrylic acid plant

The proposed model was applied to an acrylic acid production plant (Fig. 6.7) adapted from de Lira-Flores et al. (2014). The plant consists of 11 equipment items with details on equipment dimensions, costs and connectivity available in section B.6. Values for the damage index, equipment purchase cost, protection device cost, and other safety data are given in Table B.15, with four floors made available for layout considerations. 11 sample points, $\hat{k}$, were used for the piecewise linearisation of Cr_{ij} with a step size of 1. The example was solved with and without safety considerations using models A.4^{+}_IC_DHI and A.4^{+}_IC respectively. Domino escalation costs were post-processed for the solution of model A.4^{+}_IC using the same assumptions in model A.4^{+}_IC_DHI.

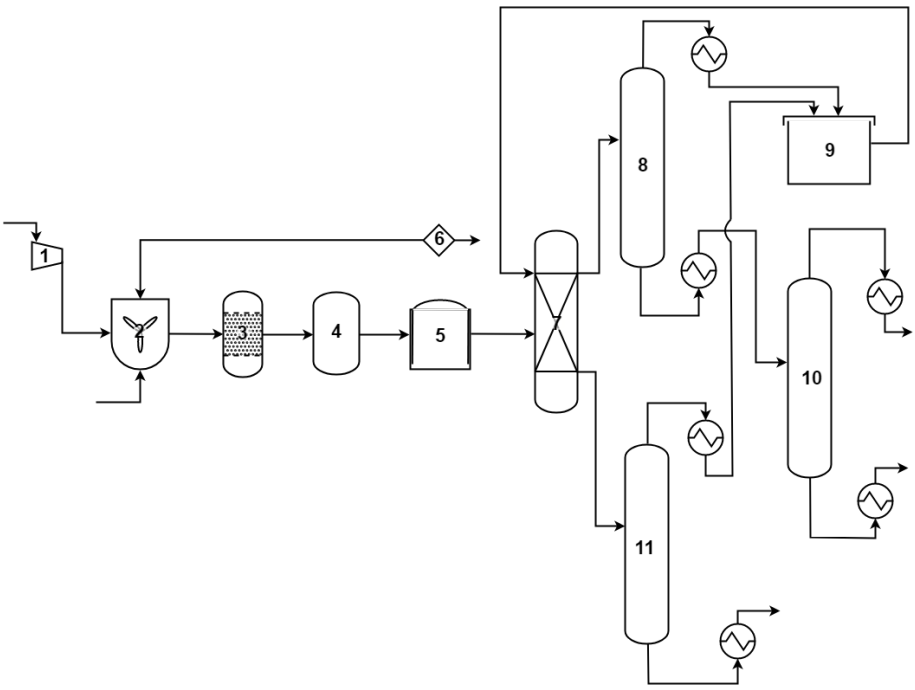

Fig. 6.7 Flow diagram of acrylic acid process plant (See Table B.14 in Appendix B for a description of the equipment item labels)

The set of highly hazardous equipment item pairs (Γ^{H}) was identified using the values in Table B.15, equation (6.1) and a lower *DI* limit of 25. The acid extractor (item 7) and solvent mixer (item 9) were identified as atmospheric equipment items (I^{A}) and also prone to

flammable vapours (I^V) having a radius of exposure for pool fire events of 3.6m and 4.0m respectively.

Table 6.3 gives a summary of the model statistics for each of the runs performed - with and without safety considerations. In both considerations, the models obtained the globally optimal solution in less than six minutes. Despite model A.4$^+$_IC_DHI having a large number of equipment items (when compared to similar attempts in literature) and a relatively larger number of decision variables, the solution was obtained in 307.3s. This shows that the model was more efficient in handling the multi-floor layout problem with safety using the Domino Hazard Index.

Table 6.3 Model Statistics & computational performance

	Without safety	With safety
Layout cost (rmu)	617,619.3	652,148.3
Domino escalation cost (rmu)	171,539.8	12,613.3
Safety device cost (rmu)	0.0	2,351.0
Total cost (rmu)	**789,159.1**	**667,112.7**
CPU (s)	7.0	307.3
Number of discrete variables	303	1578
Number of continuous variables	381	2131
Number of equations	1101	4928

Figs. 6.8 and 6.9 show the optimal layout of the AA plant without and with safety considerations having a total cost of 789,159.1 rmu and 667,112.7 rmu respectively. The same floor area of 5m$\times$10m was obtained in both cases, but when safety was considered 4 floors, compared to 3, were required. This additional floor helps to lower the risk level by providing more space for greater inter-equipment spacing as well as acting as a passive protective device. Items 7 and 9, which were particularly prone to a greater number of hazardous events than the rest, were separated from most of the other equipment items in floors 2 and 1 respectively. Item 5 (floor 3) was placed close to item 7 though as the equipment item pair was not identified as hazardous owing to the criteria in equation 6.1. As

such, the model accounts for specific interactions between equipment items based on the DHI rules to ensure minimal risk.

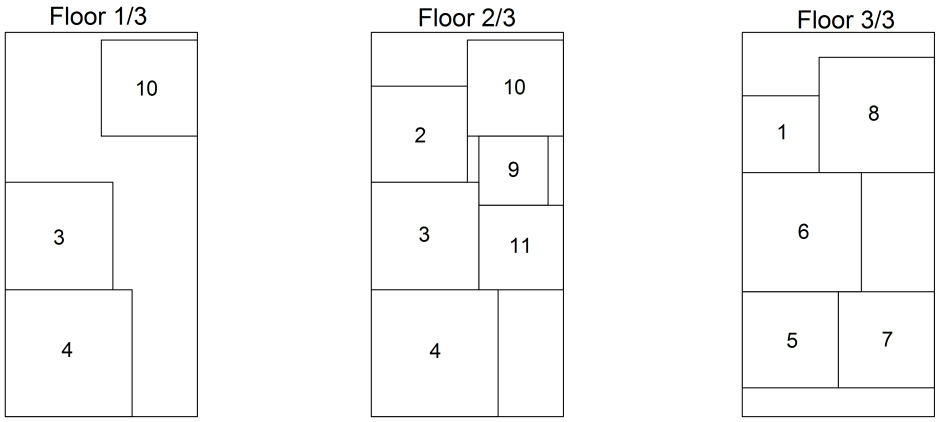

Fig. 6.8 Optimal layout of AA Plant without safety considerations

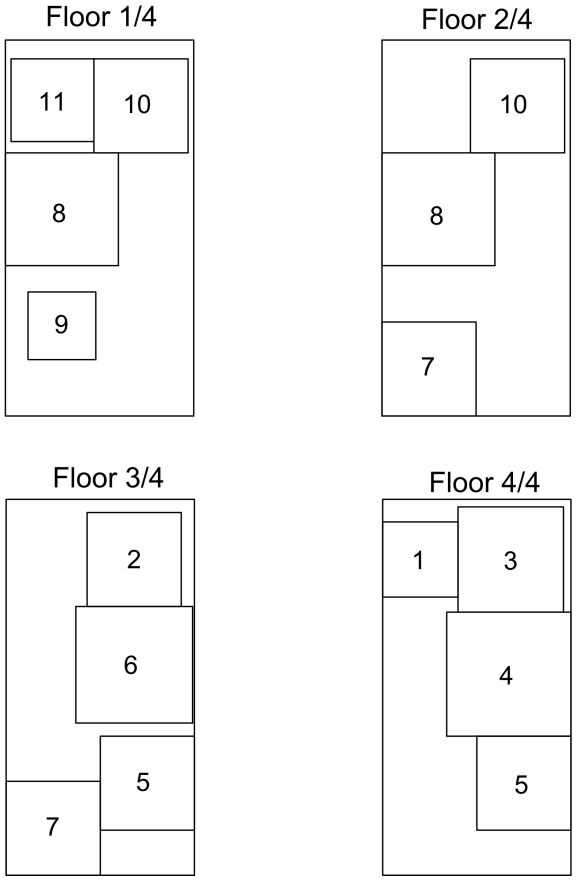

Fig. 6.9 Layout of AA Plant with safety considerations

This minimization of risk by the current layout is captured by the Domino escalation cost. Although a larger layout cost (652,148.3 vs 617,619.3 rmu) is obtained when safety is considered, a much greater reduction is achieved in terms of the financial risk (12,613.3 vs 171,539.8rmu). Layout costs encapsulate pipe installation, pumping, purchasing land and constructing the selected floors, while the Domino escalation cost deals with the purchase of all secondary units affected by the primary items event(s). Although not quantified in this case, the latter cost also affects people and the neighbouring environment by extension.

Table 6.4 shows the DHI values for each equipment item with and without safety considerations as well as the units with installed safety devices for the former case. The DHI value is the sum of scores given to the worst possible event that can occur on all secondary units, escalating from a primary unit. A score of 0 indicates an inherently 'safer' level while a higher score indicates a greater probability for domino escalation. Across all units, table 6.4 shows a reduction in the DHI with non-zero values. This denotes a general increase in the overall safety level of the plant. For some equipment items, protection devices were installed to ensure this - fire insulation on item 11. New firewalls and blastwalls were not purchased as the separating floor structure was assumed to act as such. Hence the need to purchase such devices was prevented as the solution, in most cases, placed such hazardous item pairs on different floors or outside the radius of exposure of the primary item. For example, primary item 1 and items 2 and 7 may have required a blast wall if they were closer together and on the same floor.

Table 6.4 DHI values & installed protection devices on equipment items

i	Description	DHI[1]	DHI[2]	FI	FW	BWl
1	Compressor	0.0	0.0			
2	Feed mixer	0.0	0.0			
3	Reactor	0.0	0.0			
4	Quench	0.0	0.0			
5	Absorber	0.0	0.0			
6	Splitter	10.0	0.0			
7	Acid Extractor	1.0	1.0			
8	Distillation 1	0.0	0.0			
9	Solvent mixer	32.0	5.5			
10	Distillation 2	0.0	0.0			
11	Distillation 3	10.0	0.0	✓		

[1] Without safety considerations

[2] With safety considerations

As stated earlier, the Tchebychev distance was used to calculate the separation distance between equipment items for safety considerations. This metric was adopted as it represented a better approximation to the Euclidean distance when compared to rectilinear measurements. The Euclidean distance, although a more accurate measurement, introduces non-linear terms to the model, making it difficult and/or unpredictable in obtaining solutions for different problems. For example, using the current case study, no solution was obtained using the Euclidean distance over the 3-dimensional space with GAMS/BARON within 1 hour. To demonstrate the benefits of this choice of the Tchebychev metric, the DHI value for each unit post-processed using the results obtained in the final layout with safety considerations, recalculating the separation distances from the equipment boundaries using the Euclidean distance metric. The DHI values were chosen as they have a direct effect on the overall safety level, choice of protection devices and layout configuration of the plant. The comparison is shown in table 6.5.

Table 6.5 Distance metrics comparison and the effect on DHI values

Equipment	Description	DHI_i	
		Tchebychev	Euclidean
1	Compressor	0.0	0.0
2	Feed mixer	0.0	0.0
3	Reactor	0.0	0.0
4	Quench	0.0	0.0
5	Absorber	0.0	0.0
6	Splitter	0.0	0.0
7	Acid Extractor	1.0	1.0
8	Distillation 1	0.0	0.0
9	Solvent mixer	5.5	5.5
10	Distillation 2	0.0	0.0
11	Distillation 3	0.0	0.0

As can be seen from Table 6.5, for all equipment items the DHI values calculated using the Tchebychev metric matched that obtained using the Euclidean distance. This shows that for the current case study, the Tchebychev distance was a good approximation for estimating the safety/separation distance, with the added advantage of avoiding the computational complexity when using the Euclidean metric.

6.6 Concluding remarks

In this chapter, an efficient MILP model was proposed for the multi-floor process plant layout problem considering the domino effect of hazardous events on process plant equipment items. Using the set of rules outlined by the domino hazard ranking system, primary equipment items susceptible to hazardous events including flash fires, jet fires, pool fires, fire balls and blast waves were identified, along with secondary items which could also be affected by these incidents. Using Domino Hazard Scores, the probability (and impact) of these

incidents escalating to secondary items were estimated and included in the MILP model with an objective to simultaneously minimise the total costs attributed to the layout of the equipment items, losses due to equipment damage as well as the installation of protection devices to mitigate such events.

Using an acrylic acid plant from literature, the performance and capability of the proposed model were demonstrated. Globally optimal solutions were obtained in less than six minutes considering all aforementioned incidents of fires and blast wave. Layout configurations showed that hazardous equipment items were placed outside of the primary item's radius of exposure or a form of protection device was installed. Although the total layout cost was higher when compared to the layout configuration without safety consideration, the domino escalation cost savings was far greater.

CHAPTER 7

CONCLUSIONS AND RECOMMENDATIONS

The aim of this thesis was to develop more efficient mathematical programming models to tackle the process plant layout problem towards its use in the systematic and/or automated design of layout configurations. The problem solved was characterised by as many features as addressed in literature, plus additional considerations for a more realistic evaluation of layout configurations. Novel mathematical models were developed to address a host of layout and safety features, and industry-relevant case studies were solved to demonstrate the proposed models superior performance, capabilities and unique characteristics in tackling the layout problem. In the following sections, a summary of this thesis is given and the recommendations for future work are presented.

7.1 Summary

In Chapter 2, the literature was reviewed. A background to the process plant layout problem was given highlighting its characteristics and underlying assumptions. Features of the problem considered in the past by researchers were presented showing their differing approaches in formulating the problem and solving it. The advantages of each method adopted in the past were identified, as well as the difficulties encountered and the gap that needed to be filled by current research endeavours. Two key areas were thus identified as lacking:

availability of scalable models to obtain globally optimal solutions by exact approaches, and the inclusion of a range of realistic layout features in one efficient mathematical model.

To this end, novel mixed integer linear programming (MILP) models were proposed in Chapter 3. Each of the five proposed models simultaneously handled layout features such as the placement of equipment items in multiple floors, their interconnectivity by pipes, pumping considerations within and between floors, the determination of the area required and its cost, the fixed and area-dependent construction of floors as well as the description of tall equipment items that spanned through floors. Connection points on the height of equipment items were taken at design-specified points for a more accurate representation of the inter-connectivity and pumping requirements. Using industry-relevant examples having 7 - 25 items, each of the proposed models were tested. Results showed that all the proposed models were more efficient in handling the layout problem than previously recorded in the literature. The unique characteristics and benefits of some of the proposed models were also highlighted.

In Chapter 4 the feature of segregating equipment items to common areas was introduced to the proposed models. As is common practice, the choice of which equipment item belonged to each area, referred to as a production section, was predetermined based on function and/or use. This feature had been identified as having benefits such as an increased ease of plant operation, construction, maintenance and a higher level of safety. Thus, additional constraints were included in the existing layout models in Chapter 3 for a modified layout problem with production sections. The resulting models successfully obtained the layout configurations of each production section (plot layout) and of the entire site where the sections were located. The optimal number of floors per section, production section locations and equipment item floor and spatial location were all simultaneously determined with an objective to minimise the total layout cost. With case studies having between 17 and 22 items and 3 - 6 production sections, the proposed models obtained globally optimal solutions in short computational times.

Safety considerations were addressed in Chapters 5 and 6. Two key safety indices were identified in literature as being directly affected by the layout configurations of a chemical

process plant - Dow's Fire and Explosion index (F&EI) and the Domino Hazard Index (DHI). Each of these safety indices were adopted to quantify risk within the plant as function of the inter-equipment separation distances from the hazard source. In Chapter 5, the F&EI was adopted to quantify the probability, magnitude and impact of fire and explosion events as outlined in the Dow's F&EI hazard classification guide. The probable damage to equipment items was incorporated in an MILP model with decisions to install protection device to mitigate the level of such damage. The resulting model obtained the optimal multi-floor layout and the selection of protection device configuration per item. Computationally efficient model results were obtained showing savings in layout costs and financial risk when safety factors were considered.

The Domino Hazard ranking system was adopted in Chapter 6 to address some of the limitations of the Dow's F&EI in quantifying risk. The ranking system scored each possible hazardous event on an equipment item based on the probability of escalation to a neighbouring item as a function of their relative distances and a host of other factors. Hazardous events including flash fires, fireballs, jet fires, pool fires and the effect of blast waves, were incorporated into an MILP model using the ranking system to estimate the domino escalation cost, set of protection devices to be installed and the multi-floor layout configuration. Using a case study of an acrylic acid plant with 11 major units, results showed that an optimal balance of safety and layout factors were successfully handled by the model within a modest computational time.

7.2 Recommendations for future work

The mathematical models developed in this thesis have been proven to obtain optimal solutions to the multi-floor process plant layout problem for larger problem instances in shorter computational times considering a range of features obtainable in real-life chemical process plants. Further work is still required in a number of areas.

Although the models proposed in this thesis successfully handled a larger problem instance of the layout problem than recorded in literature using an exact approach, efficient

solutions for much bigger plants still need to be obtained. Optimal layout configurations to chemical process plants with 30+ units need to be obtained in less computational times than the currently proposed models. To solve this, alternatives to the non-overlapping set of constraints in the layout model need to be developed as this presents the most computational difficulty in solving the problem. Heuristics may also be explored as most of such methods in literature are only applicable to single floor layout designs or multi-floor layout designs with each equipment item occupying only a single floor. Heuristics based on a 'divide and conquer' approach, or a construction-based approach may provide very good solutions if combined with intuitive improvement phases, especially where decision makers are more concerned with solution times rather than quality.

It may also be important to further include toxic release events to the multi-floor layout problem using the DHI, as such events readily occur in process plants. Established MINLP models exist in literature describing toxic release using the DHI for single floor cases. These may be reformulated and/or approximated to MILP models, or used as is, for multi-floor cases. Separate floors may be treated as independent entities with or without crossover of toxic gases to mimic different chemical plant designs. This additional hazardous event, along with those considered in this work, may also be explored as a multi-objective problem in order to obtain alternative layout configurations with little or no changes to the total layout costs, but with an increased safety level within the plant.

In addition to the above, comparisons need to be made between the layout results obtained using the two safety metrics adopted to quantify risk. For a particular case study, an in-depth safety analysis should be conducted to obtain necessary parameters for each index, and measurements made to establish how each index compares in quantifying the financial risk of the plant and its effect on layout configuration. Comparisons may also be made with non-linear versions of the existing models proposed. Linear approximations may lead to under(over)-estimations of the parameters that affect the layout cost and/or safety levels within a plant, as noted in this work. However, with the advent of more efficient non-linear optimisation solvers, results may now be easily obtainable for such non-linear models.

Another possible area for future work deals with the inclusion of layout decisions in optimisation-based synthesis of chemical process plants. As defined by Chen and Grossmann (2017), "process synthesis is the assembly and interconnection of units into a process network - involving different physical and chemical phenomena to transform raw material and energy inputs into desired outputs - with the goal of optimising either economic, environmental, and/or social objectives." Amongst the different applicable areas of process synthesis is the general flowsheet design were a set of alternative combinations of process unit with associated operating conditions are represented by a superstructure, for the conversion of raw materials to desired outputs. At present, design variables such as flowrates, equipment sizes, temperatures, pressures, as well as physical relations, equipment limits and system performances are included in mathematical models in order to optimise some specified performance metric such as cost minimisation (profit maximization), environmental impact minimisation, or a combination of these. However, little or no work has been done to include layout cost metrics in the decision making process. Layout factors have been shown to have an impact on capital and operational expenditures directly and indirectly, and with the availability of proven mathematical models, these can be included in existing optimisation-based process synthesis models for general flowsheet designs.

REFERENCES

Alpizar, F., Backhaus, T., Decker, N., Eilks, I., Escobar-Pemberthy, N., Fantke, P., Geiser, K., Ivanova, M., Jolliet, O., Kim, H.-S., Khisa, K., Gundimeda, H., Slunge, D., Stec, S., Tickner, J., Tyrer, D., Urho, N., Visser, R., Yarto, M., Zuin, V. G., Alo, B., Barrantes, V., Makarova, A., Chen, Y., Abdelraouf, M., and Suzuki, N. (2019). UN environment global chemicals outlook II - From legacies to innovative solutions: Implementing the 2030 agenda for sustainable development.

American Institute of Chemical Engineers (1994). *Dow's fire & explosion index hazard classification guide*, volume 7. John Wiley & Sons, Inc., Hoboken, NJ, USA.

Anjos, M. F. and Vieira, M. V. C. (2017). Mathematical optimization approaches for facility layout problems: The state-of-the-art and future research directions. *Eur. J. Oper. Res.*, 261(17):1–16.

Barbosa-Póvoa, A. P., Mateus, R., and Novais, A. Q. (2001). Optimal two-dimensional layout of industrial facilities. *Int. J. Prod. Res.*, 39(12):2567–2593.

Barbosa-Póvoa, A. P., Mateus, R., and Novais, A. Q. (2002). Optimal 3D layout of industrial facilities. *Int. J. Prod. Res.*, 40(7):1669–1698.

Caputo, A. C., Pelagagge, P. M., Palumbo, M., and Salini, P. (2015). Safety-based process plant layout using genetic algorithm. *J. Loss Prev. Process Ind.*, 34:139–150.

Castell, C., Lakshmanan, R., Skilling, J., and Bañares-Alcántara, R. (1998). Optimisation of process plant layout using genetic algorithms. *Comput. Chem. Eng.*, 22(98):S993–S996.

Chen, Q. and Grossmann, I. E. (2017). Recent developments and challenges in optimization-based process synthesis. *Annu. Rev. Chem. Biomol. Eng*, 8:249–83.

Coulson J. M.; Richardson, J. M. (1994). *Chemical engineering volume 3. Chemical & biochemical reactors and process control*, volume 3. Elsevier, 3rd edition.

Cozzani, V., Gubinelli, G., and Salzano, E. (2006). Escalation thresholds in the assessment of domino accidental events. *J. Hazard. Mater.*, 129(1-3):1–21.

D'Ambrosio, C., Lodi, A., and Martello, S. (2010). Piecewise linear approximation of functions of two variables in MILP models. *Oper. Res. Lett.*, 38(1):39–46.

Dan, S., Shin, D., and Yoon, E. S. (2015). Layout optimization of LNG-liquefaction process on LNG-FPSO preventing domino effects. *J. Chem. Eng. Japan*, 48(8):646–655.

de Lira-Flores, J., Vázquez-Román, R., López-Molina, A., and Mannan, M. S. (2014). A MINLP approach for layout designs based on the domino hazard index. *J. Loss Prev. Process Ind.*, 30(1):219–227.

de Lira-Flores, J. A., Gutiérrez-Antonio, C., and Vázquez-Román, R. (2018). A MILP approach for optimal storage vessels layout based on the quantitative risk analysis methodology. *Process Saf. Environ. Prot.*, 120:1–13.

Díaz-Ovalle, C., Vázquez-Román, R., de Lira-Flores, J., and Mannan, M. S. (2013). A model to optimize facility layouts with toxic releases and mitigation systems. *Comput. Chem. Eng.*, 56:218–227.

Díaz-Ovalle, C., Vázquez-Román, R., and Sam Mannan, M. (2010). An approach to solve the facility layout problem based on the worst-case scenario. *J. Loss Prev. Process Ind.*, 23(3):385–392.

Drira, A., Pierreval, H., and Hajri-Gabouj, S. (2007). Facility layout problems: A survey. *Annu. Rev. Control*, 31(2):255–267.

Ejeh, J. O., Liu, S., Chalchooghi, M. M., and Papageorgiou, L. G. (2018a). Optimization-based approach for process plant layout. *Ind. Eng. Chem. Res.*, 57(31):10482–10490.

Ejeh, J. O., Liu, S., and Papageorgiou, L. G. (2018b). Multi-floor process plant layout using mixed-integer optimisation. In *Comput. Aided Chem. Eng.*, volume 43, pages 633–638.

Ejeh, J. O., Liu, S., and Papageorgiou, L. G. (2018c). Optimal multi-floor process plant layout with production sections. *Chem. Eng. Res. Des.*, 137:488–501.

Ejeh, J. O., Liu, S., and Papageorgiou, L. G. (2019a). An MILP model for safe multi-floor process plant layout. In *Comput. Aided Chem. Eng.*, pages 379–384. Elsevier.

Ejeh, J. O., Liu, S., and Papageorgiou, L. G. (2019b). Optimal layout of multi-floor process plants using MILP. *Comput. Chem. Eng.*, 131:106573.

Floudas, C. A. (1995). *Nonlinear and mixed-integer optimization*. Oxford University Press.

Furuholmen, M., Glette, K., Hovin, M., and Torresen, J. (2010). A coevolutionary, hyper heuristic approach to the optimization of three-dimensional process plant layouts - A comparative study. In *IEEE Congr. Evol. Comput.*, pages 1–8. IEEE.

GAMS Development Corporation (2018). General algebraic modeling system (GAMS) release 25.0.2.

Georgiadis, M. C. and Macchietto, S. (1997). Layout of process plants: A novel approach. *Comput. Chem. Eng.*, 21:S337–S342.

Georgiadis, M. C., Schilling, G., Rotstein, G. E., and Macchietto, S. (1999). A general mathematical programming approach for process plant layout. *Comput. Chem. Eng.*, 23(7):823–840.

Guirardello, R. and Swaney, R. E. (2005). Optimization of process plant layout with pipe routing. *Comput. Chem. Eng.*, 30(1):99–114.

Han, K., Kim, Y. H., Jang, N., Kim, H., Shin, D., and Yoon, E. S. (2013). Risk index approach for the optimal layout of chemical processes minimizing risk to humans. *Ind. Eng. Chem. Res.*, 52(22):7274–7281.

Hanan, M. and Kurtzberg, J. M. (1972). A review of the placement and quadratic assignment problems. *SIAM Rev.*, 14(2):324–342.

Hosseini-Nasab, H., Fereidouni, S., Fatemi Ghomi, S. M. T., and Fakhrzad, M. B. (2018). Classification of facility layout problems: A review study. *Int. J. Adv. Manuf. Technol.*, 94(1-4):957–977.

Hwang, J. and Lee, K. Y. (2014). Optimal liquefaction process cycle considering simplicity and efficiency for LNG FPSO at FEED stage. *Comput. Chem. Eng.*, 63(63):1–33.

Jayakumar, S. and Reklaitis, G. (1994). Chemical plant layout via graph partitioning-1. Single level. *Comput. Chem. Eng.*, 18(5):441–458.

Jayakumar, S. and Reklaitis, G. V. (1996). Chemical plant layout via graph partitioning - II. Multiple levels. *Comput. Chem. Eng.*, 20(5):563–578.

Jung, S. (2016). Facility siting and plant layout optimization for chemical process safety. *Korean J. Chem. Eng.*, 33(1):1–7.

Jung, S., Ng, D., Diaz-Ovalle, C., Vazquez-Roman, R., and Mannan, M. S. (2011). New approach to optimizing the facility siting and layout for fire and explosion scenarios. *Ind. Eng. Chem. Res.*, 50(7):3928–3937.

Jung, S., Ng, D., Laird, C. D., and Mannan, M. S. (2010a). A new approach for facility siting using mapping risks on a plant grid area and optimization. *J. Loss Prev. Process Ind.*, 23(6):824–830.

Jung, S., Ng, D., Lee, J.-H., Vazquez-Roman, R., and Mannan, M. S. (2010b). An approach for risk reduction (methodology) based on optimizing the facility layout and siting in toxic gas release scenarios. *J. Loss Prev. Process Ind.*, 23(1):139–148.

Khan, F. I. and Amyotte, P. R. (2004). Integrated inherent safety index (I2SI): A tool for inherent safety evaluation. *Process Saf. Prog.*, 23(2):136–148.

Khan, F. I. and Amyotte, P. R. (2005). I2SI: A comprehensive quantitative tool for inherent safety and cost evaluation. *J. Loss Prev. Process Ind.*, 18(4-6):310–326.

Khani, E. G. and Beigi, M. A. (2015). A novel strategy for comparative points in facility layout problem with fuzzy logic. *International Journal of Management and Fuzzy Systems*, 1(2):15.

Kidam, K. and Hurme, M. (2012). Design as a contributor to chemical process accidents. *J. Loss Prev. Process Ind.*, 25(4):655–666.

Koopmans, T. C. and Beckmann, M. (1957). Assignment problems and the location of economic activities. *Econometrica*, 25(1):53.

Ku, N., Jeong, S.-Y., Roh, M.-I., Shin, H.-K., Ha, S., and Hong, J.-w. (2014a). Layout method of a FPSO (Floating, Production, Storage, and Off-loading unit) using the optimization technique. In *ASME. 33rd Int. Conf. Ocean. Offshore Arct. Eng. Vol. 1B Offshore Technol.*, page V01BT01A032. ASME.

Ku, N.-K., Hwang, J.-H., Lee, J.-C., Roh, M.-I., and Lee, K.-Y. (2014b). Optimal module layout for a generic offshore LNG liquefaction process of LNG-FPSO. *Ships Offshore Struct.*, 9(3):311–332.

Latifi, S. E., Mohammadi, E., and Khakzad, N. (2017). Process plant layout optimization with uncertainty and considering risk. *Comput. Chem. Eng.*, 106:224–242.

Lee, D. H. and Lee, C. J. (2017). The plant layout optimization considering the operating conditions. *J. Chem. Eng. Japan*, 50(7):568–576.

Lee, K. Y., Roh, M. I., and Jeong, H. S. (2005). An improved genetic algorithm for multi-floor facility layout problems having inner structure walls and passages. *Comput. Oper. Res.*, 32(4):879–899.

López-Molina, A., Vázquez-Román, R., Mannan, M. S., and Félix-Flores, M. G. (2013). An approach for domino effect reduction based on optimal layouts. *J. Loss Prev. Process Ind.*, 26(5):887–894.

Mecklenburgh, J. C. (1985). *Process plant layout*. Longman, New York.

Medina-Herrera, N., Jiménez-Gutiérrez, A., and Grossmann, I. E. (2014). A mathematical programming model for optimal layout considering quantitative risk analysis. *Comput. Chem. Eng.*, 68:165–181.

Moran, S. (2016). Process plant layout - Becoming a lost art? *Chem. Eng.*, 123(12):71–76.

Moran, S. (2017). *Process plant layout*. Butterworth-Heinemann, 2nd edition.

Papageorgiou, L. G. and Rotstein, G. E. (1998). Continuous-domain mathematical models for optimal process plant layout. *Ind. Eng. Chem. Res.*, 37(9):3631–3639.

Park, K., Koo, J., Shin, D., Lee, C. J., and Yoon, E. S. (2011). Optimal multi-floor plant layout with consideration of safety distance based on mathematical programming and modified consequence analysis. *Korean J. Chem. Eng.*, 28(4):1009–1018.

Park, K., Shin, D., and Won, W. (2018). Risk based 3-dimensional and multifloor plant layout optimization for liquefied natural gas (LNG) liquefaction process. *Korean J. Chem. Eng.*, 35(5):1053–1064.

Park, P. J. and Lee, C. J. (2015). The research of optimal plant layout optimization based on particle swarm optimization for ethylene oxide plant. *J. Korean Soc. Saf.*, 30(3):32–37.

Patsiatzis, D. I., Knight, G., and Papageorgiou, L. G. (2004). An MILP approach to safe process plant layout. *Chem. Eng. Res. Des.*, 82(5):579–586.

Patsiatzis, D. I. and Papageorgiou, L. G. (2002). Optimal multi-floor process plant layout. *Comput. Chem. Eng.*, 26(4-5):575–583.

Patsiatzis, D. I. and Papageorgiou, L. G. (2003). Efficient solution approaches for the multifloor process plant layout problem. *Ind. Eng. Chem. Res.*, 42(4):811–824.

Patsiatzis, D. I., Xu, G., and Papageorgiou, L. G. (2005). Layout aspects of pipeless batch plants. *Ind. Eng. Chem. Res.*, 44(15):5672–5679.

Penteado, F. D. and Ciric, A. R. (1996). An MINLP approach for safe process plant layout. *Ind. Eng. Chem. Res.*, 35(4):1354–1361.

Peters, M. S. and Timmerhaus, K. D. (2003). *Plant design and economics for chemical engineers*, volume 4. McGraw-Hill New York.

Realff, M., Shah, N., and Pantelides, C. (1996). Simultaneous design, layout and scheduling of pipeless batch plants. *Comput. Chem. Eng.*, 20(6-7):869–883.

Roy, N., Eljack, F., Jiménez-Gutiérrez, A., Zhang, B., Thiruvenkataswamy, P., El-Halwagi, M., and Mannan, M. S. (2016). A review of safety indices for process design. *Curr. Opin. Chem. Eng.*, 14:42–48.

Shaik, M. A. and Mathur, P. (2018). Simultaneous scheduling and routing of pipeless plants in different layouts. *Ind. Eng. Chem. Res.*, 57(29):9527–9536.

Tompkins, J. A., White, J. A., Bozer, Y. A., and Tanchoco, J. M. A. (2010). *Facilities Planning*. Wiley, 4th edition.

Tugnoli, A., Khan, F., Amyotte, P., and Cozzani, V. (2008a). Safety assessment in plant layout design using indexing approach: Implementing inherent safety perspective. Part 1 - Guideword applicability and method description. *J. Hazard. Mater.*, 160(1):100–109.

Tugnoli, A., Khan, F., Amyotte, P., and Cozzani, V. (2008b). Safety assessment in plant layout design using indexing approach: Implementing inherent safety perspective. Part 2-Domino hazard index and case study. *J. Hazard. Mater.*, 160(1):110–121.

United Nations Department of Economic and Social Affairs, Population Division (2019). World population prospects 2019: Highlights.

Vázquez-Román, R., Lee, J.-H., Jung, S., and Mannan, M. S. (2010). Optimal facility layout under toxic release in process facilities: A stochastic approach. *Comput. Chem. Eng.*, 34(1):122–133.

Wang, J. and Song, W.-h. (2013). Fire and explosion index calculation method incorporating classified safety measure credits. *J. Loss Prev. Process Ind.*, 26(6):1128–1133.

Wang, R., Wu, Y., Wang, Y., and Feng, X. (2017). An industrial area layout optimization method based on dow's Fire & Explosion Index Method. In *Chem. Eng. Trans.*, volume 61, pages 493 – 498.

Westerlund, J. and Papageorgiou, L. G. (2004). Improved performance in process plant layout problems using symmetry-breaking constraints. In *Discov. through Prod. Process Des. Proc. FOCAPD*, pages 485–488.

Westerlund, J., Papageorgiou, L. G., and Westerlund, T. (2007). A MILP model for N-dimensional allocation. *Comput. Chem. Eng.*, 31(12):1702–1714.

Wrigley, P., Wood, P., Stewart, P., Hall, R., and Robertson, D. (2019). Module layout optimization using a genetic algorithm in light water modular nuclear reactor power plants. *Nucl. Eng. Des.*, 341:100–111.

Xin, P., Khan, F., and Ahmed, S. (2016). Layout optimization of a floating liquefied natural gas facility using inherent safety principles. *J. Offshore Mech. Arct. Eng.*, 138(4):041602.

Xu, G. and Papageorgiou, L. G. (2007). A construction-based approach to process plant layout using mixed-integer optimization. *Ind. Eng. Chem. Res.*, 46(1):351–358.

Xu, G. and Papageorgiou, L. G. (2009). Process plant layout using an improvement-type algorithm. *Chem. Eng. Res. Des.*, 87(6):780–788.

PUBLICATIONS

The following is a list of journal publications (Ejeh et al., 2018a,b,c, 2019a,b) and conference presentations made based on the work in this thesis:

Articles submitted to peer-reviewed journals:

- Ejeh, J. O., Liu, S. and Papageorgiou, L. G. (*submitted*). 'An MILP model for safe multi-floor process plant layout using the domino hazard index'.
- Ejeh, J. O., Liu, S. and Papageorgiou, L. G. (2019). 'Optimal layout for multi-floor process plants using MILP'. *Comput. Chem. Eng.* 131, 106573.
- Ejeh, J. O., Liu, S. and Papageorgiou, L. G. (2018). 'Optimal multi-floor process plant layout with production sections'. *Chem. Eng. Res. Des.* 137, 488-501.
- Ejeh, J. O., Liu, S., Chalchooghi, M. M. and Papageorgiou, L. G. (2018). 'An optimisation-based approach for process plant layout'. *Ind. Eng. Chem. Res.* 57(31), 10482-10490.

Book contributions:

- Ejeh, J. O., Liu, S. and Papageorgiou, L. G. (2019). 'An MILP model for safe multi-floor process plant layout'. In *Comput. Aided Chem. Eng.* 46, 379-384. Elsevier.
- Ejeh, J. O., Liu, S. and Papageorgiou, L. G. (2018). 'Multi-floor process plant layout using mixed integer optimisation'. In *Comput. Aided Chem. Eng.* 43, 633-638. Elsevier.

Presentations made at conferences:

- Ejeh, J. O., Liu, S. and Papageorgiou, L. G. (*accepted*). 'Towards a system for optimal multi-floor process plant layout design'. 2020 AICHE Annual Meeting, San Francisco, USA.

- Ejeh, J. O., Liu, S. and Papageorgiou, L. G. (2019). 'An MILP model for safe multi-floor process plant layout'. ESCAPE 29, Eindhoven, The Netherlands.
- Ejeh, J. O., Liu, S. and Papageorgiou, L. G. (2018). 'Multi-floor process plant layout using mixed-integer optimization'. ESCAPE 28, Graz, Austria.
- Ejeh, J. O., Liu, S. and Papageorgiou, L. G. (2017). 'An optimisation-based approach for process plant layout'. Poster presentation at ChemEngDay Uk 2017, 27-28th March, 2017, Birmingham, UK
- Ejeh, J. O., Liu, S. and Papageorgiou, L. G. (2017). 'An optimisation-based approach for process plant layout'. Poster presentation at 2nd year PhD Poster competition, Department of Chemical Engineering, UCL, UK.

APPENDIX A

LITERATURE MODEL FOR MULTI-FLOOR PROCESS PLANT LAYOUT

The MILP model proposed by Patsiatzis and Papageorgiou (2003) for the multi-floor process plant layout problem is presented below:

A.1 Floor constraints

Each equipment item available should be assigned to only one floor:

$$\sum_{k} V_{ik} = 1 \qquad \forall\, i \tag{A.1}$$

The value of N_{ij} is obtained by:

$$N_{ij} \geq V_{ik} + V_{jk} - 1 \qquad \forall\, i, j > i, k \tag{A.2}$$

$$N_{ij} \leq 1 - V_{ik} + V_{jk} \qquad \forall\, i, j > i, k \tag{A.3}$$

$$N_{ij} \leq 1 + V_{ik} - V_{jk} \qquad \forall\, i, j > i, k \tag{A.4}$$

As such, the variable N_{ij} is forced to the value of 1 if and only if item i and j are on the same floor. An item can only be assigned to a floor that exists:

$$V_{ik} \leq W_k \qquad \forall\, i,k \tag{A.5}$$

A floor can only be available if the preceding floor is occupied:

$$W_k \leq W_{k-1} \qquad \forall\, k > 1 \tag{A.6}$$

The number of floors required for the process is then given by:

$$NF \geq \sum_k W_k \tag{A.7}$$

A.2 Equipment orientation constraints

Each equipment item is allowed rotation in the x-y plane by 90^o as deemed optimal:

$$l_i = \alpha_i O_i + \beta_i (1 - O_i) \qquad \forall\, i \tag{A.8}$$

$$d_i = \alpha_i + \beta_i - l_i \qquad \forall\, i \tag{A.9}$$

A.3 Non-overlapping constraints

The following constraints prevent items i and j from occupying the same location if they exist on the same floor ($N_{ij} = 1$). Each combination of the values of the binary variable $E1_{ij}$ and $E2_{ij}$ activates one of the four constraints, which prevents an overlap of any two equipment items.

$$x_i - x_j + BM(1 - N_{ij} + E1_{ij} + E2_{ij}) \geq \frac{l_i + l_j}{2} \qquad \forall\, i,j > i \tag{A.10}$$

$$x_j - x_i + BM(2 - N_{ij} - E1_{ij} + E2_{ij}) \geq \frac{l_i + l_j}{2} \qquad \forall\, i,j > i \tag{A.11}$$

$$y_i - y_j + BM(2 - N_{ij} + E1_{ij} - E2_{ij}) \geq \frac{d_i + d_j}{2} \qquad \forall\, i, j > i \tag{A.12}$$

$$y_j - y_i + BM(3 - N_{ij} - E1_{ij} - E2_{ij}) \geq \frac{d_i + d_j}{2} \qquad \forall\, i, j > i \tag{A.13}$$

where BM is an appropriately large number.

A.4 Distance constraints

The constraints that follow determine the distances in the x, y, and z planes respectively;

$$R_{ij} - L_{ij} = x_i - x_j \qquad \forall\, i, j : f_{ij} = 1 \tag{A.14}$$

$$A_{ij} - B_{ij} = y_i - y_j \qquad \forall i, j : f_{ij} = 1 \tag{A.15}$$

$$U_{ij} - D_{ij} = FH \sum_k k(V_{ik} - V_{jk}) \qquad \forall i, j : f_{ij} = 1 \tag{A.16}$$

and the total rectilinear distance between any two items i and j, connected to each other is given as:

$$TD_{ij} = R_{ij} + L_{ij} + A_{ij} + B_{ij} + U_{ij} + D_{ij} \qquad \forall i, j : f_{ij} = 1 \tag{A.17}$$

A.5 Area constraints

In order to avoid bilinear terms, the value of the floor area, FA, is selected from a set of S predefined rectangular area sizes, AR_s, with dimensions $(\overline{X}_s, \overline{Y}_s)$.

$$FA = \sum_s AR_s Q_s \tag{A.18}$$

$$\sum_s Q_s = 1 \tag{A.19}$$

The floor length and breadth is selected from the chosen rectangular area size dimensions:

$$X^{max} = \sum_s \overline{X}_s Q_s \tag{A.20}$$

$$Y^{max} = \sum_{s} \overline{Y}_s Q_s \tag{A.21}$$

Also, a new term NQ_s is introduced in order to linearise the cost term associated with the number of floors in the objective function.

$$NQ_s \leq \mid K \mid Q_s \qquad \forall s \tag{A.22}$$

$$NF = \sum_{s} NQ_s \tag{A.23}$$

A.6 Layout design constraints

Layout design constraints are included to avoid placement of equipment items outside of the boundary of the floor area. The lower bound constraints are:

$$x_i \geq \frac{l_i}{2} \qquad \forall i \tag{A.24}$$

$$y_i \geq \frac{d_i}{2} \qquad \forall i \tag{A.25}$$

and the upper bound:

$$x_i + \frac{l_i}{2} \leq X^{max} \qquad \forall i \tag{A.26}$$

$$y_i + \frac{d_i}{2} \leq Y^{max} \qquad \forall i \tag{A.27}$$

A.7 Objective Function

$$\begin{aligned} min \sum_{i,j \neq i / f_{ij}=1} & \left(C^c_{ij} T D_{ij} + C^v_{ij} D_{ij} + C^h_{ij} (R_{ij} + L_{ij} + A_{ij} + B_{ij})\right) \\ & + FC1 \cdot NF + FC2 \cdot \sum_{s} AR_s \cdot NQ_s + LC \cdot FA \end{aligned} \tag{A.28}$$

APPENDIX *B*

DATA FOR CASE STUDIES CONSIDERED

B.1 Ethylene oxide plant

The dimensions of equipment items in the ethylene oxide plant are given in Table B.1. Table B.5 shows the connection cost, connection heights, horizontal and vertical pumping costs, as well as other required data.

Table B.1 Equipment dimensions & purchase cost for ethylene oxide plant

Equipment item	Description	α_i(m)	β_i(m)	γ_i(m)	Purchase cost (rmu)
1	Reactor	5.22	5.22	4.50	335,000
2	Heat exchanger 1	11.42	11.42	2.21	11,000
3	Ethylene oxide absorber	7.68	7.68	7.42	107,000
4	Heat exchanger 2	8.48	8.48	2.21	4,000
5	CO_2 absorber	7.68	7.68	6.40	81,300
6	Flash tank	2.6	2.6	3.50	5,000
7	Pump	2.4	2.4	1.20	1,500

Table B.2 Pertinent item system factors; EO plant

Equipment item	Description	Material factors	D_i^e	DF_i
1	Reactor	29	40	0.87
3	Ethylene oxide absorber	29	21.8	0.73
5	CO_2 absorber	24	18.06	0.66

Table B.3 Protection device data for the Reactor, item 1 (Patsiatzis et al., 2004)

Configuration (p)	Device	CF_{ip}	C_{ip}^p
1	–	1	0
2	1	0.900	5,000
3	3	0.750	15,000
4	1,3,6	0.365	40,000
5	1,3,5,6	0.292	60,000
6	1,3,4,5,6	0.117	125,000

CF_{ip} - loss control credit factor of protection device configuration p for item i

C_{ip}^p - purchase and installation cost of protection device configuration p for item i

Table B.4 Protection device data for the Ethylene oxide, item 3, and CO_2 absorber, item 5 (Patsiatzis et al., 2004)

Configuration (p)	Device	CF_{ip}	C_{ip}^p
1	–	1	0
2	1	0.900	5,000
3	2	0.760	20,000
4	1,2	0.684	25,000
5	1,7	0.612	35,000
6	1,2,7	0.465	55,000

CF_{ip} - loss control credit factor of protection device configuration p for item i

C_{ip}^p - purchase and installation cost of protection device configuration p for item i

Table B.5 Parameters for the ethylene oxide plant

(a) Connection and pumping costs, and connection heights

Connection	C^c_{ij}(rmu/m)	C^h_{ij}(rmu/m)	C^v_{ij}(rmu/m)	OP_{ij}(m)	IP_{ij}(m)
1.2	200	400	4000	4.5	1.11
2.3	200	400	4000	1.11	3.71
3.4	200	300	3000	7.42	1.11
4.5	200	300	3000	1.11	3.2
5.1	200	100	1000	6.40	2.25
5.6	200	200	2000	0.0	1.75
6.7	200	150	1500	0.0	0.60
7.5	200	150	1500	1.20	4.80

(b) Other Parameters

Parameters	Value
K	3
$FC1$(rmu)	3,330
$FC2$ (rmu/m^2)	6.6
LC (rmu/m^2)	26.6
FH (m)	5

B.2 Urea production plant

The dimensions of equipment items in the urea production (UR) plant are given in Table B.6. Table B.7 shows the connection cost, connection heights, horizontal and vertical pumping costs, as well as other required data.

Table B.6 Equipment dimensions for the urea production plant

Equipment item	Description	α_i(m)	β_i(m)	γ_i(m)
1	Flash drum	1.9812	1.9812	6.0960
2	Reactor 1	2.4384	2.4384	28.956
3	Reactor 2	1.5240	1.5240	5.7912
4	Distillation column 1	1.0668	1.0668	14.6304
5	Distillation column 2	0.6096	0.6096	7.3152
6	Reactor 3	0.7620	0.7620	3.3528
7	Reactor 4	1.2192	1.2192	5.0292
8	Separator	1.0668	1.0668	3.6576

Table B.7 Parameters for the urea production plant

(a) Connection and pumping costs, and connection heights

Connection	C^c_{ij}(rmu/m)	C^h_{ij}(rmu/m)	C^v_{ij}(rmu/m)	OP_{ij}(m)	IP_{ij}(m)
1.4	38.0	662.2	6621.8	0.0000	12.8016
4.3	161.0	513.3	5133.4	14.6304	4.6330
4.7	25.0	332.2	3321.8	0.0000	1.0058
7.8	25.0	332.2	3321.8	1.0058	2.9261
3.2	124.0	803.5	8035.1	1.1582	0.0000
2.1	103.0	803.5	8035.1	28.9560	4.5720
1.5	62.0	141.3	1413.3	6.0960	1.8288
8.6	14.0	59.0	590.0	3.6576	3.3528
6.5	13.0	59.0	590.0	3.3528	5.4864
5.3	17.0	156.2	1561.7	0.0000	4.6330

(b) Other Parameters

Parameters	Value
$\mid K \mid$	4
$FC1$(rmu)	3,200
$FC2$ (rmu/m^2)	120
LC (rmu/m^2)	420
FH (m)	8.0

B.3 Crude distillation plant with pre-heating train (CDU) plant)

The dimensions of equipment items in the CDU plant are given in Table B.8. Table B.9 shows the connection cost, connection heights, horizontal and vertical pumping costs, as well as other required data.

Table B.8 Equipment dimensions for the CDU plant

Equipment item	Description	α_i(m)	β_i(m)	γ_i(m)
1	Crude preheater 1	6.000	0.974	0.974
2	Crude preheater 2	2.550	0.620	0.620
3	Desalter	5.572	3.715	3.715
4	Preflash heater	2.550	0.774	0.774
5	Preflash drum	5.251	5.251	7.877
6	Fired heater (CDU)	3.922	3.922	17.600
7	Crude distillation tower	12.300	12.300	14.500
8	Naphtha condenser	1.789	1.193	1.193
9	Kerosene SS	1.500	1.500	3.900
10	Diesel SS	1.500	1.500	3.900
11	AGO SS	1.500	1.500	3.900
12	Fired heater (VDU)	3.922	3.922	17.600
13	Vacuum distillation tower	9.410	9.410	4.500
14	Kerosene reboiler	3.050	2.033	2.033
15	Debutaniser	5.337	5.337	24.750
16	Stabilised naphtha condenser	1.789	1.193	1.193
17	Debutaniser reboiler	1.789	1.193	1.193

Table B.9 Parameters for the CDU plant

(a) Connection and pumping costs, and connection heights

Connection	C^c_{ij}(rmu/m)	C^h_{ij}(rmu/m)	C^v_{ij}(rmu/m)	OP_{ij}(m)	IP_{ij}(m)
1.2	550.3	2,481.0	24,810.0	0.000	0.620
2.3	550.3	2,481.0	24,810.0	0.000	3.715
3.4	550.3	2,481.0	24,810.0	1.857	0.774
4.5	531.4	2,395.6	23,955.8	0.000	3.938
5.6	519.2	2,340.5	23,405.0	0.000	0.000
6.7	519.2	2,340.5	23,405.0	4.280	0.750
7.1	245.3	1,106.0	11,059.9	10.000	0.974
7.2	155.0	698.9	6,988.8	6.250	0.620
7.4	161.6	728.4	7,284.1	3.750	0.774
1.7	245.3	1,106.0	11,059.9	0.000	10.750
2.7	155.0	698.9	6,988.8	0.000	6.750
4.7	161.6	728.4	7,284.1	0.000	4.250
7.8	206.1	929.2	9,291.8	14.500	0.597
8.7	102.1	460.2	4,602.0	0.000	14.250
7.9	57.4	258.6	2,586.4	10.250	3.650
9.7	11.0	49.7	496.9	3.900	10.750
9.14	67.9	306.2	3,061.9	0.000	0.000
14.9	21.6	97.2	972.4	2.033	2.650
7.10	117.5	529.8	5,297.9	6.250	3.650
10.7	17.4	78.5	785.2	3.900	6.750
7.11	31.4	141.7	1,416.6	3.750	3.650
11.7	8.0	36.0	359.6	3.900	4.250
7.12	248.3	1,119.2	11,191.6	0.000	0.000
12.13	248.3	1,119.2	11,191.6	4.280	0.250
8.15	99.0	446.2	4,462.2	0.000	12.925
15.16	50.6	228.3	2,282.8	24.750	0.597
15.17	212.7	958.7	9,587.5	0.000	0.000
16.15	30.4	137.0	1,369.7	0.000	24.475
17.15	133.9	603.8	6,038.4	1.193	0.275

(b) Other Parameters

Parameters	Value
$\mid K \mid$	7
$FC1$(rmu)	3,330
$FC2$ (rmu/m^2)	33.3
LC (rmu/m^2)	666
FH (m)	5.0

B.4 Liquefied natural gas (LNG) plant

Table B.10 shows the dimensions of equipment items and Table B.11 shows the connection cost, connection heights, horizontal and vertical pumping costs, as well as other required data for the LNG plant.

Table B.10 Equipment dimensions for the LNG plant

Equipment item	Description	α_i(m)	β_i(m)	γ_i(m)
1	PMR compressor LP suction drum	3.613	3.613	4.603
2	PMR compressor HP suction drum	3.217	3.217	4.900
3	PMR compressor	18.809	5.939	5.741
4	PMR compressor cooler	2.969	1.979	2.969
5	Overhead crane for PMR compressor	22.769	15.839	5.939
6	SW cooler 1	7.919	1.979	4.949
7	SW cooler 2	7.919	1.979	4.949
8	PMR receiver	4.157	4.157	9.800
9	LP precool exchanger	4.157	4.157	21.086
10	HP precool exchanger	4.355	4.355	21.779
11	Joule–Thomson valve 1	0.989	0.989	0.989
12	Joule–Thomson valve 2	0.989	0.989	0.989
13	MR separator 1	4.454	4.454	12.869
14	MCHE	5.642	5.642	41.579
15	MR compressor suction drum	5.444	5.444	8.909
16	MR compressor	17.126	5.939	5.939
17	MR compressor cooler	2.969	1.979	2.969
18	Overhead crane for MR Compressor	22.769	15.839	5.939
19	SW cooler 3	3.959	2.474	2.969
20	SW cooler 4	3.959	2.474	2.969
21	Joule–Thomson valve 3	1.484	1.484	1.484
22	Joule–Thomson valve 4	1.484	1.484	1.484

Table B.11 Parameters for the LNG plant

(a) Connection and pumping costs, and connection heights

Connection	C^c_{ij}(rmu/m)	C^h_{ij}(rmu/m)	C^v_{ij}(rmu/m)	OP_{ij}(m)	IP_{ij}(m)
2.3	150	750	7500	2.4500	2.8705
3.6	150	750	7500	2.8705	2.4745
3.7	150	750	7500	2.8705	2.4745
7.2	150	750	7500	2.4745	2.4500
8.10	150	750	7500	8.9000	4.0000
10.11	150	750	7500	18.8895	0.4945
11.10	150	750	7500	0.4945	18.8895
9.10	150	750	7500	4.0000	18.8895
10.9	150	750	7500	18.8598	4.0000
12.9	70	250	2500	0.4945	18.5430
9.12	70	250	2500	18.4530	0.4945
13.14	150	750	7500	4.0000	12.0000
14.15	150	750	7500	4.0000	4.0000
15.16	150	750	7500	8.4545	2.9695
16.17	150	750	7500	2.9795	1.4845
17.16	150	750	7500	1.4845	2.9695
14.21	70	250	2500	28.0000	0.7420
21.14	70	250	2500	0.7420	28.0000
16.19	150	750	7500	2.9695	1.4845
19.16	150	750	7500	1.4845	2.9695
16.20	150	750	7500	2.9695	1.4845
20.16	150	750	7500	1.4845	2.9695
22.14	150	750	7500	0.7420	36.7895
14.22	150	750	7500	36.7895	0.7420
10.2	150	750	7500	12.0000	2.4500
9.1	150	750	7500	12.0000	2.3015
6.8	150	750	7500	2.4745	8.9000
14.9	150	750	7500	20.0000	12.0000
10.13	150	750	7500	4.0000	4.0000

(b) Other Parameters

Parameters	Value
$\mid K \mid$	5
$FC1$(rmu)	4,600
$FC2$ (rmu/m^2)	33.3
LC (rmu/m^2)	666
FH (m)	8.0

B.5 Crude oil & gas processing (COGP) plant

Table B.12 shows the dimensions of equipment items and Table B.13 shows the connection cost, connection heights, horizontal and vertical pumping costs, as well as other required data for the COGP plant.

Table B.12 Equipment dimensions for the COGP plant

Equipment item	Description	α_i(m)	β_i(m)	γ_i(m)
1	Separator	20.000	5.000	5.000
2	KO drum	16.000	4.000	4.000
3	Contactor 1	3.000	3.000	8.000
4	Contactor 2	2.000	2.000	5.333
5	Compressor 1	8.000	3.000	3.000
6	Compressor 2	5.333	2.000	2.000
7	Mixer 1	1.000	1.000	1.000
8	Heat exchanger 1	8.000	2.500	2.500
9	Heat exchanger 2	9.600	3.600	3.600
10	Heat exchanger 3	14.400	4.500	4.500
11	Contactor 3	3.000	3.000	9.000
12	Contactor 4	3.600	3.600	10.800
13	Contactor 5	5.400	5.400	16.200
14	Compressor 3	6.400	2.400	2.400
15	Compressor 4	7.680	2.880	2.880
16	Compressor 5	11.520	4.320	4.320
17	Heat exchanger 4	6.000	1.875	1.875
18	Heat exchanger 5	7.200	2.700	2.700
19	Heat exchanger 6	10.800	3.375	3.375
20	Contactor 6	2.400	2.400	7.200
21	Contactor 7	2.880	2.880	8.640
22	Contactor 8	4.320	4.320	12.960
23	Compressor 6	5.760	2.160	2.160
24	Compressor 7	6.912	2.592	2.592
25	Compressor 8	10.368	3.888	3.888

Table B.13 Parameters for the COGP plant

(a) Connection and pumping costs, and connection heights

Connection	C^c_{ij}(rmu/m)	C^h_{ij}(rmu/m)	C^v_{ij}(rmu/m)	OP_{ij}(m)	IP_{ij}(m)
1.7	50.00	225.00	2250.0	0.000	1.000
1.2	200.00	900.00	9000.0	0.000	2.000
2.4	72.00	324.00	3240.0	0.000	2.667
4.6	72.00	324.00	3240.0	5.333	2.000
6.7	72.00	324.00	3240.0	2.000	1.000
5.7	108.00	486.00	4860.0	3.000	1.000
2.3	108.00	486.00	4860.0	0.000	4.000
3.5	108.00	486.00	4860.0	8.000	3.000
7.8	57.50	258.75	2587.5	0.000	2.500
7.9	69.00	310.50	3105.0	0.000	3.600
7.10	103.50	465.75	4657.5	0.000	4.500
8.11	57.50	258.75	2587.5	0.000	4.500
11.14	46.00	207.00	2070.0	9.000	2.400
14.17	46.00	207.00	2070.0	2.400	1.875
17.20	46.00	207.00	2070.0	0.000	3.600
20.23	41.40	186.30	1863.0	7.200	2.160
9.12	69.00	310.50	3105.0	0.000	5.400
12.15	55.20	248.40	2484.0	10.800	2.880
15.18	55.20	248.40	2484.0	2.880	2.700
18.21	55.20	248.40	2484.0	0.000	4.320
21.24	49.68	223.56	2235.6	8.640	2.592
10.13	103.50	465.75	4657.5	0.000	8.100
13.16	82.80	372.60	3726.0	16.200	4.320
16.19	82.80	372.60	3726.0	4.320	3.375
19.22	82.80	372.60	3726.0	0.000	6.480
22.25	74.52	335.34	3353.4	12.960	3.888

(b) Other Parameters

Parameters	Value
$\mid K \mid$	7
$FC1$(rmu)	3,330
$FC2$ (rmu/m^2)	33.3
LC (rmu/m^2)	666
FH (m)	5.0

B.6 Acrylic acid (AA) plant

Table B.14 shows the dimensions of equipment items and Table B.16 shows the connection cost, connection heights, horizontal and vertical pumping costs, as well as other required data for the acrylic acid (AA) plant.

Table B.14 Equipment dimensions for the AA plant

Equipment item	Description	α_i(m)	β_i(m)	γ_i(m)
1	Compressor	2.0	2.0	2.0
2	Feed mixer	2.5	2.5	3.5
3	Reactor	2.8	2.8	5.2
4	Quench	3.3	3.3	6.4
5	Absorber	2.5	2.5	7.0
6	Splitter	3.1	3.1	3.1
7	Acid extractor	2.5	2.5	5.5
8	Distillation column 1	3.0	3.0	7.2
9	Solvent mixer	1.8	1.8	1.8
10	Distillation column 2	2.5	2.5	5.8
11	Distillation column 3	2.2	2.2	4.7

Table B.15 Equipment item parameters for safety considerations

i	Description	DI_i	C_i^p(rmu)	$C_{i,FI}$(rmu)	$C_{i,FW}$(rmu)	$C_{i,BWl}$(rmu)	P_i^{lo}(m)	P_i^{up}(m)
1	Compressor	7	6,000	563	8,000	8,000	-	-
2	Feed mixer	29	41,735	2,661	20,000	58,000	8.8	13.6
3	Reactor	47	88,906	2,925	20,000	61,429	19.5	30.0
4	Quench	25	45,836	2,787	20,000	53,636	14.8	22.9
5	Absorber	30	62,335	2,212	20,000	48,400	14.5	22.7
6	Splitter	21	23,365	1,640	15,000	30,645	5.6	8.4
7	Acid Extractor	30	67,876	2,506	20,000	54,800	-	-
8	Distillation 1	22	94,909	2,117	20,000	42,000	22.0	16.0
9	Solvent mixer	20	33,417	2,273	20,000	54,444	-	-
10	Distillation 2	21	48,898	2,212	20,000	48,400	13.0	9.0
11	Distillation 3	27	59,236	2,351	20,000	53,636	22.0	16.0

Table B.16 Parameters for the AA plant

(a) Connection and pumping costs, and connection heights

Connection	C^c_{ij}(rmu/m)	C^h_{ij}(rmu/m)	C^v_{ij}(rmu/m)	OP_{ij}(m)	IP_{ij}(m)
1.2	166.13	863.876	8,638.76	0.00	3.50
2.3	166.13	863.876	8,638.76	0.00	2.60
3.4	166.13	863.876	8,638.76	0.00	3.20
4.5	166.13	863.876	8,638.76	0.00	3.50
5.6	166.13	863.876	8,638.76	7.00	1.55
5.7	166.13	863.876	8,638.76	0.00	2.75
6.2	166.13	863.876	8,638.76	1.55	3.50
7.8	166.13	863.876	8,638.76	5.50	3.60
7.11	166.13	863.876	8,638.76	0.00	2.35
8.9	166.13	863.876	8,638.76	7.20	0.90
8.10	166.13	863.876	8,638.76	0.00	2.90
11.9	166.13	863.876	8,638.76	4.70	0.90

(b) Other Parameters

Parameters	Value
$\mid K \mid$	4
$FC1$(rmu)	3,330
$FC2$ (rmu/m^2)	1,000
LC (rmu/m^2)	5,000
FH (m)	5.0

APPENDIX *C*

LAYOUT RESULT PLOTS OF PROPOSED MODELS

C.1 Layout result plots for Chapter 2: Multi-floor process plant layout

C.1.1 Ethylene oxide plant

The layout plans for the models proposed for the Ethylene oxide plant are shown below in Figs (C.1) - (C.4):

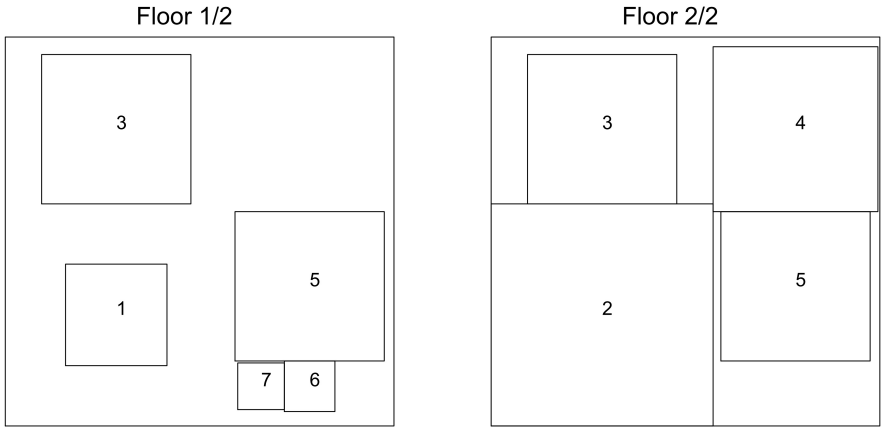

Fig. C.1 EO plant layout plan; Model A.2

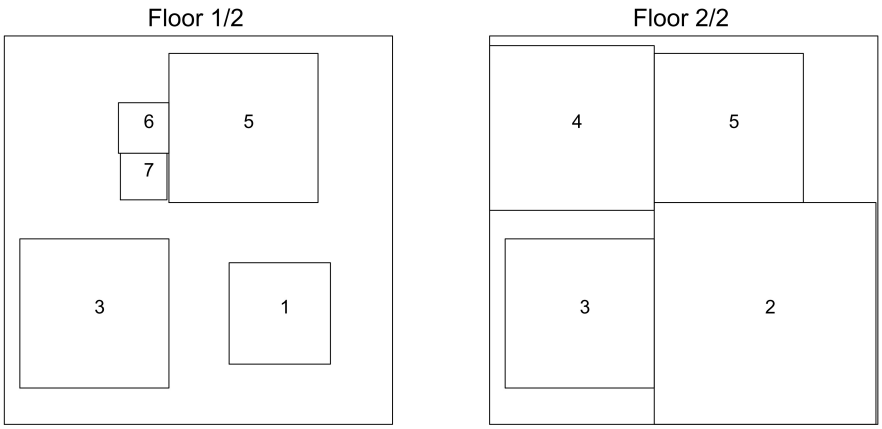

Fig. C.2 EO plant layout plan; Model A.3

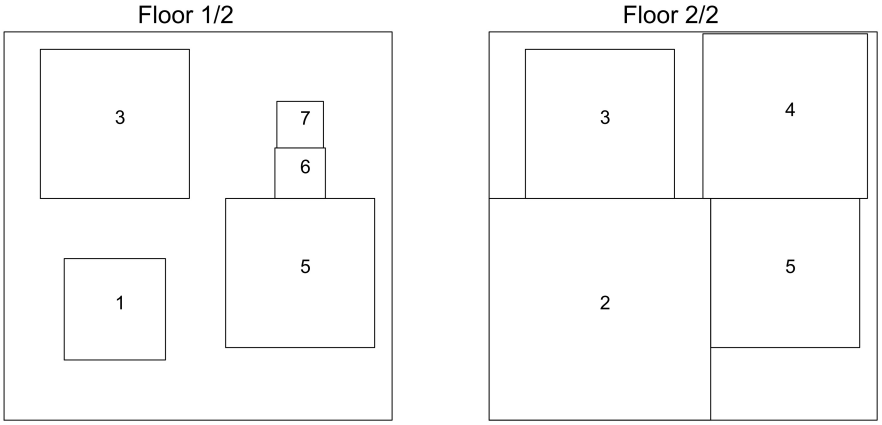

Fig. C.3 EO plant layout plan; Model A.4

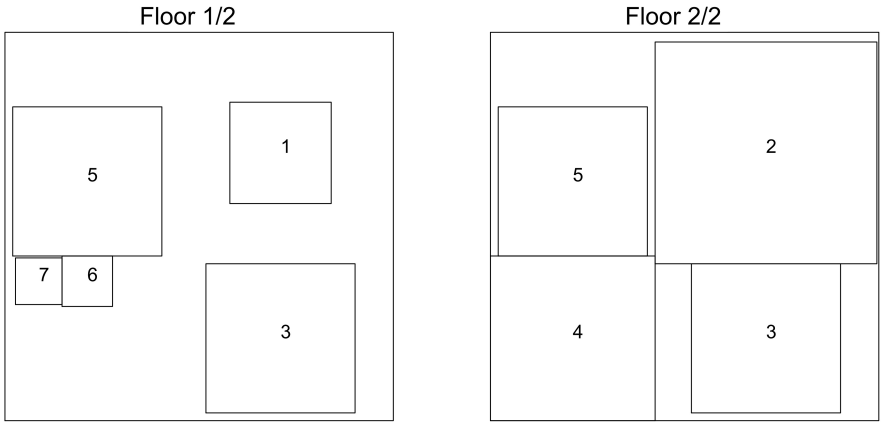

Fig. C.4 EO plant layout plan; Model B

C.1.2 Urea production plant

The layout plans for the models proposed for the Urea production plant are shown below in Figs (C.5) - (C.8):

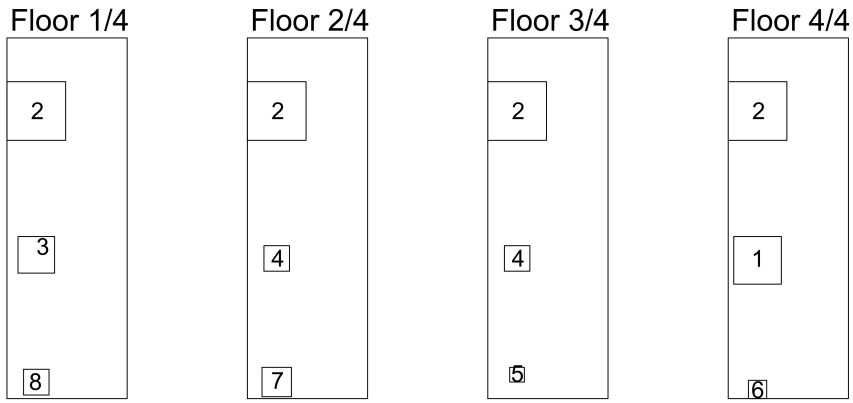

Fig. C.5 UR plant layout plan; Model A.2

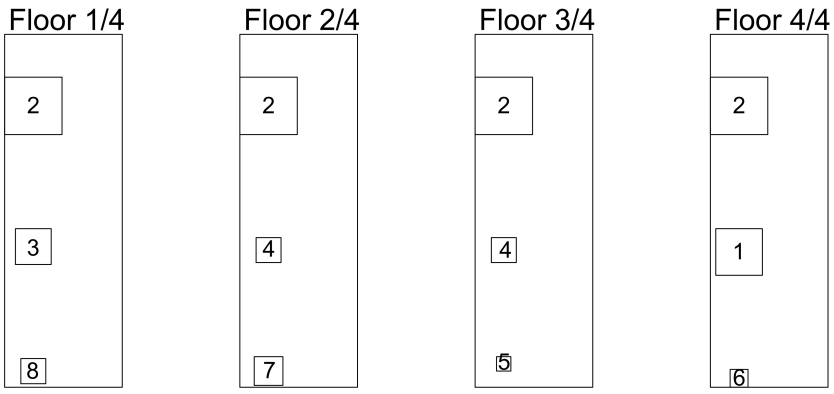

Fig. C.6 UR plant layout plan; Model A.3

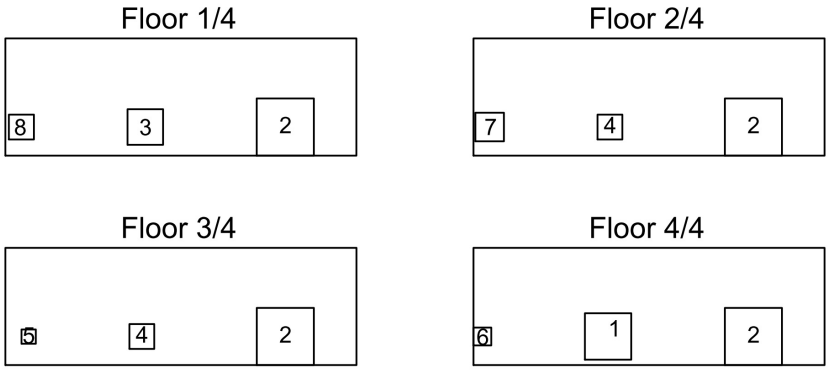

Fig. C.7 UR plant layout plan; Model A.4

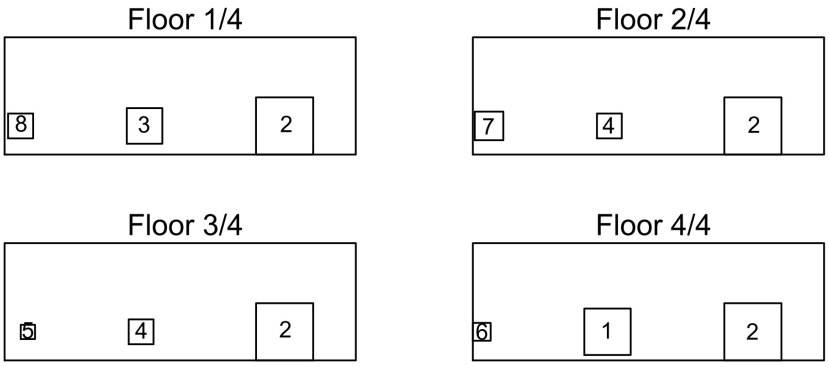

Fig. C.8 UR plant layout plan; Model B

C.1.3 Crude distillation plant with pre-heating train (CDU) plant)

The layout plans for the models proposed for the CDU plant are shown below in Figs (C.9) - (C.12):

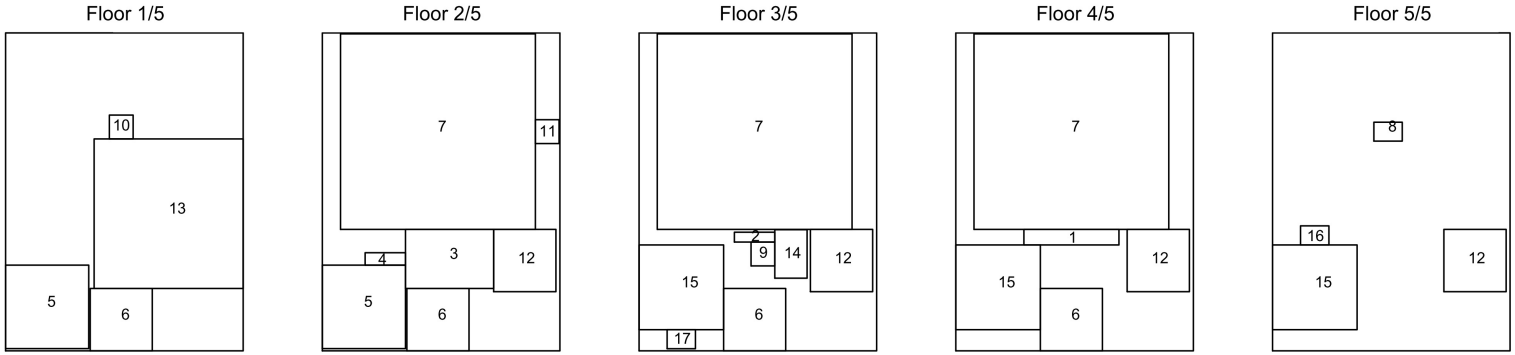

Fig. C.9 CDU plant layout plan; Model A.2

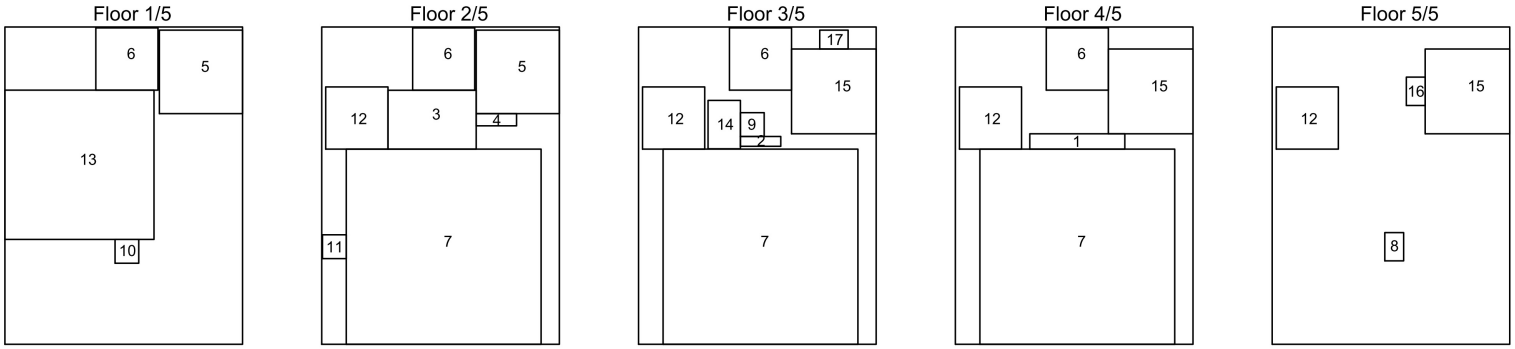

Fig. C.10 CDU plant layout plan; Model A.3

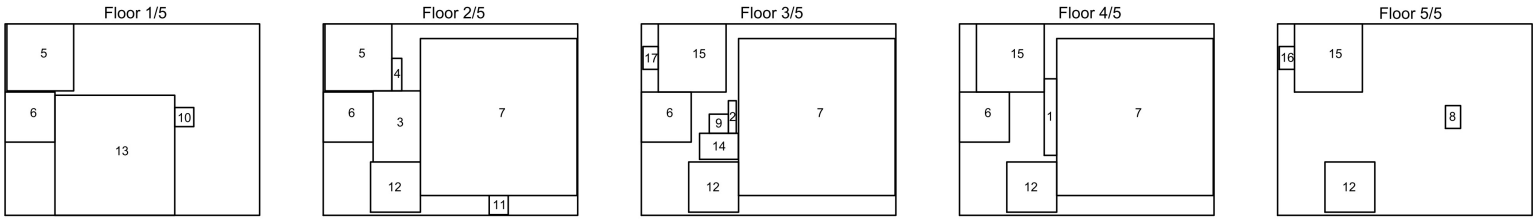

Fig. C.11 CDU plant layout plan; Model A.4

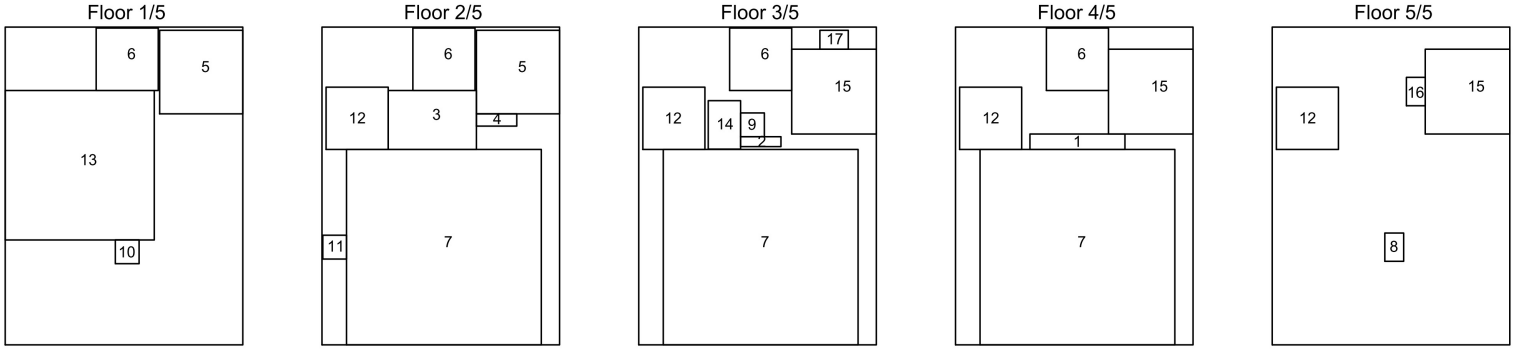

Fig. C.12 CDU plant layout plan; Model B

C.1.4 Liquefied natural gas (LNG) plant

The layout plans for the models proposed for the LNG plant are shown below in Figs (C.13) - (C.16):

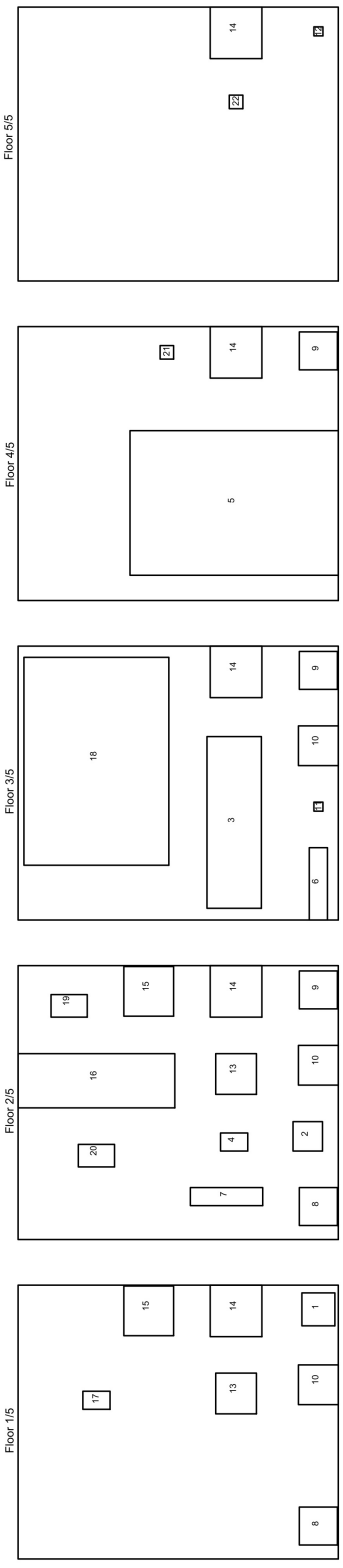

Fig. C.13 LNG plant layout plan; Model A.2

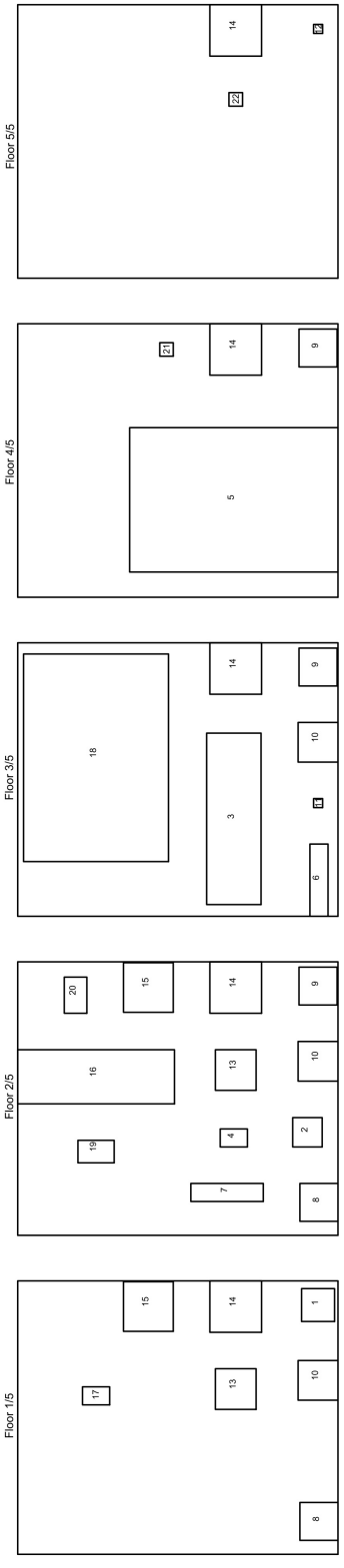

Fig. C.14 LNG plant layout plan; Model A.3

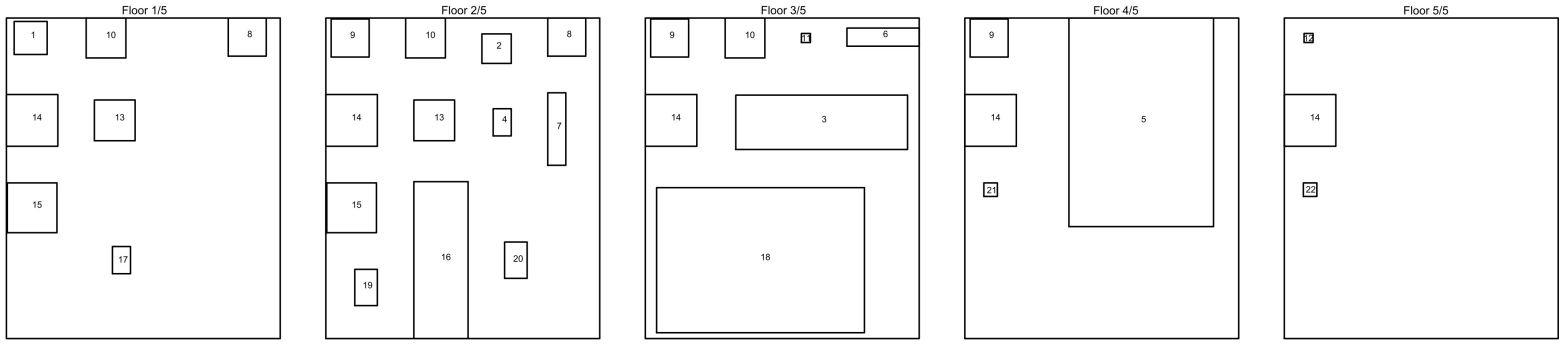

Fig. C.15 LNG plant layout plan; Model A.4

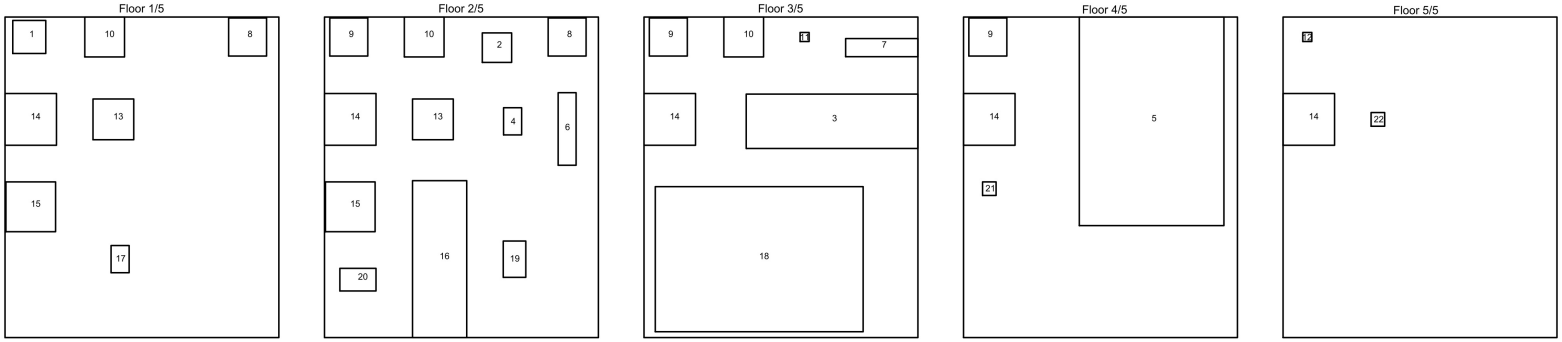

Fig. C.16 LNG plant layout plan; Model B

C.1.5 Crude oil & gas processing (COGP) plant

The layout plans for the models proposed for the COGP plant are shown below in Figs (C.17) - (C.20):

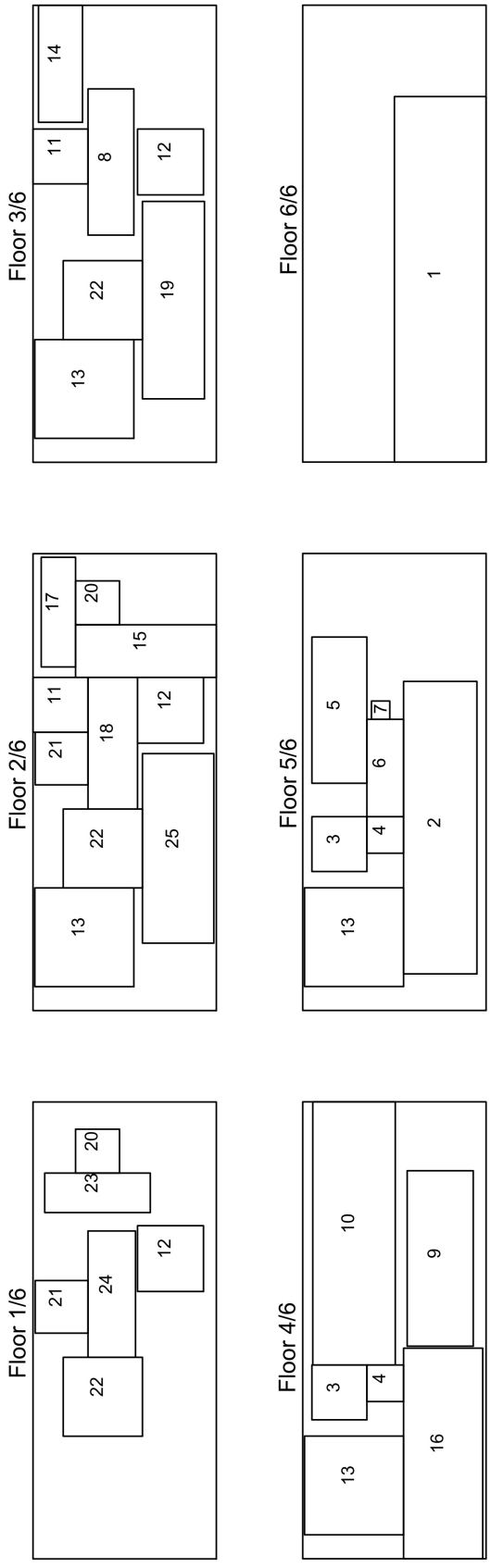

Fig. C.17 COGP plant layout plan; Model A.2

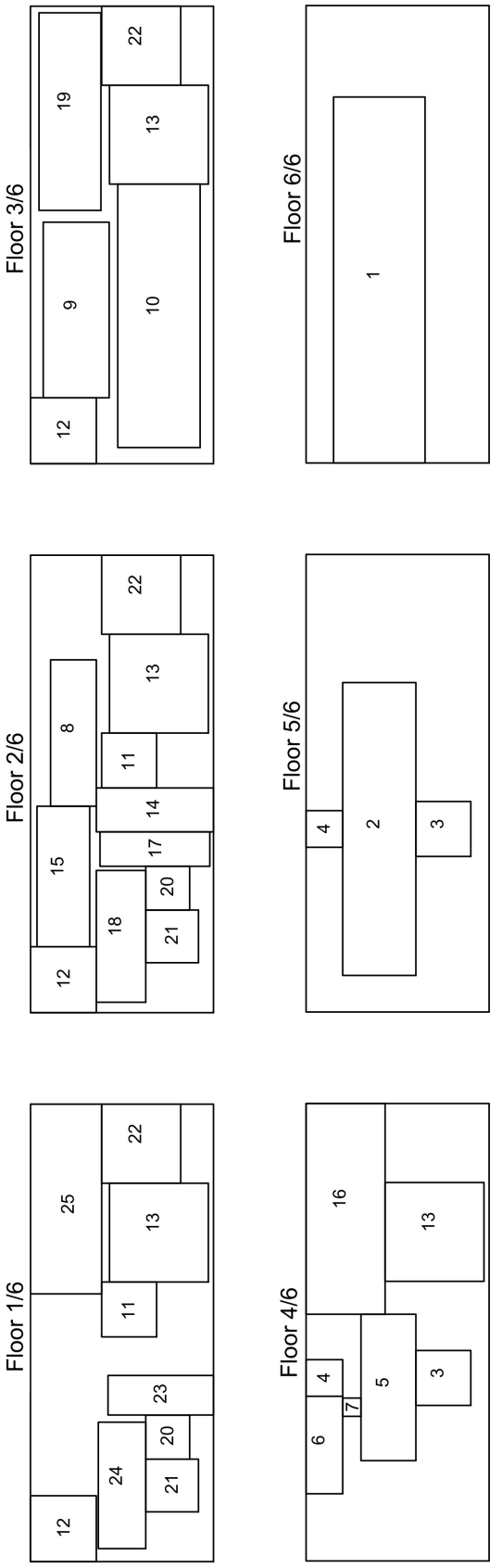

Fig. C.18 COGP plant layout plan; Model A.3

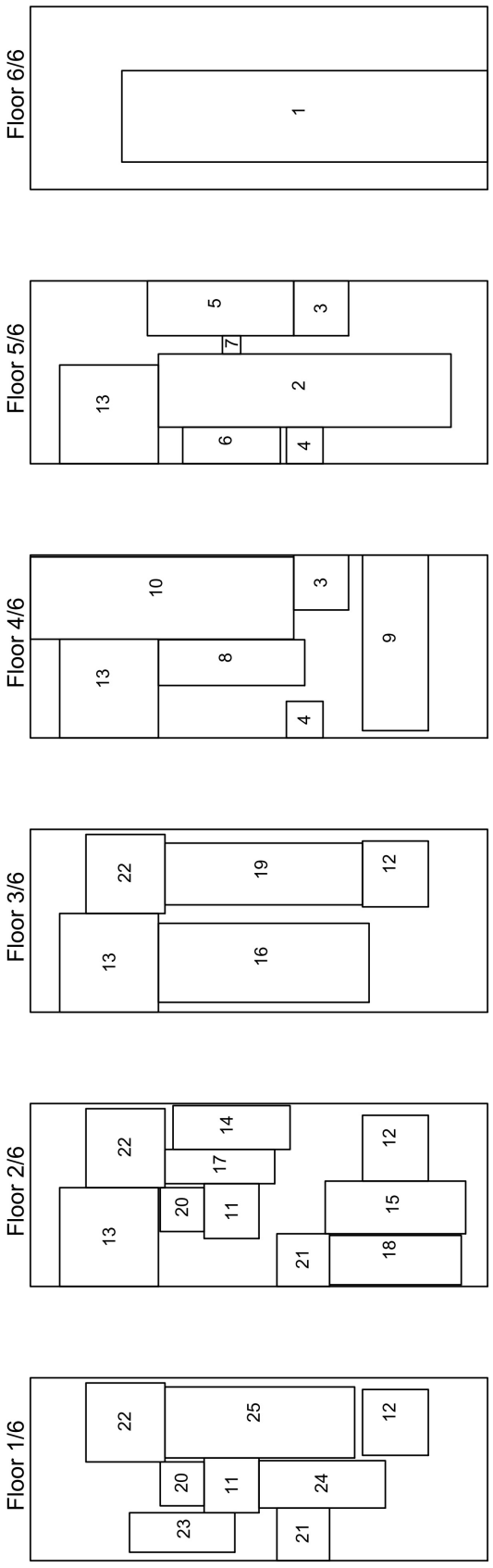

Fig. C.19 COGP plant layout plan; Model A.4

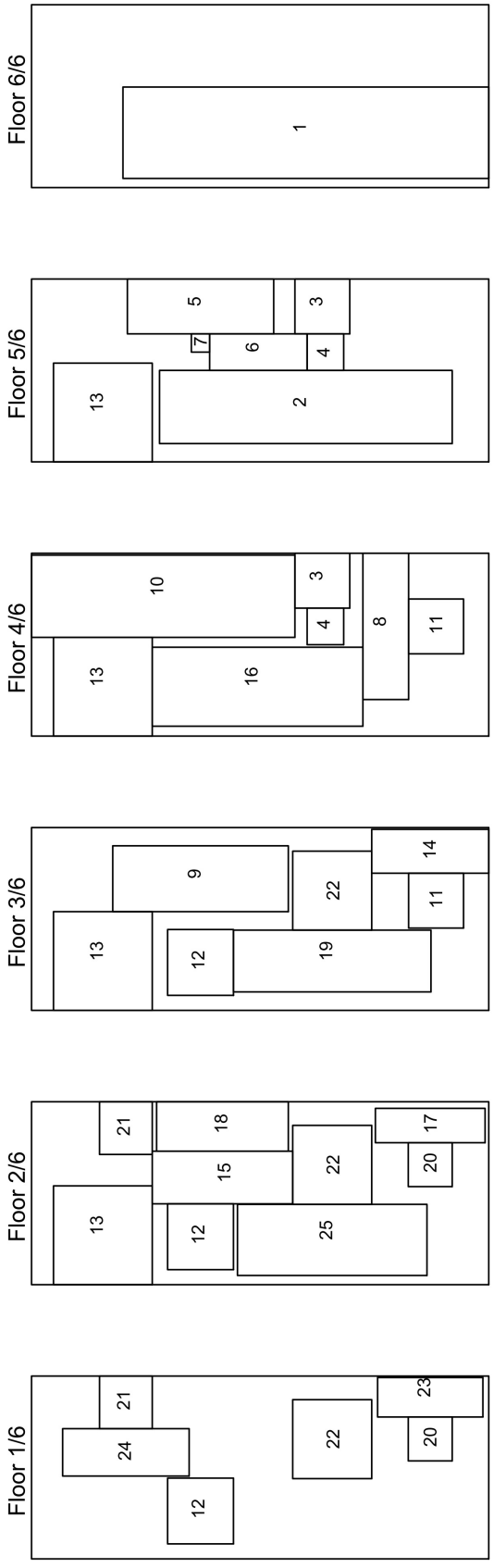

Fig. C.20 COGP plant layout plan; Model B

C.2 Layout result plots for Chapter 3: Multi-floor process plant layout with production sections

C.2.1 CDU plant: Function-based sections

The layout plans for the models proposed for the CDU plant are shown below in Figs (C.21) - (C.24):

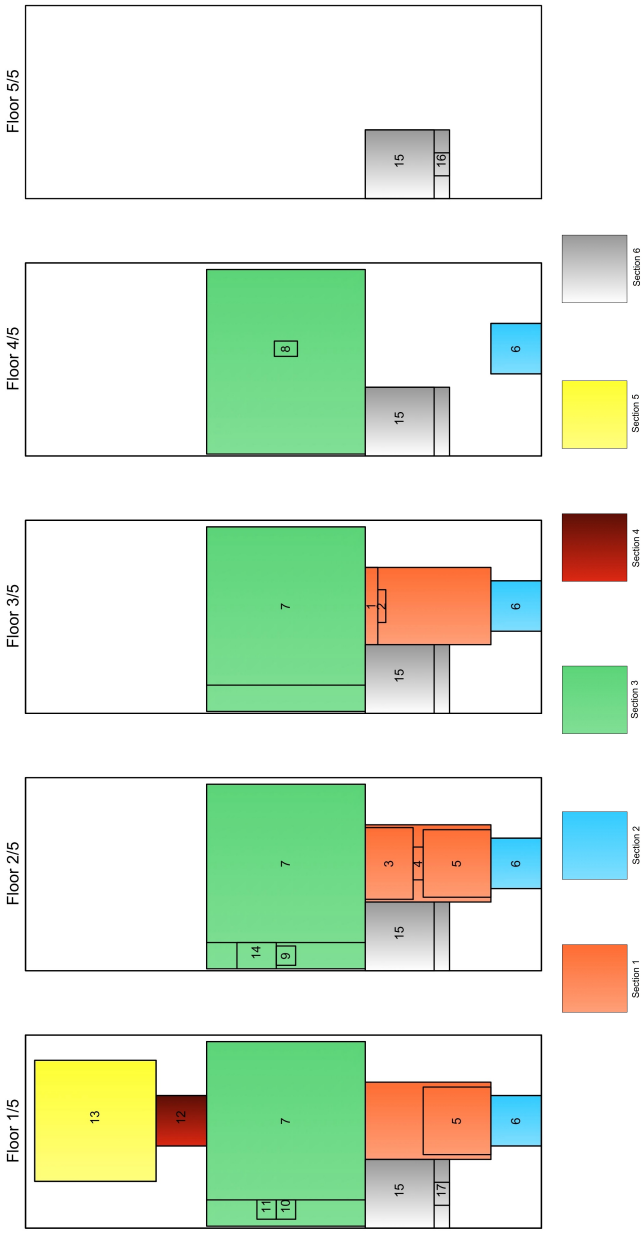

Fig. C.21 CDU plant layout plan, Function-based sections; Model A.2

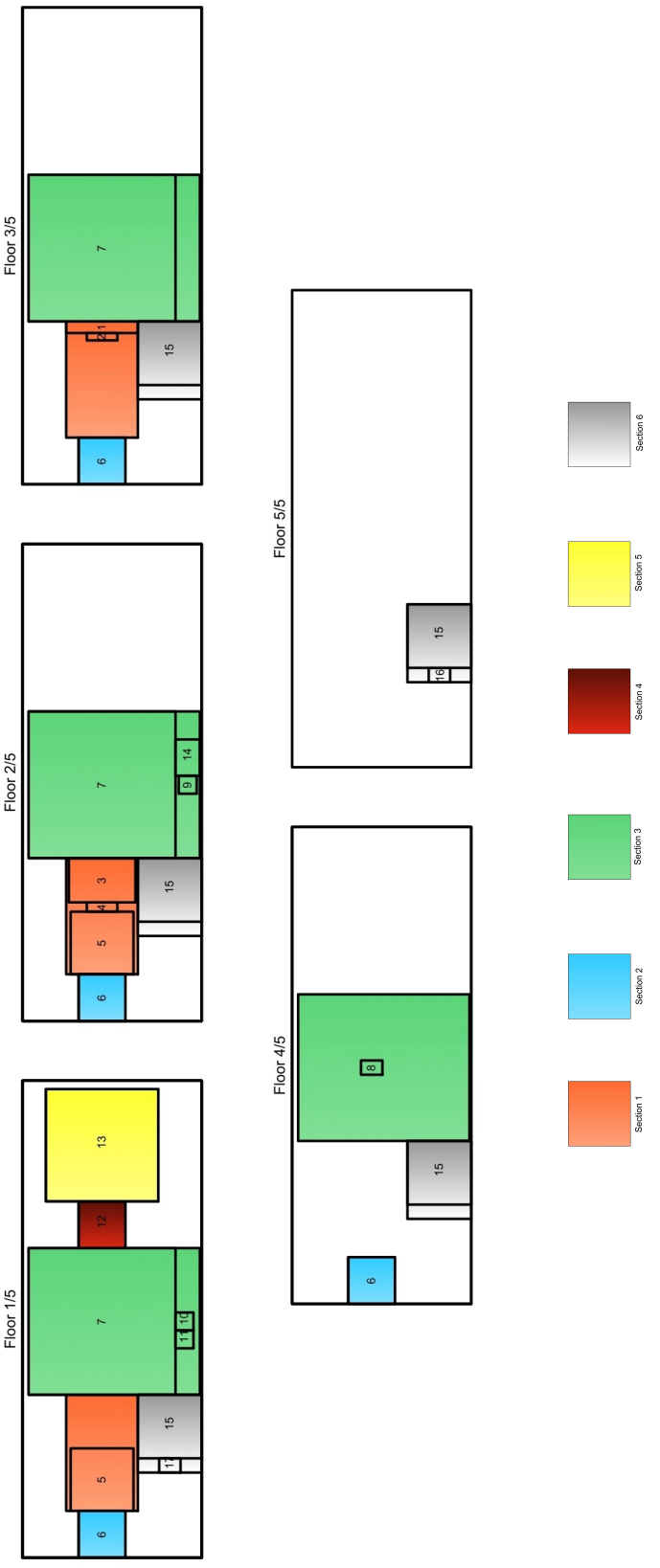

Fig. C.22 CDU plant layout plan, Function-based sections; Model A.3

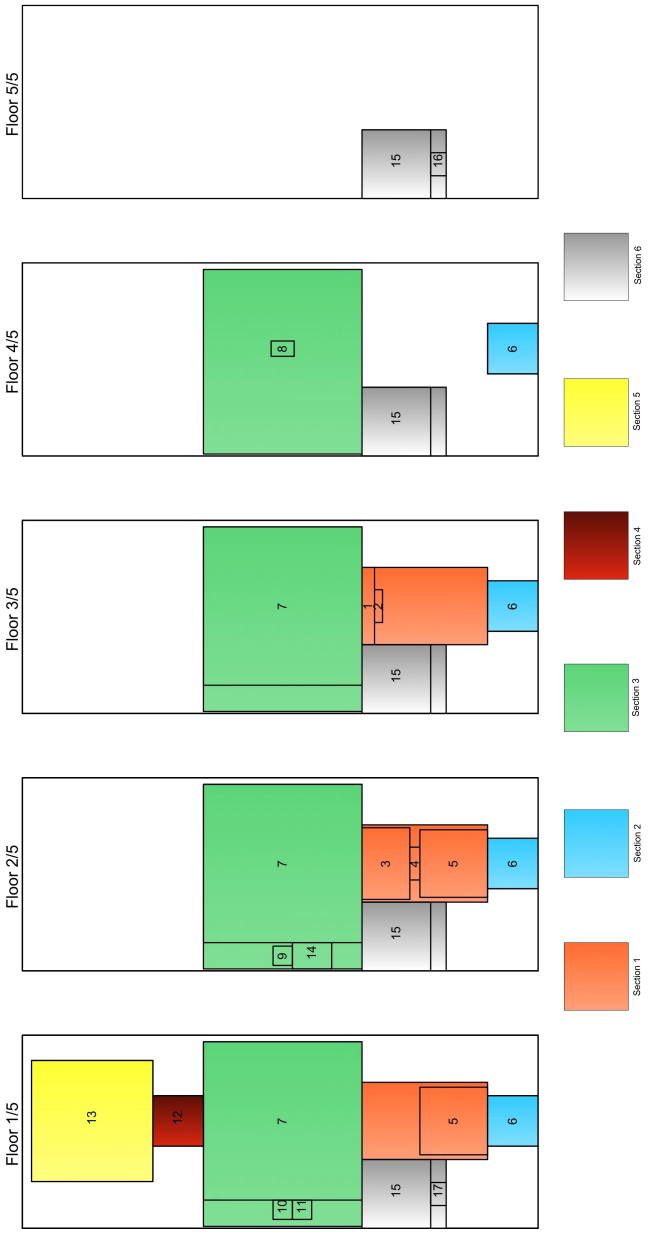

Fig. C.23 CDU plant layout plan, Function-based sections; Model A.4

Fig. C.24 CDU plant layout plan, Function-based sections; Model B

C.2.2 CDU plant: Unit-based sections

The layout plans for the models proposed for the CDU plant are shown below in Figs (C.25) - (C.28):

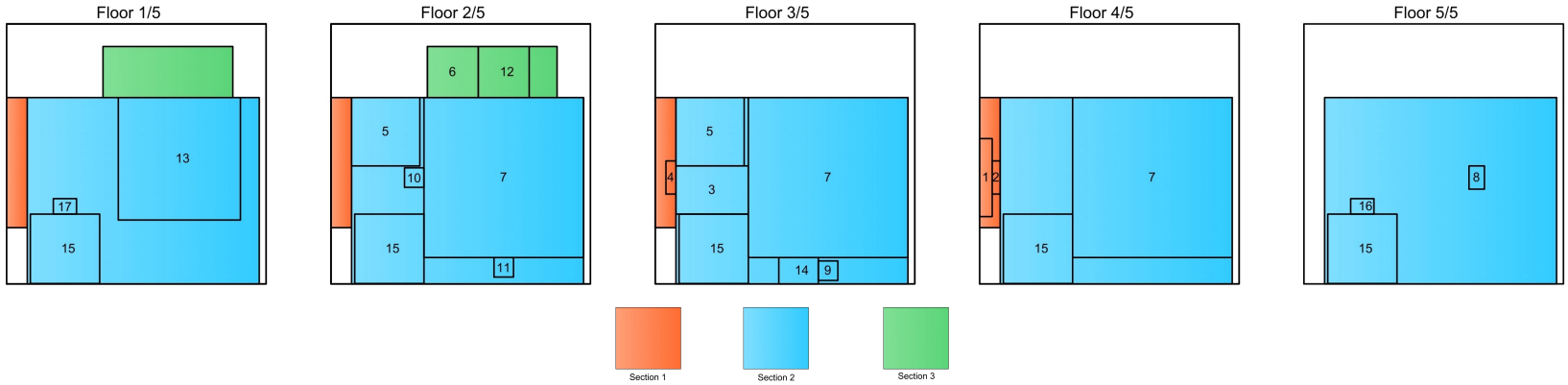

Fig. C.25 CDU plant layout plan, Unit-based sections; Model A.2

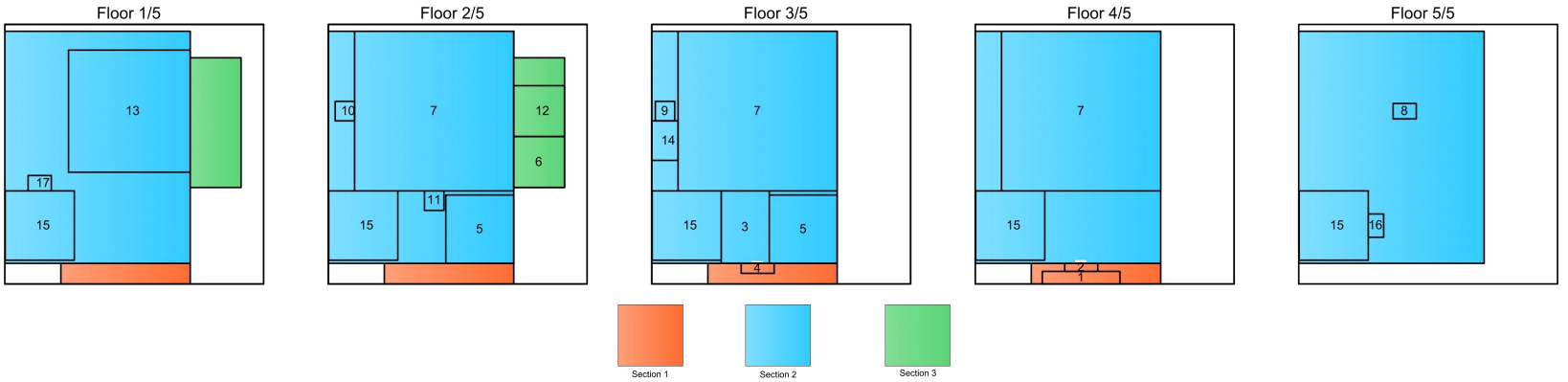

Fig. C.26 CDU plant layout plan, Unit-based sections; Model A.3

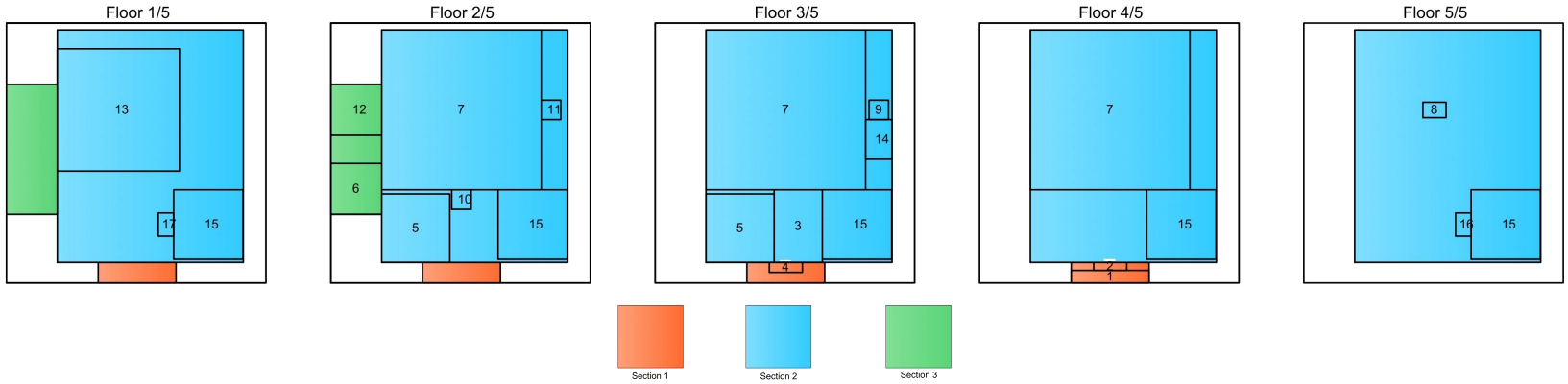

Fig. C.27 CDU plant layout plan, Unit-based sections; Model A.4

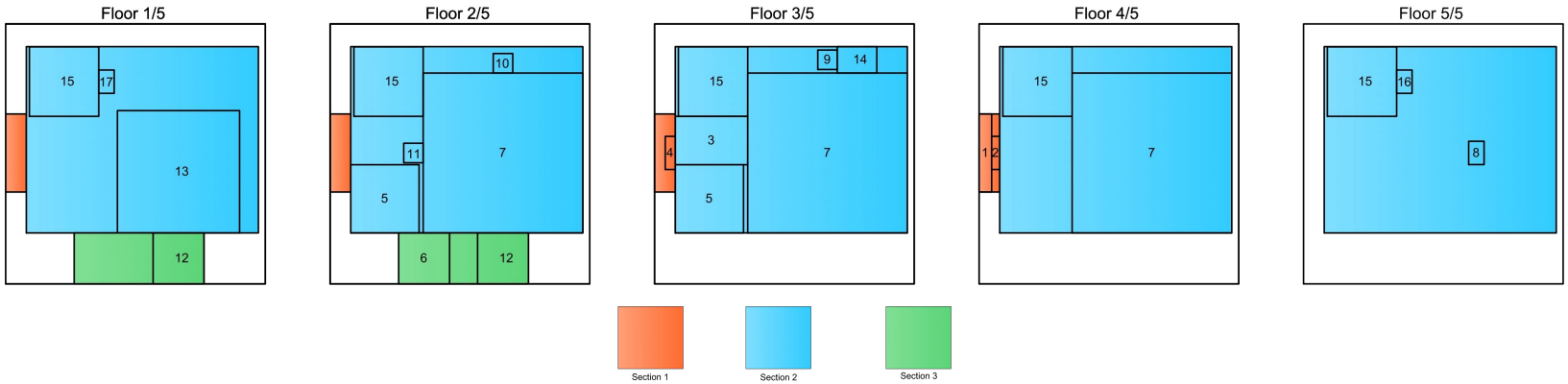

Fig. C.28 CDU plant layout plan, Unit-based sections; Model B

C.2.3 Liquefied natural gas (LNG) plant

The layout plans for the models proposed for the LNG plant are shown below in Figs (C.29) - (C.32):

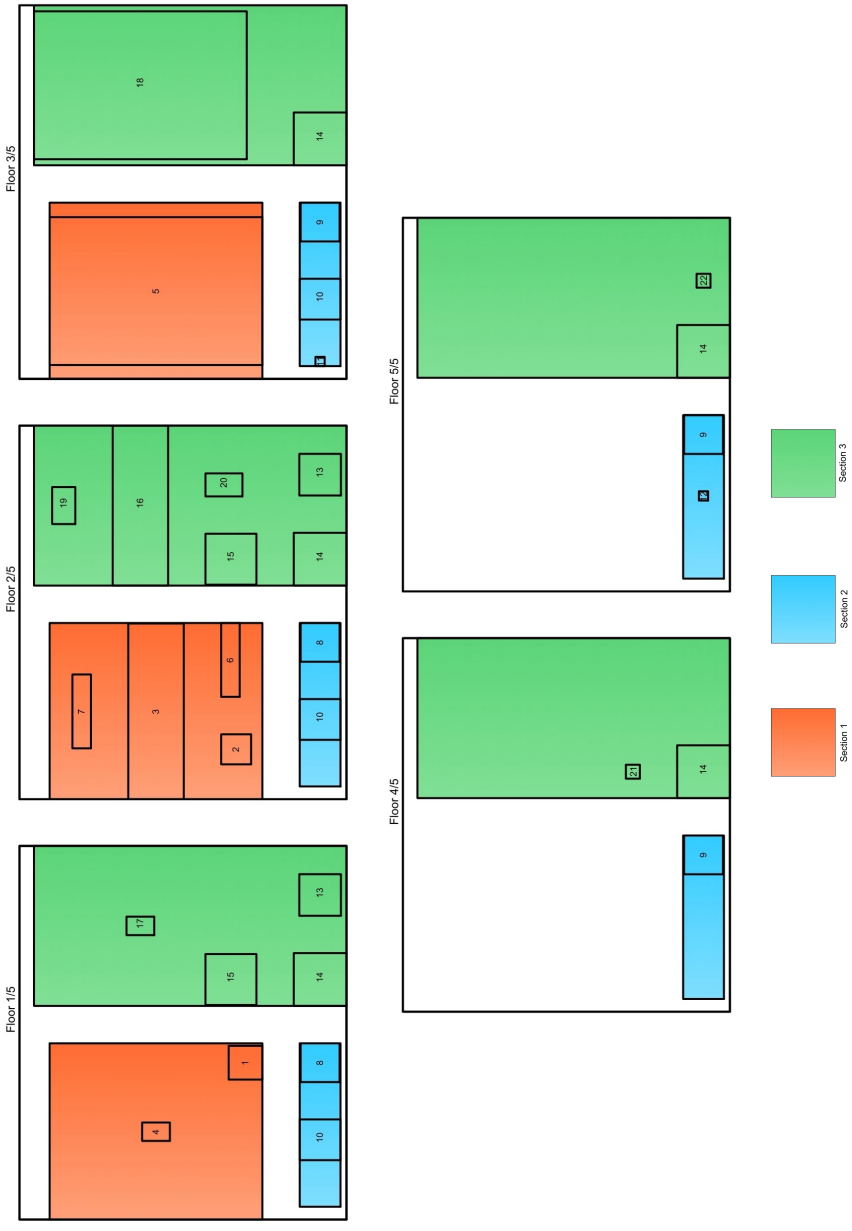

Fig. C.29 LNG plant with sections layout plan; Model A.2

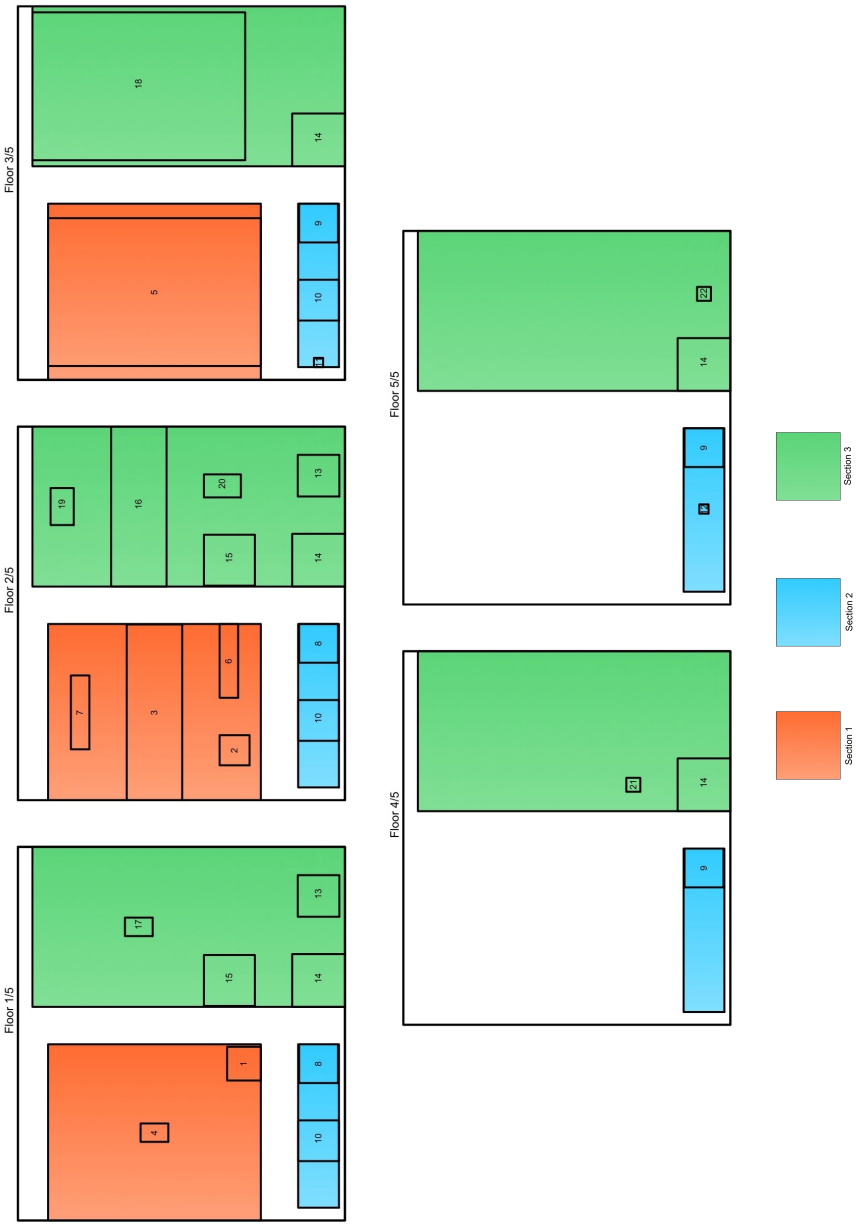

Fig. C.30 LNG plant with sections layout plan; Model A.3

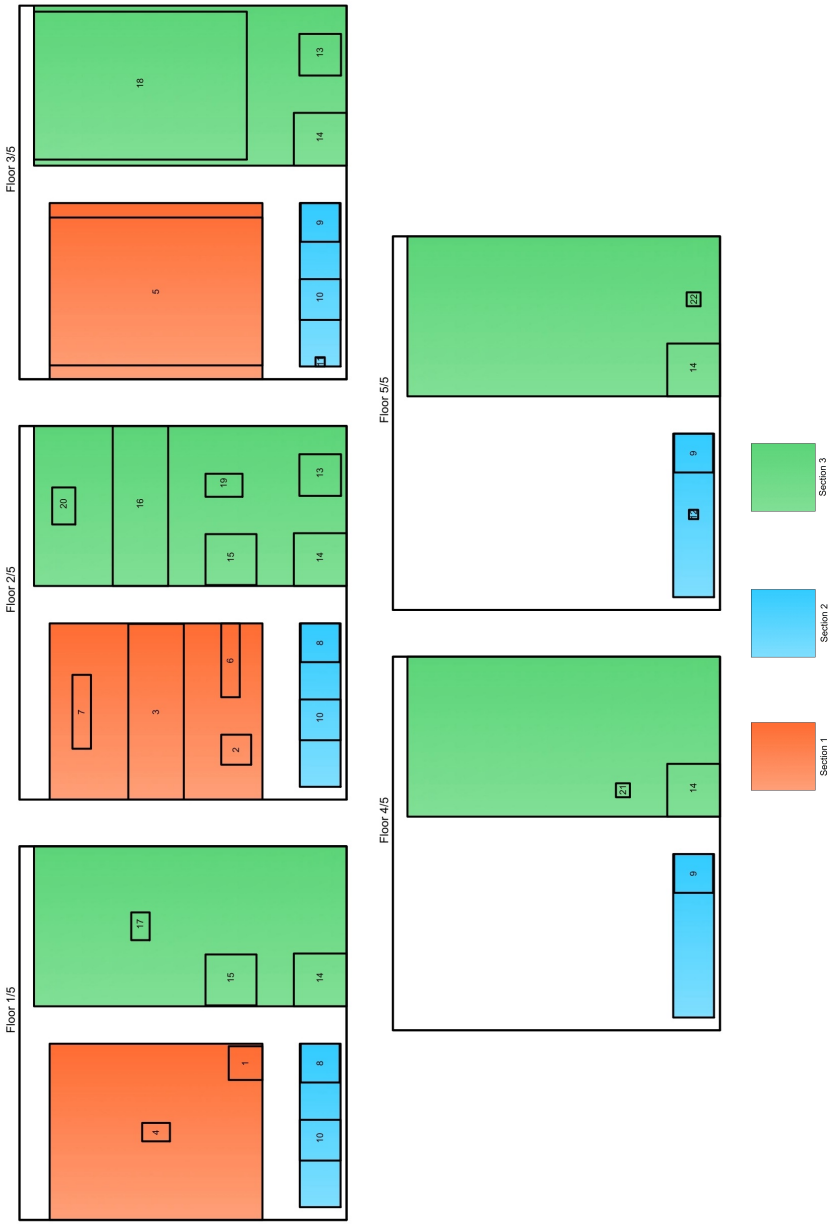

Fig. C.31 LNG plant with sections layout plan; Model A.4

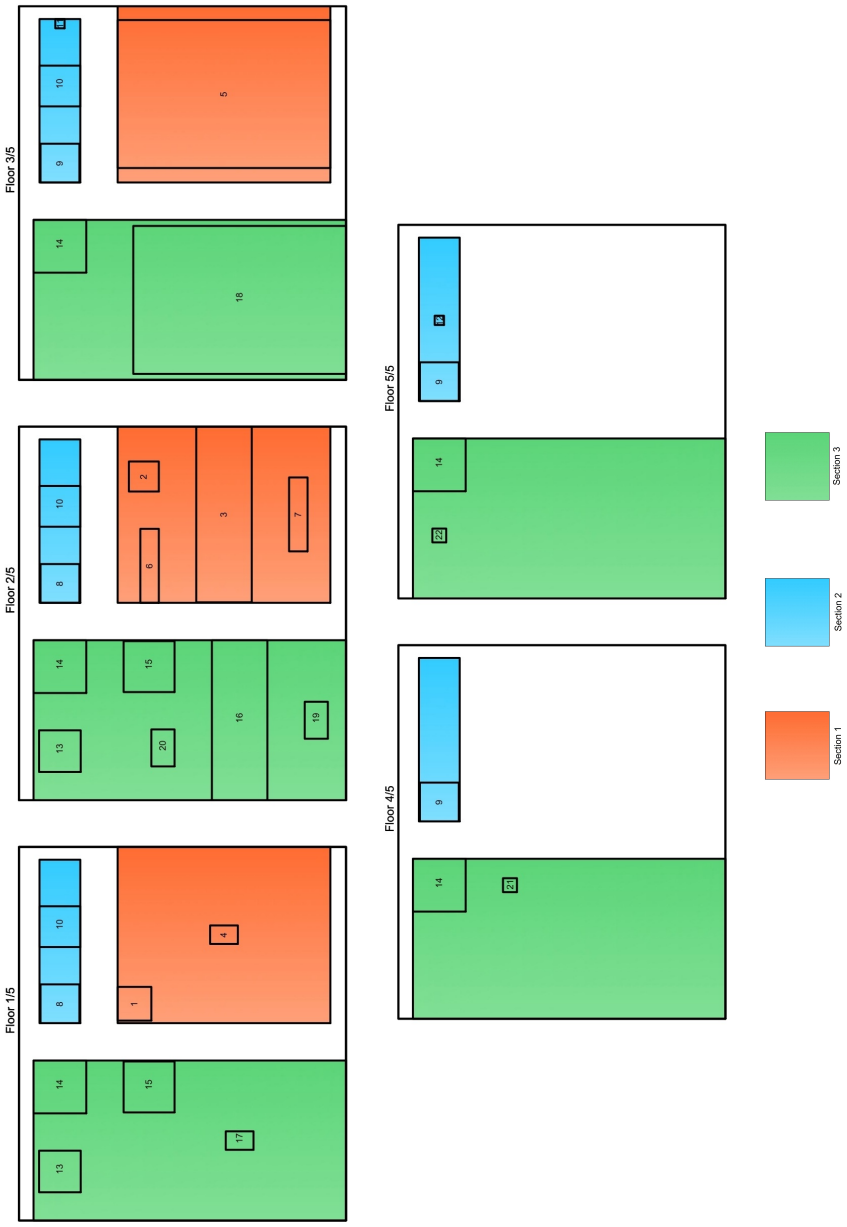

Fig. C.32 LNG plant with sections layout plan; Model B